THE TRANSPORT OF SOLIDS IN ROTATING DRUMS.

William James Scott.

Ph.D.
University of Edinburgh.
1986.

To Mum, Dad, Angus and Janice.

I declare that the work described in this Thesis has been carried out by me.

William James Scott.

I've started so I'll finish.

Magnus Magnusson.

ACKNOWLEDGEMENTS.

During the course of this work I have had help from many people. I particularly wish to acknowledge the following.

Dr Jack Ponton for his guidance and encouragement during my time at Edinburgh. My thanks are due for many stimulating discussions and useful suggestions. I would also like to thank Jack for his occasional social "events" which were greatly appreciated and enjoyed.

ICI Mond Division for their financial contribution to the project and my living expenses. For the use of their translating facility and for the assistance of my industrial supervisors Bill Kenny and John Edgley.

Dave Ketchin and his workshop staff for all the work on the apparatus and a good deal of advice freely given.

My office companions. Graham Aird for timely insights into the applications of fundamental calculus and much enjoyable combat on the chess board. Caroline Shirridan for wit, wisdom and many lively debates.

My wife Janice for her patient support as this Thesis took shape and for all the efforts and sacrifice made that it might progress.

CHAPTER 4 (Cont)

ABSTRACT.

This work considers the mathematical modelling of the motion of material inside an unflighted rotating drum in order to predict the degree of filling in the drum and the mean residence time and bed profile of the solid. The drum may be horizontal or sloping and may have one or more constrictions in the form of annular weirs along its length.

A critical review of previous work in this area is presented in which a mathematical description of the components of material motion is to be found. The approximations and limitations in the assumptions on which this description is based are addressed and further developed to provide an improved model for solids transport. One particular advantage introduced is the ability to model drums with internal weirs.

The model is tested using both experimental and literature data. It predicts filling to within 15% over a wide range of operating conditions. Areas for which agreement is worse can be identified in advance. The comparison of drum data on a dimensionless basis is also considered. The model is used to help determine a parameter which allows comparison over a much wider feed rate and drum dimension range than hitherto.

CHAPTER 1 - INTRODUCTION

Introduction

Rotating drums are widely used in industry to process granular or powdery material. Drying, cooling, size reduction and thermal decomposition are among the operations commonly carried out. Industrial production rates often require that the drums for such processes be very large with diameters of up to 4 m and lengths of 30 m or more. They are usually inclined at some small angle to the horizontal, sloping down from feed to discharge end and operated with continuous flow through of material.

A knowledge of the amount of material contained (hold up) in a rotating drum under normal operating conditions is of fundamental importance. It is used both in equipment design and process operation since for a fixed feed rate to the drum, varying the hold up allows the mean residence time to be changed.

The aim of this investigation was to devise a means of modelling the transport (or movement) of the solid material within a rotating drum so that the hold up and residence time could be accurately predicted.

A preliminary examination of the available literature indicated that it would be prudent to restrict the field of study due to the impracticality of dealing with all of the various types of drums and drum/solid systems available. The following four criteria were chosen to define a suitable field of study:

1 The Geometry of Internal Fixtures

Rotating drum equipment can be split into two broad categories viz flighted or unflighted drums. Flighted drums are so called because they contain longitudinal flights or "lifters" attached to the inside of the drum shell and protruding some distance in towards the centre. These carry material up the side of the drum and shower it across the drum cross section (Figure 1.1). The flights can have various shapes and are usually found in rotary driers or coolers. The initiator for the present investigation was the operation of calciners, reactors and kilns, all of which are generally operated without flights, so it was decided to exclude flighted drums from the field of study.

One internal fixture often encountered in unflighted drums is an annular constriction (Figure 1.2). This may be included by design in an effort to influence the residence time of material in the drum by increasing the hold up behind the constriction. Alternatively it may occur naturally in some rotating drum processes in which sintering or agglomeration occurs and material builds up into a "nose ring". Such constrictions located at any point along the drum length were considered to be of interest and were included in this study. This in addition to the obvious open ended unflighted drum.

2 **Presence of an Induced Air Flow**

A counter or co-current stream of air may be used to cool or dry the product. This is almost always encountered in association with a flighted drum in which the product is showered through the air stream. Since such drums were excluded from this study the effects of an induced air flow were also not considered.

3 **Variation of Physical Properties along the Length of the Drum**

As material is processed in a rotating drum, properties such as density and angle of repose may change due to the effects of heat and/or mass transfer. It was decided for simplicity to examine systems with no axial variation of solid physical properties in the expectation that the resulting model could be combined with an appropriate heat or mass transfer model to deal with systems in which solid physical properties change.

4 **Segregation Effects**

Only materials of uniform particle size and bulk density have been considered. This was not thought to be a serious limitation as many industrial processes operate with essentially uniform feed material.

Although the above restrictions to the field of study have been made explicit it was recognised that all rotating drum literature has a common heritage and recourse has been made to papers dealing with "excluded" topics.

Chapter 2 now examines the available literature on the topic of solids movement in rotating drums. This provides a basic model of motion which is further developed in Chapter 3. The details of an experimental

system used to examine both solids motion itself and the accuracy of the model in describing it are given in Chapter 4. Chapter 5 discusses the results of these experiments and also those of previous workers in the light of the new model. The conclusions of this work and recommendations for further work are given in Chapter 6.

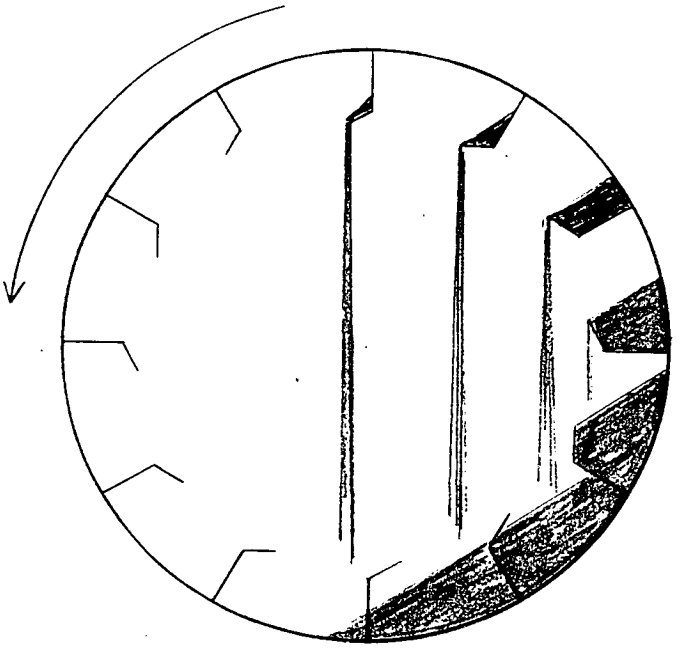

Figure 1.1 Cross Section of flighted Drum Showing Material Cascade (From Miller, Smith and Schuette [M6] (1942))

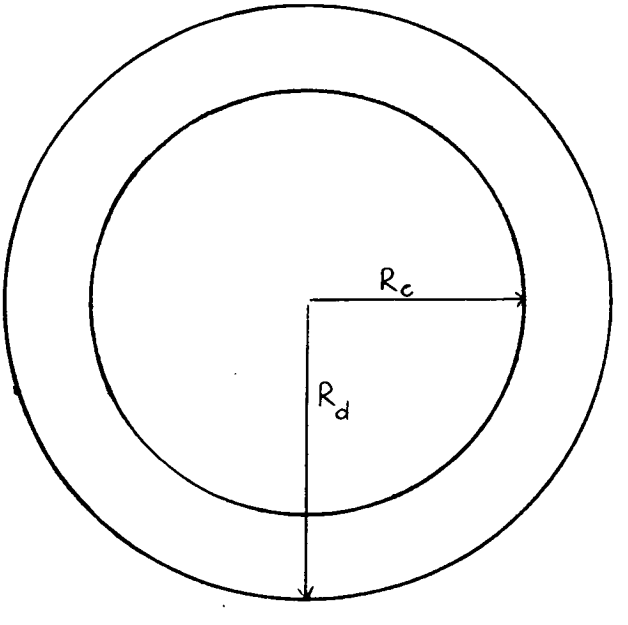

Figure 1.2 Cross Section of Drum of Radius R_d with Annular Constriction of Radius R_c

CHAPTER 2 - LITERATURE REVIEW

Introduction

In this chapter previous work on the transport of solids through unflighted rotating drums which may have one or more constrictions in the form of annular weirs along their length is reviewed. Both empirical correlations and theoretical models for mean residence time, hold up and bed profile are considered. Section 2.1 considers first the case of the open ended drum and Section 2.2 the constricted drum.

In addition, radiotracer and Residence Time Distribution Studies are considered in Section 2.3 and overall simulation of rotating drum plant in Section 2.4. These topics although they have not been studied in detail in this investigation are nonetheless relevant as they provide an indication of the wider context into which a detailed model of solids transport should fit. A summary of what has been achieved in the literature and an introduction to the work of this investigation is given in Section 2.5.

Throughout the text equations taken from the literature have been expressed in a common notation. The details of experimental work in the literature, used either to derive or verify equations, have largely been omitted from the main text, they have instead been collected together in Tables 2.1 and 2.2 at the end of this chapter.

2.1 The unconstricted drum

The first published results of a detailed investigation into the behaviour of material in a rotating drum are those of Sullivan, Maier and Ralston in 1927 [S1]. They studied the motion of solids in inclined drums with and without discharge and internal constrictions. Details of their experimental equipment and materials are given in Tables 2.1 and 2.2 at the end of this chapter.

Sullivan et al note that under normal operating conditions the bulk of the solid material rotates with the drum until carried past its static angle of repose α_s. This is a characteristic angle for any given material though slight variations for the same material may be observed depending on the method of measurement [T1]. One common method is to measure the angle which the edge of a conical heap of material makes with the horizontal. Once carried beyond the static angle of repose the uppermost particles fall back down the surface of the bed and re-enter it somewhere below the midpoint whence the process is repeated. The bed is thus composed of two regions, the larger plug flow region moving in unison with the drum and the thin surface cascade layer with dynamic angle of repose α_d as shown in Figure 2.1. The dynamic angle of repose is the angle which the surface of the bed in cross section makes with a plane tangential to the lowest point of the drum circumference.

It is while cascading down the surface of the bed that the axial transport can take place. If the surface is inclined to the horizontal in the axial direction then a particle will descend at some angle ϕ to the cross section of the bed from which it has just emerged, thus it will advance along the drum as shown in Figure 2.2. The particle moves from A to B by rotation with the drum and from B to C by cascading on the surface. If the drum itself is inclined then this may provide the necessary slope for the surface to effect axial transport with no change in bed height, otherwise the bed itself must increase in depth from the discharge to the feed end to provide the surface slope. A continuous increase in bed depth is necessary in horizontal drums but it may also occur or be part of the bed profile in an inclined drum as in Figure 2.2. This is because the depth at which transport may be effected with no change in bed height in inclined drums

becomes larger for larger feed rates and there must be a finite length over which the bed builds up to this height from the minimum at the discharge end. The bed depth at which no further increase is necessary is known as the "limiting filling".

Sullivan et al worked with drums whose feed rate and operating conditions were such that limiting filling existed over essentially the whole of the drum length. Various feed rates, drum parameters and operating conditions will allow a drum to operate with near uniform bed depth over its whole length, these may be determined but the basis for this depends on much of the theory yet to be discussed and uniform bed depth criteria are therefore discussed later in this chapter. It may be said however that in general the conditions require very low feed rates and result in correspondingly low drum hold up, thus the following empirical expression for the mean residence time in an open ended inclined drum presented by Sullivan et al is of very limited use.

$$t = \frac{1.77\ L \alpha_d^{\frac{1}{2}}}{\psi N D} \qquad (2.1)$$

Where t is the residence time in minutes, L is the length of the drum (m), D its diameter (m), ψ is the drum slope in degrees and N the rotational speed (RPM).

In 1932 Gilbert [G1] carried out experiments using sand in bench scale drums 76.2 cm long with diameters of 5.1, 6.35 and 7.1 cm all with fixed slope of 1 in 25 (2.29°). Here again the drum was operated under conditions which would result in a nearly uniformbed depth over the entire length, Gilbert's analysis is certainly based on this assumption. The drum was fed in a batchwise manner and rotated by hand for a fixed number of revolutions between feeds until the rate of discharge equalled the rate of feed. This procedure would result in a discontinuous motion not wholly compatible with steady state operation, nonetheless Gilbert's results are of interest.

For the drums described above with fillings up to 9% (fc = 0.09) Gilbert states that the amount of charge retained in the drum is directly proportional to the rate of feed per revolution,

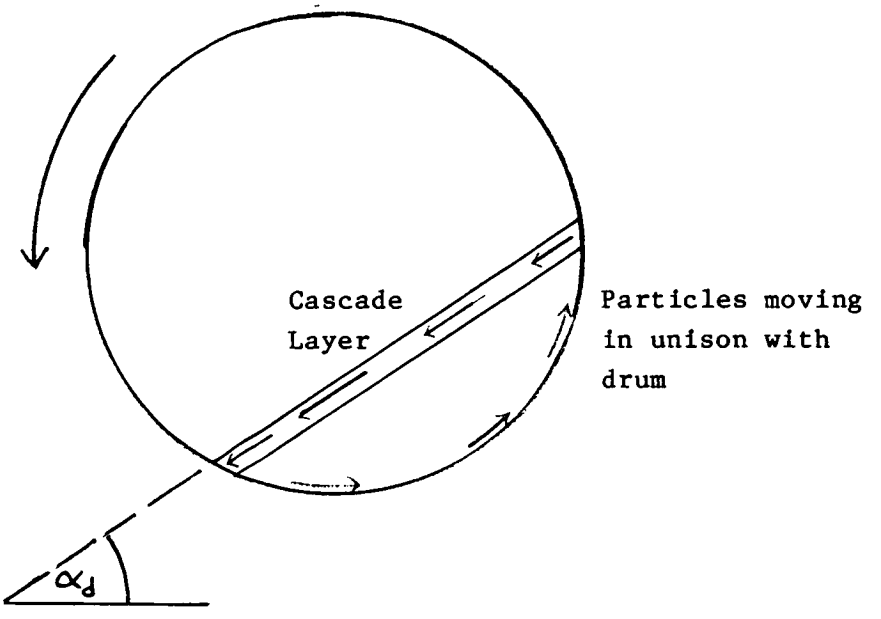

Figure 2.1 - Transverse Section through the solid bed in a rotating drum

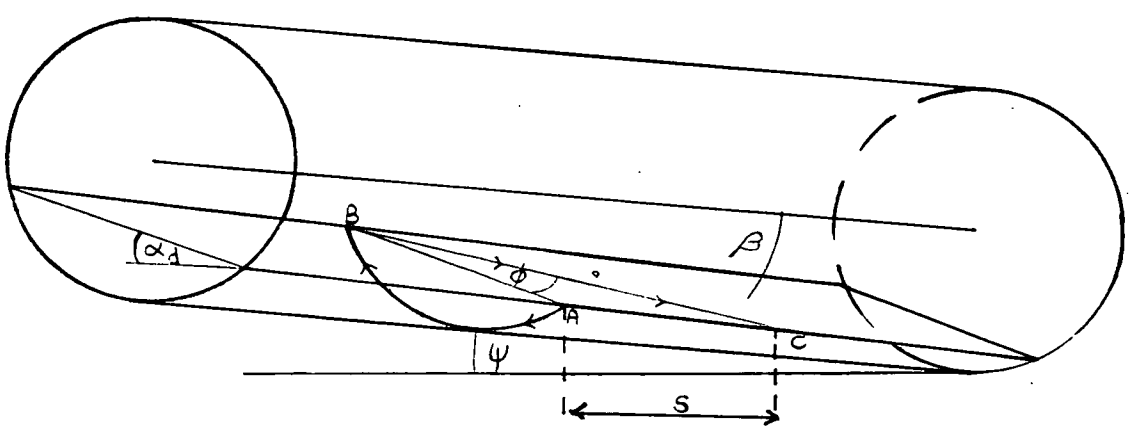

Figure 2.2 - Section of drum showing mechanism of particle motion along the drum

$H \propto F/N$

where H is the hold-up (Kg) and F is the mass feed rate (Kg/s). Since the hold-up is also equal to the mean residence time multiplied by the mass feed rate,

$$H = tF$$

the proportionality is equivalent to

$$t \propto N^{-1}$$

which is in agreement with equation 2.1 of Sullivan et al. Gilbert also states that the rate of advance of the charge is independent of the charge volume and equal to 23.3% of the drum diameter per revolution. The mean residence time would thus be expressed by the following equation.

$$t = \frac{L}{0.233DN} = \frac{4.29L}{DN} \qquad (2.2)$$

If equation 2.1 is applied to Gilbert's drum with slope 2.29° using a common value for the static angle of repose for sand of 34° for α_d (not unreasonable since the motion in the drum was discontinuous) the following is obtained.

$$t = \frac{4.49L}{DN} \qquad (2.3)$$

This differs from (2.2) by less than 5% which, given the limitations of Gilbert's technique, suggests that the findings of Sullivan et al and Gilbert for inclined drums with low fractional fillings are in agreement.

Gilbert also notes that by plotting the fractional filling in drums of different diameters against the feed rate to the drum, expressed as q/ND^3 where q is the volumetric feed rate in (m^3/min), the points for different drums lie on a single line. This is the first indication that drum data may be compared on a dimensionless basis, further application of this technique does not occur until much later.

The empirical correlation of Ginstling, Zil'berman and Gvozdev (1939) [G2] for the mean residence time of material in an inclined rotating furnace is presented by Friedman and Marshall [F1] in the introductory section of their paper on the hold-up in flighted drums, viz:

$$t = \frac{26.81L}{\psi ND} \qquad (2.4)$$

They compare this directly with the equation of Sullivan et al. If however the original Russian paper is examined it can be seen from the diagram and equations that the correlation is semi-empirical and derived on the basis of "slumping" motion. This type of motion arises when the coefficient of friction between the solid bed and the drum wall is not sufficient to carry the bed past its static angle of repose and thus induce turnover or cascading. Instead the motion is oscillatory, the bed being carried part way up the drum wall and then sliding back en masse to a lower position whence the process is repeated. A similar analysis to that of Ginstling et al is presented by Van Krevelen and Hoftjizer [V1] in which a general equation is derived. The degree to which the charge is carried up the drum wall is assumed fixed at some arbitrary value which is independent of drum speed, inclination and diameter. This results in the equation for the mean residence of a particle containing a constant k which has to be empirically determined.

$$t = \frac{kL}{DN\tan\psi} \qquad (2.5)$$

The absence of any dependence on α_d is characteristic of equations for this oscillatory slumping. Ginstling et al essentially fitted the constant k in (2.5) for the prevailing conditions in a rotary furnace which they investigated and found k = 26.81 (2.4). The simplification of setting the value $\tan\psi$ equal to its radian angle is quite often encountered in early work as it introduces very little error for small drum slopes. Although (2.4) is similar in form to that of Sullivan et al the constant of proportionality results in answers around 2.5 times those of (2.1). This highlights the operating condition specific nature of such correlations. Some attempt was made to make things more

general by incorporating user-fitted constants such as 'k' in the following equation of Gibbs (1942) [G3] for industrial kilns.

$$T_d = kLD^2/100 \qquad (2.6)$$

Where T_d is the tons of finished material per day and the constant k is dependant on the type of material being processed. Various guidelines are given as to the value of k but again this equation is of limited accuracy and application. In recognition of this perhaps Gibbs went on to publish a "Chart for estimating performance and production rates in rotary kilns" (1943) [G4] which was based on (2.1). This is for use with kilns having a slope of 2.4° which "seems to be most generally used" and it was hoped would aid the maximum production of suitable finished material for the war effort!

The first claim to a theoretically derived equation came from Bayard (1945) [B1]. He states that his equations are based on a geometrical derivation and that the total time in the kiln may be expressed as

$$t = \frac{0.037(\alpha_d+24)L}{\psi ND} \qquad (2.7)$$

Where ψ is measured in inches per foot. This is said to represent the length of the kiln divided by the distance moved along its major axis per cycle multiplied by the time taken to complete a cycle. If ψ is converted to degrees however, then (2.6) becomes

$$t = \frac{0.176(\alpha_d+24)L}{\psi ND} \qquad (2.8)$$

This has the form of (2.1) with $1.77\alpha_d^{\frac{1}{2}}$ replaced by $0.176(\alpha_d+24)$. It is interesting to note that over a range of commonly reported values for α_d of 30-45 degrees these functions differ by 2% at most. This, and the fact that the diagrams accompanying Bayard's text show that he too was concerned with drums which had a uniform bed depth, indicates that (2.7) is subject to the same limitations as (2.1) of Sullivan et al.

Since "kiln operators are interested chiefly in results" Bayard does not present the derivation of (2.7). This is unfortunate since

as will be shown later the axial transport distance per cycle is not a linear function of α_d, neither is it possible to find an obvious substitution or approximation which would make it so. Thus if some legitimate assumption has indeed been made, Bayard's brevity disserves him since later workers all refer to his work as empirical [F1,S2].

The fundamentals of a mathematical model for solids transport, based on the already well understood mechanism of motion, were developed between 1949 and 1952. Vahl (1949) [V2] was the first to consider transport in horizontal drums due solely to an increase in bed height from discharge to feed end. He presents an equation for the flowrate in horizontal drums whose derivation is given later by Vahl and Kingma (1952) [V3]. Pickering Feakes and Fitzgerald (1951) [P1], Saeman (1951) [S2, reprinted in S3] and Kramers and Krookewit (1952) [K1] all developed equations for inclined drums. All except Pickering et al included the effect of any increase in bed height on transport as well as the fundamental effect of drum slope.

The following assumptions are common to all of this early theoretical work:

(1) The bed cross-section has a flat surface of slope α_d with respect to a plane tangential to the lowest point on the drum circumference.

(2) The time spent cascading on the surface is negligible compared to that spent locked in the bed.

(3) The thickness of the cascade layer is negligible with respect to the bed depth.

(4) All particles re-enter the bed at the same radial distance from which they left.

(5) There is no change in the physical properties of the solid material over the length of the drum.

Assumption 4 may be justified as follows. Since particles enter the bed surface at all points along its upper half and re-enter it all along its lower half, to maintain a steady motion all particles must

on the average re-enter the bed at the same radial element from which they left. This results in a segregated path flow pattern. As pointed out much later by Mu and Perlmutter (1980) [M1] however, another steady flow in which the particles re-enter the bed at a fixed distance (equal to half the bed surface length) from their point of emergence is a possibility. This would result in a maximum mixedness of flow. Comparison of both assumptions suggests that the former models the physical situation best and is presented in Chapter 3 Section 3.3. The segregated path model is indeed used exclusively in all published work concerned with developing expressions for the variation in filling along a drum length. Mu and Perlmutter, whose work is discussed later in Section 2.3, did not consider particle paths for this purpose.

The model building procedure is common to all of the above workers [K1, P1, S2, V2, V3]. First of all the axial distance travelled when a particle cascades down the bed surface is determined by geometry. This is then divided by the time taken for that particle to complete the cycle of being locked in the bed and cascading on the surface (assumed equal to the time spent in the bed - assumption 2 above) thus the axial transport velocity of the particle is obtained. This velocity is found to be a function of the radial position of the particle path. At this stage, for drums with small bed depths, variation in bed height along the drum may be neglected and certain angles which define the bed surface may be approximated by geometrical ratios. The variation in axial velocity with radial position may also be neglected if the effective average radius of particle paths is considered as closely approaching the radius of the drum R_d. In this way the velocity equation may be simplified and combined with the drum length L to produce an equation for the mean residence time in lightly loaded drums. This procedure is well illustrated by Saeman who shows that such simplifications result in an equation which corresponds closely to that of Sullivan et al.

Pickering et al did not consider variation of bed height along the drum and further simplified their model by neglecting terms which accounted for the variation in cycle time with radial position. Their model derivation is thus analogous to the simplification of the general solution by Saeman and results in an equation similar to that of Sullivan et al, limited in application to drums with very low fractional fillings. Their derivation of the axial advance per cascade also has a minor error as outlined in Appendix 1.

For drums with relatively large fractional fillings simplification of the velocity equation is not possible. It is instead expanded to a volumetric basis by multiplying by the incremental area associated with each particle path and then integrating this across the drum cross section. The result is given in (2.9) below

$$q = \frac{4}{3}\pi N\left(\frac{\tan\Psi + \tan\beta \cos\alpha_d}{\sin\alpha_d}\right)(R_d^2 - b^2)^{3/2} \qquad (2.9)$$

Where q is in (m^3/s), β is the angle between the surface of the bed and the axis of the drum and b is the distance between the same, perpendicular to the bed surface. This equation was used as the basis of a solution for mean residence time by Saeman, Kramers and Krookewit and, with $\Psi = 0$, Vahl and Kingma. Its derivation, discussed above in general terms, is given in Appendix 1 along with a discussion of the simplifications incorporated in it. Saeman presents (2.9) with $\tan\psi$ and $\tan\beta$ approximated by their radian angles which for small angles introduces negligible error. Simplifications of this sort are prevalent in all of the early theoretical modelling of solids motion and have already been seen when discussing the empirical work of G'instling et al and Van Krevelen and Hoftjizer.

Equation 2.9 corresponds with equation 18 of Saeman, equation 2 of Kramers and Krookewit and equation 5 of Vahl and Kingma ($\psi = 0$). The latter papers express

$$\tan\beta \text{ as } -dh/dx$$

and

$$b \text{ as } (R_d - h)$$

where h is the bed height at any axial position x along the drum, thus the equivalence is not immediately apparent. Expressing $\tan\beta$ as dh/dx (or -dh/dx depending on whether the feed end of the drum is considered as x=0 or x=L) is the key to the solution of (2.9) as it allows an expression for the variation in bed height along the drum to be determined. Saeman expressed

$$\tan\beta \text{ as } db/dx$$

and produced the following equation

$$\frac{db}{dx} = \frac{3q\sin\alpha_d}{4\pi N(R_d^2-b^2)^{3/2}\cos\alpha_d} - \frac{\tan\psi}{\cos\alpha_d} \qquad (2.10)$$

The limits of integration are from $b=(R_d-h_o)$ where h_o is the bed height at the drum outlet, to $b=(R_d-h_i)$ where h_i is the bed height at the drum inlet. Saeman recognised that due to the approximations made in its derivation (2.10) is not valid in regions of rapid decrease in bed height (large db/dx) such as exist at the discharge end of a drum. He observes however that in general the region of collapse is "so short that it is of little or no value to know either the length in which this occurs or the value of β over this length". He therefore suggests setting h=0 which is equivalent to zero filling at the discharge end. This lower limit of integration for b was also used by Vahl and Kingma and by Kramers and Krookewit with much less deliberation. Whilst this procedure may be acceptable for long drums with uniform filling over almost all of their length, the error introduced will be greater for short drums and those with increasing bed depth over much (or in horizontal drums, all) of their length.

Even if the approximations which make (2.10) inapplicable for large db/dx are removed however, the assumption of $h_o=0$ at x=0 is still incorrect. This reflects of the fact that this condition is not a true representation of the physical situation, there can be no transport with zero fractional filling. The mathematics of this inconsistency and the minimum filling for which the model (further refined) will hold are presented by Austin and Flemmer (1974) [A2] and detailed later in this chapter. For the time being however it is accepted that a lower bound for the integration has been established and (2.10) can yield a relationship between h and x along the drum length.

The integration of (2.10) proved extremely difficult in pre computer days. Saeman presented no general solution and the later work of Kramers and Krookewit and Vahl and Kingma (with $\psi=0$) introduced simplified functions to represent the integral over bed depth, they were greatly aided in this by the assumption $h_o=0$ at x=0. Vahl and Kingma present a general solution for horizontal drums in terms of volumetric flowrate as follows

$$q = 0.68(h_i/D)^{2.08} \frac{D^4 N \cot \alpha_d}{L} \qquad (2.11)$$

Due to the limited accuracy of mathematical approximation incorporated in the solution this applies for $0.15 \leq h_i/D \leq 0.45$. Vahl and Kingma compared this equation with the results of their own experiments (details given in Tables 2.1 and 2.2) and found that theory underpredicted flowrate by an average of 13%. This is equivalent to an overprediction of residence time which would not perhaps be expected when the effects of the following assumptions inherent in (2.10) are considered:

(i) Assuming zero filling at the discharge end will tend to underpredict drum holdup reducing t.

(ii) Assuming the distance travelled in the bed surface is equal to the axial advance (see Appendix 1) will have the same effect and

(iii) Assuming the particle travels through the drum faster than it actually does (neglecting the cascade time) should also underpredict t.

The discrepancy between what might be the expected direction of a systematic error and what is actually observed may be partly due to the simplified form of the solution function but on examining the photograph of the experimental set up it appears likely that it may be due to experimental error. This is suggested since later workers report marked differences in drum hold-up for even slight deviations from the horizontal [S4] and the method of drum support shown by Vahl and Kingma's paper does not look particularly accurate. The underprediction of (2.11) is compensated for by changing the value of the constant from 0.68 to 0.74 and the exponent from 2.08 to 2.05.

This modified equation defines a relationship between bed height and distance along the drum, since however it is the hold-up in the drum which is sought in order to determine the mean residence time, the relationship between bed height and drum filling is now introduced. For a linear transverse bed profile the bed height at any axial position x is related to the filling angle θ_x, half the angle subtended by the bed surface at the centre of the drum (see figure 2.3),

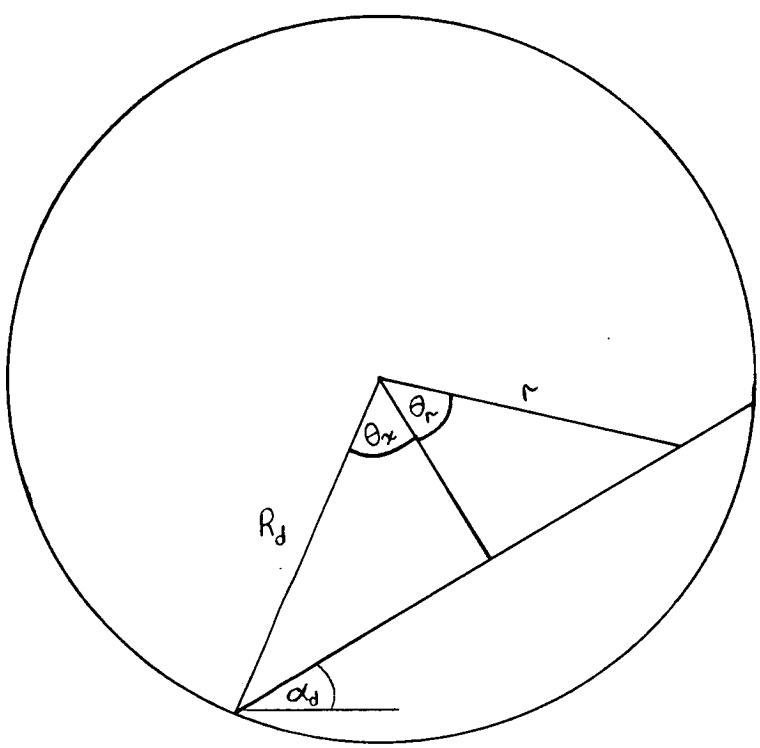

Figure 2.3 - Notation for transverse section at any distance x along the drum

at that point as follows.

$$h = R_d(1 - \cos\theta_x) \qquad (2.12)$$

The filling angle is in turn related to the fractional filling fc of the drum cross section at x.

$$fc = (1/\pi)(\theta_x - (\sin 2\theta_x)/2) \qquad \theta_x \leq \pi/2 \qquad (2.13)$$

and the cumulative filling in the drum is found by integrating the point fillings of (2.13) over the drum length as follows

$$FC = (1/L) \int_0^L fc(x)\, dx \qquad (2.14)$$

The cumulative filling can now be used with the drum volume and material bulk density to calculate the hold-up in the drum, which when combined with the flow rate through the drum allows the mean residence time to be determined. Vahl and Kingma use a simplified form of (2.13) in terms of h and produce the following expression for mean residence time.

$$t = 0.91\left(\frac{L}{D}\right)^2\left(\frac{D}{h_i}\right)^{0.6} \frac{\tan\alpha_d}{N} \qquad (2.15)$$

This is now rather unsatisfactory in that the solution is essentially empirical and requires that the bed height at inlet be known.

The solution for the inclined drum case presented by Kramers and Krookewit is more complex. Prior to integration the expression containing b in (2.10) is linearised. The two variables of the equation, h and x, are made dimensionless and the solution expressed in terms of the resulting groups. Here again a simplified version of (2.13) is used to obtain values of the overall filling FC. The results are expressed in the following form

$$FC.N_q = f(N_q N_L) \qquad (2.16)$$

for different values of the dimensionless parameter $h_o/(R_d N_q)$. In which h_o the bed height at the outlet of the drum, considered to be equal to the height of the discharge lip. N_q and N_L are dimensionless numbers defined as:

$$N_q = \frac{q.\sin\alpha_d}{wR_d^3\tan\varphi} \qquad (2.17)$$

a modified version of the ratio earlier identified by Gilbert, and

$$N_L = \frac{R_d\cos\alpha_d}{L\tan\varphi} \qquad (2.18)$$

Kramers and Krookewit also carried out experiments and compared their theoretical solution with the results of these and with the data of Sullivan et al. There is a systematic discrepancy which causes the calculated value of FC to be too low for low drum fillings and too high for higher drum fillings, agreement is best for $0.05 \leqslant FC \leqslant 0.1$. "Deviations of greater than 30% seldom occur" however, and the mean square deviation is around 15%. Also noted are the asymptotes of the solution one of which shows that for long drums with low feedrates and large slope no increase in bed height is required to achieve transport and the other defines the case in which axial surface slope is mainly responsible for transport.

Further development of the analytical model for solids transport did not occur until 1974. Between 1952 and 1974 much of the literature on rotating drums was concerned with qualitative investigations on operating plant especially using the technique of radioactive tracers. The results of this type of investigation are of interest but little direct use in model building. Work of this kind will be discussed in Section 2.3. Another topic of interest during this period was overall simulation of rotary kiln or reactor plant. This was primarily concerned with heat and mass transfer and in some instances reaction kinetics throughout the drum. The models of solid motion used in these simulations were invariably extremely simple and are discussed in Section 2.4.

In 1961 Varentsov and Yufa [V4] attempted to describe the transport of solids in an industrial kiln (with air flow) using dimensional analysis. One of the fundamental groups derived

however, a Reynolds number for the gas in the kiln, based on the solid particle diameter, is not dimensionless as the wrong units for viscosity have been used. This, coupled with the fact that the final expression includes an empirical constant to account for kiln diameter effects somewhat limits its usefulness. Another investigation using the technique of dimensional analysis was presented by Zablotny (1965) [Z1]. This considered the more familiar case of a uniform bulk solid's motion in the absence of any influences other than the drum rotation. The fractional filling and axial rate of advance were considered to be independent of each other. The analysis was carried out for these two variables separately and five groups in all were developed, one of which was that previously noted by Gilbert [G1]. Length was not considered to be a variable which influenced overall filling thus the equations developed apply only to drums with uniform filling over their entire length. The groups were correlated for a series of experiments at low rotational speed and low fillings in which uniform filling would largely prevail. Further dimensional analysis is contained in the work of Vogel (1965) [V5, V6]. The groups determined here match those of Zablotny and further introduce a dependence on drum length and are therefore no longer limited to uniformly filled drums. No general correlation was presented however and most of Vogel's work was concerned with analysing the motion, characteristic of very low drum fillings, in which there is no turnover of the bed. One such motion, oscillatory "slumping", has been discussed previously. Vogel also considered the motion which can occur at higher rotational speeds in which the bed surface is stationary with some angle of repose α less than the static angle and the particles progress through the drum by a "jostling" of each other. The use of dimensionless groups is considered further in Chapter 5 in which theory and experiment from this investigation are compared.

In 1972 Jinescu and Jinescu [J1] attempted to derive an expression for the mean residence time in a uniformly filled inclined drum. The same basic approach as Pickering et al [P1] was adopted but the expression for the axial advance of the particle per cascade is fundamentally wrong and gives quite the wrong dependence on angle of repose.

Another model for uniformly filled inclined drums which contains the same error was presented in the same year by Rykvin, Telyatnikov and Broginskii [R1]. The mechanism of motion in this case is slightly different in that the continuous collapse of a wedge of material lifted past its static angle of repose is considered. The time associated with any axial advance is also incorrectly defined thus invalidating the further development and resulting equations of Rykvin et al's model. The final expression also includes an empirical factor to account for physical properties.

Abouzeid (1973) [A1] carried out an experimental investigation into the behaviour of material in both open ended and constricted discharge drums. The use of dimensionless parameters for scale-up is considered as is the axial dispersion in rotating drum systems and its effect on residence time distributions. The latter topics are considered in Section 2.3. The work was not reported in the open literature until much later (1980) [A4, A5].

Cross (1974) [C2] considers the motion of pellets in a rotary kiln in which the filling was uniform over the entire length of the drum. The drum filling appears explicitly in his derived expression for volumetric flow rate making the equations of little use for filling prediction. There appears to be reasonable agreement between theory and experiment over a limited range of drum speeds but very little information of the experimental set up is given. A criterion for the transition between surging and cascading motion was presented based on a consideration of the balance between the torque acting on the bed due to the drum wall and that due to gravity.

Shoji (1974) [S4] and Hogg, Soji and Austin (1974) [H1] examine the axial transport of dry powders through horizontal cylinders. In this instance however the equation for the axial advance of the particle is correctly expressed as the distance moved parallel to the drum axis and not that travelled in the surface of the bed, (these will only be equal for inclined drums with uniform filling).

When this distance is combined with the time taken to complete a cycle in order to compute the axial velocity, the cycle time is no longer assumed equal to that spent locked in the bed but instead is considered proportional to it and a constant of proportionality, B, is introduced. The velocity equation of a particle with path radius r is next combined with the incremental area of the path as before and integrated across the drum cross section to give the following expression

$$q = (2/3)BR_d^3 w \sin^3\theta_x \tan\phi \cos\beta \qquad (2.19)$$

B is defined as the time spent locked in the bed divided by the total cycle time (-), w is the angular velocity of the drum (rad/s) and ϕ is the angle at which a particle rolls down the bed surface (see figure 2.2) Hogg et al present (2.19) in terms of a mass feed rate F with the bulk density of the material appearing explicitly on the right hand side of their equation. In order to maintain continuity of notation and ease comparison with previous and future work in which volumetric flow rate through the drum has been used, the mass flow rate and bulk density have been combined in this and all subsequent work in which they appear explicitly. The derivation of (2.19) is given by Hogg et al and repeated in Appendix 2. Equation 2.19 corresponds with equation 2.9, the expression

$$(R_d^2 - b^2)^{3/2}$$

has been replaced by the equivalent

$$R_d^3 \sin^3\theta_x$$

noting that

$$\cos\theta_x = b/R_d$$

It should also be noted that any dependence on angle of repose or drum slope is still contained in $\tan\phi$ as is any further dependence on the angle β . The term $\cos\beta$ appears explicitly at this stage since this is what relates distance travelled in the surface of the bed to equivalent distance along the drum axis.

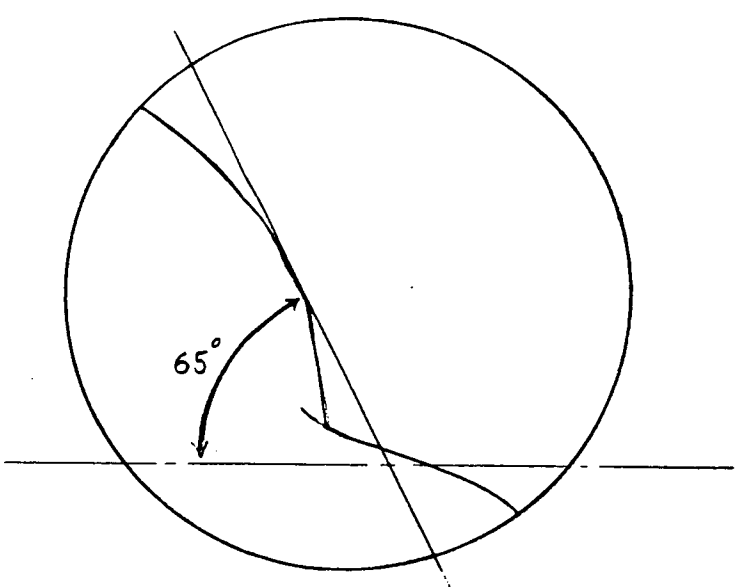

Figure 2.4: Effective dynamic angle of repose of 35x60 mesh silicon in an 8 inch cylinder, rotated at 67% of the critical speed from Shoji [S4]

The functional form of $\tan\phi$ is found by considering the line of steepest descent of a particle on the bed surface. This procedure is illustrated in Appendix 3 for the general case of an inclined drum with axial surface slope. The expression is also derived in a later paper by Austin, Shoji, Hogg, Carlson and Flemmer [A3] upon consideration of a force balance on a particle in the bed surface, perhaps not as intuitively obvious as maximising an angle of descent. Hogg et al present the form of $\tan\phi$ for a horizontal drum, a logical reduction of the expression derived in Appendix 3 and in [A3], as being simply based on the geometry of the system

$$\tan\phi = \cot\alpha_d \sin\beta \qquad (2.20)$$

Which when substituted into equation 2.19 gives

$$q = (2/3)BR_d^3 w \sin^3\theta_x \cot\alpha_d \cos\beta \sin\beta \qquad (2.21)$$

Here again however as with Saeman and Vahl and Kingma the assumption that β is small is introduced and the approximations $\sin\beta \simeq \tan\beta$ and $\cos\beta \simeq 1$ are made. The discharge end is considered as x=0 so that $\tan\beta = -db/dx$, this is coupled with the fact that $b=R_d\cos\theta_x$ to give

$$\frac{db}{dx} = -R_d \sin\theta_x \frac{d\theta_x}{dx} \qquad (2.22)$$

Substitution of the above into equation 2.21 gives

$$\frac{d\theta_x}{dx} = \frac{3q}{2B\cot\alpha_d w R_d^4 \sin^4\theta_x} \qquad (2.23)$$

a relationship now between filling angle and axial position. Noting that $\cos\theta_x = b/R_d$ this compares with (2.10) (with ψ =0). Equation 2.23 is solved by Hogg et al again using the incorrect boundary condition θ_x=0 at x=0. The solution function for θ_x is modified to approximate the fractional filling (2.13) and the following form of the solution of (2.23) results

$$fc = 0.875 \left[\frac{qx}{B\cot\alpha_d w R_d^4}\right]^{0.64} \qquad (2.24)$$

Due to the limits of the mathematical approximations employed this applies for $0.04 \leq fc \leq 0.4$. This expression is then integrated according to (2.13) to give the following equation for the cumulative filling.

$$FC = 0.534 \left[\frac{q}{B\cot \alpha_d w R_d^4}\right]^{0.64} \qquad (2.25)$$

Experiments were carried out on a small rotating drum (Tables 2.1 and 2.2) rotating at the relatively high speed of $67w_c$ where w_c is the critical speed of the drum defined as

$$w_c \equiv \sqrt{(g/R_d)} \qquad (\text{rad/s})$$

Where g is the acceleration due to gravity. The critical speed is the speed at which, assuming no slip between the particles and the drum wall, centrifuging of the particles can occur whereby they adhere to the drum wall at all points. The expression for w_c simply represents equality between the gravitational acceleration g and the centrifugal acceleration w^2R_d which will allow particles to be carried past the highest point in the drum's rotation. Such high rates of rotation were used because Shoji was primarily concerned with the operation of ball mills which have characteristic operating speeds of $0.55\text{-}0.85w_c$ [R3]. Rotary Kilns, calciners and reactors are generally operated in the range $0.04\text{-}0.2w_c$. The experiments of Hogg et al were used to determine the value of the constant B as 0.51. In order to obtain this value however, the static angle of repose α_s was used in (2.24) and (2.25) in place of α_d. In their diagram and in the derivation of their equations however Hogg et al clearly show that α (they do not differentiate between static and dynamic angles of repose in notation) was considered as the dynamic angle of repose. An explanation for this discrepancy may be found by examining the diagram of the bed cross section profile for these experiments contained in Shoji's thesis and reproduced in Figure 2.4. Here it can be seen that the assumption of a linear transverse bed profile inherent in the derivation of (2.19) is violated. If the suggested effective dynamic angle of repose of 65° is used in the expressions developed by Hogg (this would seem entirely logical from the presentation of the work) a value for B of 1.41 is needed to fit the data. This cannot be since B is defined as the ratio of the time a particle spends locked in the bed to the total cycle time, (that spent cascading on the surface plus that spent locked in the bed). Clearly the physical model described by Hogg et al does not hold for high rotational speed, and/or non-linear transverse profiles but it has been made to fit by wrongly using the static angle of repose in place of the dynamic.

Comparison of theory and experiment showed that the agreement was worst for high feed rates and short drums or for short distances along a drum if cumulative filling with distance was compared. These are conditions for which the assumption that β is small is not obeyed (bed collapse) and the underprediction of FC associated with the assumption of $\theta_x=0$ at x=0 has maximum effect.

The error in assuming $\theta_x=0$ at the discharge end is addressed later in the same year by Austin and Flemmer [A2]. Austin was one of the contributors to Hogg et al [HI]. Throughout the paper however the error is referred to as being that of Vahl and Kingma's. Austin and Flemmer note that for a constant volumetric flowrate, as the filling considered becomes lower and lower the value of β must be increased to maintain a constant flowrate and in the limit of zero fractional filling is therefore inconsistent with the basis on which the model is derived, which requires that there be a finite bed surface in order to pass material. The limit in filling to which the model can be applied may be determined if the approximation of:-

$$\sin\beta\cos\beta=\tan\beta$$

is replaced with the identity $\tan\beta/(1+\tan^2\beta)$ (2.26) and this is substituted into (2.21) yielding.

$$q=K\sin^3\theta_x\tan\beta/(1+\tan^2\beta) \qquad (2.27)$$

where

$$K=(2/3)BwR_d^3\cot\alpha_d$$

(Austin and Flemmer erroneously omit B from this expression when referring to the work of Hogg et al). From this it can be seen that the minimum filling, corresponding to a minimum in $\sin\theta_x$ will occur for maximum $\tan\beta/(1+\tan^2\beta)$ which is for $\tan\beta=0.5$ or $\beta=45°$. The minimum filling for which the model applies can now be found from:-

$$\sin^3\theta_x=2.5q/K \qquad (2.28)$$

(Austin and Flemmer wrongly put 2 instead of 2.5 here). Equation 2.28 defines the lower bound for the integration of the equation for $d\theta/dx$. The latter is now more complex than (2.23) as

substituting the full expression for $\sin\beta\cos\beta$ in (2.21) requires that it be rearranged as a quadratic in $\tan\beta$ and the roots extracted before the introduction of $\tan\beta = R_d \sin\theta_x d\theta_x/dx$ be made. The result is shown below.

$$\frac{d\theta_x}{dx} = \frac{1}{R_d \sin\theta_x}\left[\left(\frac{K\sin^3\theta_x}{2q}\right) - \sqrt{\left(\frac{K\sin^3\theta_x}{2q}\right)^2 - 1}\right] \qquad (2.29)$$

This does not readily lend itself to the simplified solution techniques which result in (2.24) and (2.25). The solution is instead obtained by numerical integration and Austin and Flemmer compare results with those of (2.24) and (2.25). The deviation between the original model and the modified version was shown to be greatest for large dimensionless flowrate (q/K), precisely the conditions under which Hogg et al's solutions deviate most from experiment. One example was given by Austin and Flemmer to show the improved agreement between theory and experiment which resulted from using (2.29) rather than (2.23). The value of K for this example is that determined previously by Hogg et al.

Austin and Flemmer found that the assumption that minimum filling occurred exactly at the discharge end lead to overprediction of the cumulative filling FC. They therefore moved this lower bound for integration inside the drum a distance Δx (see Figure 2.3) and assumed that from this point the bed collapsed to the end of the drum at an angle of repose of 45°. This forms an isosceles triangle in which $\Delta x = h_m$ where h_m is the height associated with the minimum fractional filling and is determined using the filling angle found from (2.28) combined with (2.12) (Austin and Flemmer present an approximate relationship between fractional filling and h).

This effort to correct overprediction of FC was dispensed with when the case of inclined drums was considered in a paper by Austin, Shoji, Hogg, Carlson and Flemmer [A3] (1978). Here again the equation developed by Shoji and presented in Hogg et al (2.19) was used as the starting point. $\tan\phi$ must now be determined for the inclined drum case. The derivation of the expression for $\tan\phi$ has been discussed previously and is presented in Appendix 3, it is also given by Austin et al based on different considerations. The result is as follows:

$$\tan\phi = (\cos\alpha_d \sin\beta + \tan\psi\cos\beta)/\sin\alpha_d \qquad (2.30)$$

Which reduces to equation (2.20) for horizontal drums (ψ =0). Following the procedure previously described for horizontal drums this is substituted into (2.19) to give

$$q = K\sin^3\theta_x \cos\beta \sin\beta \,(1 + C/\tan\beta) \qquad (2.31)$$

Where: $C \equiv \tan\psi/\cos\alpha_d$. Once again the identity (2.26) is introduced giving

$$q = K\sin^3\theta_x \left(\frac{\tan\beta}{1 + \tan^2\beta}\right)\left(1+ \frac{C}{\tan\beta}\right) \qquad (2.32)$$

Which when rearranged as a quadratic in $\tan\beta$ gives

$$\tan\beta = \left(\frac{K\sin^3\theta_x}{q}\right) \pm \sqrt{\left(\frac{K\sin^3\theta_x}{q}\right)^2 - \left(1 - \frac{CK\sin^3\theta_x}{q}\right)} \qquad (2.33)$$

Where the negative sign is applicable. As before $\tan\beta$ is replaced by $R_d\sin\theta_x d\theta_x/dx$ to obtain

$$\frac{d\theta_x}{dx} = \frac{1}{(R_d \sin\theta_x)}\left[\left(\frac{K\sin^3\theta_x}{q}\right) \pm \sqrt{\left(\frac{K\sin^3\theta_x}{q}\right)^2 - \left(1- \frac{CK\sin^3\theta_x}{q}\right)}\right] \qquad (2.34)$$

the relationship for filling angle versus distance for an inclined drum, which reduces to the horizontal equivalent (2.29) for C=0. There are two things to note about this solution.

(i) The minimum filling now determined for maximum $(\tan\beta/(1+\tan^2\beta))(1+C/\tan\beta)$ in (2.32) is the lower bound for integration and is assumed to apply from the discharge end exactly.

(ii) It can be seen that $d\theta_x/dx$ equals zero for values of $\sin^3\theta_x$ equal to q/CK. This determines the filling angle for which transport may be achieved in inclined cylinders with no increase in bed height.

This relationship between θ_x and x is linked to the corresponding fractional filling variation with x and then the cumulative filling by (2.13) and (2.14) as before.

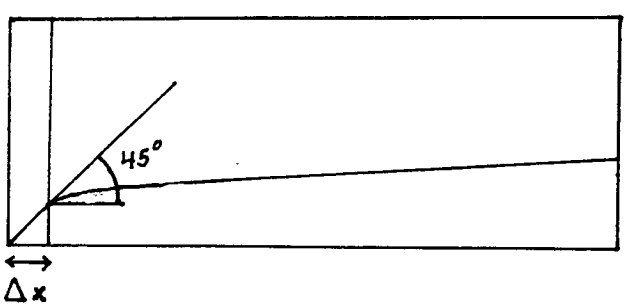

Fig 2.5 Proposed model of transfer of powder along cylinder applies over x: Δx is region where powder collapses through end of cylinder.

The comparison between theory and experiments (carried out for relatively low fractional fillings) was found to be very good. Details of the experiments used to compare theory and experiment are not given, but it is obvious from the figures presented that they are the inclined drum experiments from Shoji's thesis [S4]. Indeed the value of K used to solve (2.34) is that determined for the horizontal drum case earlier by Hogg et al [H4]. As was previously discussed the static angle of repose has been used in place of the dynamic in calculating K. Austin et al however use the effective dynamic angle of repose of 65° to calculate C! This use of two different angles represented by one symbol in (2.34) cannot be detected without recourse to the paper of Hogg et al. The reader is instead led to believe that one angle, the dynamic angle of repose α_d has been used throughout.

2.2 The Constricted Drum

Early work on the transport of solids through open ended inclined drums was concerned with drums in which the transport could be effected with no change in bed height (limiting filling attained a short distance in from the discharge). This was also the case when constricted drums were first considered. The profiles which may exist in a constricted discharge drum operating with limiting filling are shown in figure 2.6.

Equation 2.34 illustrates the stage to which the model for solids transport in a rotating drum had been developed when this investigation was started in October 1981. Other papers relevant to the subject appeared and are discussed below but none developed further the fundamental mathematical description of the solids motion.

Fritts (1976) [F2] reports an empirical expression for Portland cement kilns quite similar in form to that of Gibbs (1942) equation (2.6). Empirical correlations and limited theoretical derivations which were produced in this period in the eastern european countries have not been detailed since they are at best as limited as the equation of Sullivan et al. A summary of the equations is given by Akerman (1973) [A7] and some are reported in Vogel (1965) [V5] who examined their limitations in more detail. One such published in English is given by Sribner (1979) [S5]. The equations for mean residence time and related quantities such as volumetric flow rate require that the fractional filling be known before they can be used.

For nonuniform bed depth the slope of the bed surface with respect to the drum axis is required, this is assumed equal to the static angle of repose at the discharge end, further variation is then found by "sequential approximation" for which no general solution or example is given.

Sullivan et al [S1] produced a group of correction factors which could be used to multiply their basic open ended drum equation for mean residence time (equation 2.1). The form of the correction factor was empirically determined and depends on whether the uniform filling bed height is greater than, equal to, or less than the height of the weir (curves a, b and c respectively in figure 2.6). The equations are thus of no use for residence time prediction where the bed profile is unknown. They are limited also in being "tied" to the open ended drum equation which is only applicable to drums with relatively small feed rates.

Bayard [B1] also produced a correction factor for multiplying on to his equation for open ended drums. As for the original equation the correction factor is based on a "geometrical derivation" but again this is not presented and the derivation is not obvious. His equation also requires that the bed profile be known in advance. A further extremely limited empirical expression is presented by Mukherjee and Ghosh (1977) [M3]. They derive an expression for a kiln with a constriction located at a fixed distance in from the discharge end which is only useful for drums of similar dimensions and inclinations.

Moving on from expressions which consider uniform filling alone, Saeman suggests setting bed height equal to the height of the constriction in order to define a boundary condition for the integration of (2.10). The error associated with this will obviously increase with increasing feed rate which requires a greater bed depth over the constriction to transport it. He also suggests that this approach is suitable for bed profiles such as c in figure 2.6. In this case he suggests integrating from the constriction height down to the uniform filling height whose value may be found by setting $db/dx = 0$ in (2.10). It seems unlikely that an equation derived on the basis of axial advance along an inclined surface should apply when the motion is effectively in a direction opposite to the bed gradient. This is the situation which arises when a constriction forces the bed to build up behind it. Further

use of (2.10) for situations in which dh/dx is negative (x = 0 at the discharge end) was made by Kramers and Krookewit. It is perhaps noteworthy that of the results for constricted inclined drums which they report only 4 of the 28 sets of data are for drums whose constriction height is greater than the bed height required for uniform filling and these represent four of the highest deviations between experiment and theory in their data. Alternative solution techniques are discussed in Chapter 3. Saeman and Kramers and Krookewit are the only authors to have considered the solution of the equation derived from a theoretical model of solids motion for the case of an inclined constricted drum. All published work from this point on is concerned with horizontal constricted discharge drums.

The possibility of the discharge lip height being greater than bed height further back up the drum, brought about by the ability of inclined drums to sustain uniform filling, cannot occur in horizontal drums. Here the discharge end constriction is truly a lower boundary condition form which the integration of the equation for the variation of filling along the drum length must commence. Hogg et al [H1] solve their equation (2.23) with the boundary condition $\theta_x = \theta_x(0)$ for constricted drums in addition to the (incorrect) boundary $\theta_x=0$ for open ended drums. $\theta_x(0)$ is the filling angle corresponding to the filling fc(0) at the constricted discharge. Once $\theta_x(0)$ is determined the solution technique is analagous to that previously discussed for the open ended drum case and Hogg et al presented the following equation for overall filling in a horizontal drum with constricted discharge opening.

$$FC = \frac{0.751\ B\ Cot\alpha_d w R_d^4 fc(0)^{2.56}}{qL}\left[\left(1 + \frac{0.812qL}{BCot\alpha_d w R_d^4 fc(0)^{1.56}}\right)^{1.64} - 1\right] \qquad (2.35)$$

Their equation has been rearranged in the above form to facilitate comparison with later workers who use this form.

The problem of defining the filling at a constricted discharge other than by assuming the bed height equals the constriciton height was first addressed by Hogg et al. Their answer was to develop the following empirical correlation between discharge end filling, feed rate and discharge opening

$$fc(0) = [1 + (F/K_1)^{1/m}]\ \ fc_{\ min} \qquad (2.36)$$

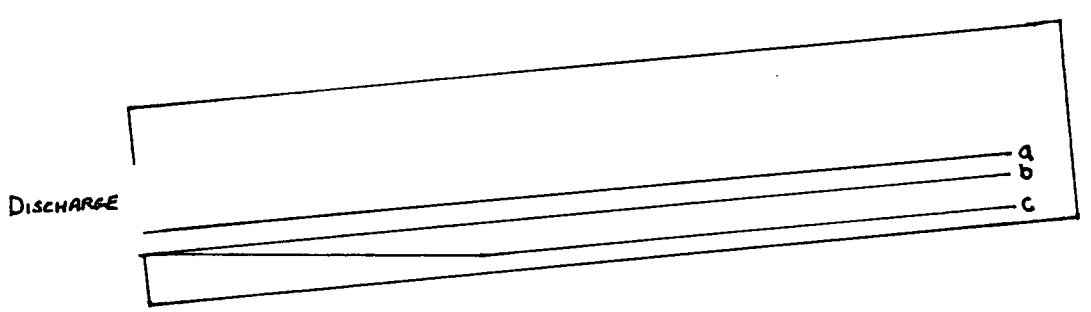

Figure 2.6 - Bed profiles for uniform filling in a constricted drum

a) bed height > constriction height
b) bed height = constriction height
c) bed height < constriction height

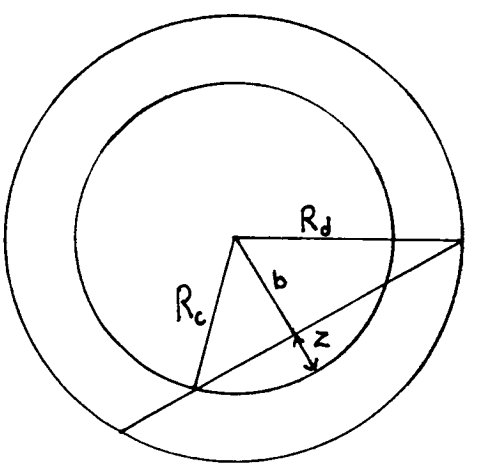

Figure 2.7 - Schematic diagram of discharge end of constricted drum

Where K_1 and m are empirically determined constants and fc_{min} is the filling corresponding to a bed height which is the same as the constriction depth (found using (2.12) and (2.13) with h = constriction height). The constants K_1, m and B in (2.35) and (2.36) were fitted using the data of Shoji [S4], and the static angle of repose was used in place of the dynamic in order that B might have a value consistent with its definition. Discussion of this illogical procedure has been presented when the work of Hogg et al for open ended drums was considered.

All other published work on the prediction of filling in constricted discharge drums has also considered only horizontal drums and has used (2.35) to calculate overall filling in the drum. As discussed below however the value of B has been fitted by each author using their own data. Empirical correlations different from (2.36) were also developed to determine the discharge end filling. Karra and Fuerstenau [K2] (1978) studied the hold up in horizontal drums with a grate-discharge. Though this type of constriction, an end plate with a pattern of holes or slots in it, is quite different from the annular weir presently under consideration, the form of the equations developed by Karra and Fuerstenau was later used by workers concerned with weir type end constrictions. Unlike Hogg et al, Karra and Fuerstenau carried out their investigations over a range of drum speeds from 10% to 75% w_c. They did not find a constant value for B in (2.35) but instead calculated it using the following expression

$$B \cot \alpha_d = -K_1 (w/w_c) + K_2 \qquad (2.37)$$

Where K_1 and K_2 are empirically determined constants. Karra and Fuerstenau did not constrain B to be less than or equal to unity and used an unsubscripted α, considered simply an "angle of repose" for α_d (α_d is clearly the correct angle as can be seen in the derivation of Hogg et al - thus it has been subscripted here). Karra and Fuerstenau also used the static angle of repose to calculate values of B though they need not have specified any angle but simply considered B $\cot \alpha_d$ as a single parameter.

It can be seen then that in order to fit experimental data, Karra and Fuerstenau, Hogg et al and Austin et al have all had to violate fundamental relationships contained in the model on which the derivation of (2.34) and (2.35) are based. They use these

equations therefore essentially as dimensionless correlations with empirically determined coefficients in which the dimensionless groups have been suggested on the basis of a model, rather than as the solution of a model with certain empirically determined parameters. It is believed this has arisen through using the model for situations in which it does not hold, viz high rotational speeds in the case of Hogg et al and Austin et al and a combination of high speed and probably the effect of a grate discharge in the case of Karra and Fuerstenau.

Karra and Fuerstenau found they could correlate the discharge end filling fc(0) with the following expression

$$fc(0) = K_3\left(\frac{q}{w_c D^3}\right)^{K_4} \qquad (2.38)$$

Where K_3 and K_4 are empirically fitted constants. This expression takes no account of discharge plate geometry and Karra and Fuerstenau only used one configuration in their investigation. The discharge end filling, used as a fitted parameter in Hogg et al's model by Karra and Fuerstenau is shown to be greater than the cumulative filling over much of the drum. This emphasises the fact that although the discharge end filling and the constant 'B' retain their terminology - the values fitted to them do not have any physical significance.

Equation (2.35) was also used to predict the filling in a horizontal constricted discharge drum by Abouzeid and Fuerstenau (1980) [A4]. They presented the equation in the following form

$$FC = \frac{fc(0)^{2.56}\ Aw^*D}{21.31\ F^*L}\left[\left(1 + \frac{12.99\ F^*L}{fc(0)^{1.56}\ Aw^*D}\right)^{1.64} - 1\right] \qquad (2.39)$$

Where the terms A, w* and F* are defined as follows

$$F^* \equiv q/w_c D^3 \qquad (2.40)$$

This is the group in brackets on the right hand side of (2.38) used by Karra and Fuerstenau.

$$w^* \equiv w/w_c \qquad (2.41)$$

(w* is wrongly defined in words in the paper as simply the drum speed in rpm) and

$$A = B\cot\alpha_d \qquad (2.42)$$

Abouzeid and Fuerstenau [A4] use the same expression as Karra and Fuerstenau to determine B (equation 2.37) which, using their notation is

$$A = -K_1 w^* + K_2 \qquad (2.43)$$

They also use (2.38) to determine discharge end filling, but in two stages. The right hand side of (2.38) is not used to determine the filling directly but to find the filling over the weir as follows

$$K_3(F^*)^{K4} = \frac{1}{\pi}\left[\cos^{-1}\left(\frac{R_c-Z}{R_c}\right)-\left(\frac{R_c-Z}{R_c}\right)\sqrt{1-\left(\frac{R_c-Z}{R_c}\right)^2}\right] \qquad (2.44)$$

Where Z is the bed height above the weir as shown in Figure 2.7. The right hand side of (2.44) defines the filling over the weir. Once Z has been determined the filling at the discharge end is found as follows

$$fc(0) = \frac{1}{\pi}\left[\cos^{-1}\left(\frac{R_c-Z}{R_d}\right)-\left(\frac{R_c-Z}{R_d}\right)\sqrt{1-\left(\frac{R_c-Z}{R_d}\right)^2}\right] \qquad (2.45)$$

The constants K_1-K_4 used in (2.43) and (2.44) are evaluated for a small scale drum of fixed discharge constriction radius operated over speeds between 6 and 75% of the critical speed. The values of K_1 and K_2 thus determined are such that B is greater than one for all common values of α_d in (2.43). It is noteworthy that no expression used to determine discharge end filling (equations 2.36, 2.28, 2.44 and 45) has had any dependency on drum speed. It should also be noted that the fractional fillings reported in [A4] and presented as percentages on the ordinates of their graphs are not the fraction of the total drum volume occupied by the solid bed. They are instead the filled fraction of the drum volume which remains if the volume of a "core cyclinder" whose radius is equal to that of the discharge constriction is considered removed from the total drum volume. No mention of this is made in the text of the paper.

A subsequent paper by Abouzeid and Fuerstenau (1980) [A5] presents exactly the same equations as in [A4] but modifies some of the definitions. This can only be detected by detailed comparison of both papers. The latter paper replaces the group F*L/w*D in (2.39) with one symbol Ψ where Ψ is defined as

$$\Psi = qL/BwD^4 \qquad (2.46)$$

This is not consistent with the expansion of the group according to the definition in [A4] and requires that the value of A in [A5] be simply $\mathrm{Cot}\,\alpha_d$. Another paper by Abouzeid, Fuerstenau and Sastry [A10] (1980) also shows that B in (2.46) has been considered equal to $\pi\,\mathrm{Cot}\,\alpha_d$ though no mention was made of this at the time.

The expression in (2.46) is shown to be useful for comparing the holdup in drums of various dimension which are operated at the same fraction of their critical speed and which have the same ratio of discharge constriction radius to drum radius. Equation (2.39) with variables determined by (2.43), (2.44) and (2.45) (with definition presumably according to [A5]) is shown to underpredict filling in general, the deviation increasing with increasing L/D of the drum [A5]. Equations (2.35) and (2.39) with the various attendant empirical expressions for discharge end filling which have just been discussed represented the most up to date expressions for the prediction of filling in (horizontal) constricted drums at the time of this investigation.

2.3 Tracer and Residence time distribution studies

Between 1952 and the early 1970's much of the literature on the motion of solids in rotating drums was concerned with the use of radioactive tracer methods in full scale industrial equipment. First reported was an account of a test made with "sticky and non granular" finely chopped seaweed in a rotary drier carried out by Gardner, Mitchell and Scott (1952) [G5]. A quantity of seaweed which had absorbed radioactive orthophosphoric acid was introduced into the feed to the drum at time t_o and the discharge thereafter sampled at discrete time intervals until the radioactive material was all or almost all discharged. A plot of discharge concentration versus time gave a now familiar age distribution curve from which Gardner et al only wished to extract the modal residence time. Similar limited use of

residence time distribution (RTD) information was previously made by Pickering et al who used dyed bulk solid particles and Van Krevelen and Hoftjizer who simply introduced a fixed mass of material to an empty drum.

Radioactive tracer techniques serve to illustrate the complexity of material motion in industrial processes. This is highlighted in a paper by Rutle (1955) [R2] concerned with movement of material in long wet process rotary cement kilns (lengths of 80-115m, L/D $\sim$34 and residence times of the order of 5 hours). Here again the technique of irradiating a portion of feed is employed and RTD curves obtained in a manner similar to that described above. Since the tracer was added over an extended period of time the curves are only used to get a qualitative idea of the extent of mixing in a kiln. In addition however the rate of advance of the material along the kiln was measured by placing detectors along its length and following the "activity peaks" of an added portion of radioactive feed. It was observed that the material had different rates of advance in different sections of the kiln. This is attributed to the change in physical properties of the charge as it moves from the environment of a nodulising zone to burning and calcination zones. The effect of CO_2 driven off in the calcination zone is also noted as this had a fluidising effect on the charge producing a rapid advance due to the combined effects of "airslide" and drum slope.

Boguslavskii (1956) [B2] combines empirical expressions for the variation in bulk density and angle of repose along the drum with the expression developed by Saeman (equation 2.10) in an effort to improve the prediction of the bed profile in certain horizontal kilns for the calcination of sodium bicarbonate. Unfortunately no measure of the degree of success is given. Jinescu and Jinescu also considered accounting for varying physical properties with length by splitting the drum into sections of known properties and applying their equation, discussed in Section 2.1, to each of these in turn.

Many investigations of similar type and scope to that of Rutle were carried out, for example [A6, G6, H2, Z2] and many papers were concerned with the details of tracer techniques and correct analysis and interpretation of the results of such investigation [C1, L1, O1]. The inevestigation of Shevstov et al [S6] (1971) used a refractory brick "capsule" to contain the radioactive source. This was significantly larger than the bulk solid material thus their results are only of qualitative significance since the rates of advance for the capsule and bulk solid will be different though they were claimed to be "roughly the same".

In all of the above tracer investigations rarely is sufficient data given to allow the RTD results to be used to compare with a theoretical model for RTD. Such models as have been developed shall now be considered, the discussion being kept general as no development of RTD work was carried out in the present investigation.

The axial dispersion of solid particles in a rotating drum was first considered by Fan and Ahn (1961) [F3]. They believed that mixing in the radial direction was extremely rapid and that longitudinal dispersion could be represented by the one dimensional diffusion model. The unsteady state material balance for tracer was expressed as follows

$$\frac{dC_t}{dt} = D \frac{d^2C_t}{dx^2} \qquad (2.47)$$

Where D is the longitudinal dispersion coefficient m^2/S, C_t is the concentration of tracer (kgm^{-3}) and t the time from its introduction to the system. The solution of this equation for an impulse response is presented and the parameters fitted to the data of Miskell and Marshall [M4] who performed impulse input RTD experiments on a flighted drum. A correlation between the Peclet Number

$$Pe = \frac{D}{UL} \qquad (2.48)$$

Where U is the flow velocity (m/s) found by dividing volumetric flowrate by the drum area, and the dimensionless feed rate

$$\frac{q}{N\psi D^3}$$

is presented. The Peclet number is found from the variance of the RTD curve. Approximations are presented for low values of Peclet or variance such as were encountered in the data of Miskell and Marshall. Rutgers (1965) [R3] also uses the one dimensional diffusion model but refers to the quantity defined by (2.48) as the Bodenstein Number. He carried out extensive experiments for drums with different inlet and outlet configurations and various operating conditions. The effect of the various conditions on longitudinal dispersion, as measured by the Bodenstein number calculated from tracer response curves, is discussed in general terms.

No general correlation was presented. The mathematical relationship between the form of the tracer response curve, its variance and the Bodenstein Number calculated on the assumption of a log-normal distribution of tracer as opposed to the diffusion model is considered by Ivanets, Moiseenko and Lukyanov [I1] (1969).

Austin Luckie and Atey [A8] (1971) consider RTD in cement mills and present the mathematics for analysing impulse response curves which must be corrected for recycle streams. Merz and Molerus [M5] (1972) also consider RTD in ball mills with high rates of rotation ($>0.5w_c$), up to 60% drum filling and a grate discharge. A fuller review of the workers who have considered RTD in ball mills, drum mixers, flighted drums and "plain" drums and the models they have used to describe the RTD is presented by Abouzeid, Mika, Sastry and Fuerstenau [A9] (1974). They carried out experiments on small scale drums to determine the effect of operating variables on the mean and variance of the RTD for a constricted discharge drum. The results are analysed in terms of the axially dispersed plug flow model and the applicability of this model for non segregating particulate material transport is established.

A similar analysis is carried out by Karra and Fuerstenau (1977) [K3] on the same apparatus used by Abouzeid et al. This time the effect of discharge plate geometry is studied in isolation.

Hehl, Kroger, Helmrich and Schugerl [H3] (1978) investigated RTD in a laboratory scale horizontal rotary drum with an end constriction using fine sodium carbonate as bulk material. All previous investigations have used more granular substances. The effects of rotational speed and feed rate were studied and the mean residence times measured were found to compare well with those predicted by a modified version of Vahl and Kingma's solution at low feed rates. Deviations occurred however at higher feed rates. Rogers and Gardner (1979) [R4] also considered horizontal drums and the physical model of Vahl and Saeman but this they used as a base on which to superimpose a Monte Carlo simulated degree of dispersion. Empirical data on the dispersion of particles in a batch system is required to provide a distribution curve for the angle at which a particle tumbles down the surface.

Abouzeid, Feurstenau and Sastry [A10] (1980) investigated the scale-up of RTD using the axial dispersion model. Here again a good review of the published literature on RTD is given. A dimensionless mean residence time is derived by dividing the

fractional hold up in the drum (expressed as the volume of material hold-up divided by the drum volume) by the dimensionless feed rate expression (2.46) which is found in the solution to the mass transport equation of Hogg et al. The dimensionless mean residence time derived can be related to a dimensionless variance of the RTD curve using the axial dispersion model. This was done and data were correlated for one set of drum dimensions and used to predict the variance for other sizes with dimensions of similar order of magnitude but differing L/D ratio.

The work of Mu and Perlmutter (1980) [M1, M2] was concerned with the development of a wholly new model to describe solids mixing and material transport in a rotating drum. The model is based on a description of the solid bed in terms of model blocks linked by transfer functions (eg plug flow section and cascade region with by pass and recycle). The essential parameters are number of stages, volume fractions of mixed flow and plug flow in each stage, recycle ratio and by-pass ratio, these must be determined empirically. The model was used to determine RTD, in order to define the number of turnover stages, the relationship between filling angle and distance is required however and for this a modified version of Hogg et al's solution was employed based on (2.21) but with only β and θ_x left as variables, all other terms being grouped into one factor which must be determined empirically. As pointed out by Abouzeid [A10] multi parameter models have greater potential for the accurate fitting of experimental data but are perhaps less useful for comparing various systems or for scaling them up.

2.4 Overall simulation of rotating drum plant

An accurate model of solids transport should allow the design of rotating drum equipment to be carried out on the basis of residence time, hold-up and bed profile criteria. Better use could perhaps be made of such a model if it were combined with heat and mass transfer information and reaction kinetics to provide an overall desription of the process being carried out in the drum. This should provide an improved basis for design and a useful tool for control models and even operator training.

Such work as has been done in this area has universally adopted the simplest of models for solids transport in assuming a uniform hold-up which is proportional to the feedrate and inversely proportional to the drum speed [D1, G7, K4, L2, L3, L4, R5, S6]. Much of the work was performed on analog or hybrid computers. With the increasing availability of powerful digital computing time today the building of a model which accurately predicts the changing physical processes and properties for a given rotating drum application is an attractive proposition. Some papers which give details of processes carried out in rotating drums along with reaction rate constants, temperature profiles, heat transfer coefficients and emissivities where appropriate are those of Lyons, Min, Parisot and Paul [L3], Kroger, Hehl, Helmrich and Schugerl [K4]. One paper which has considered the fundamental nature of the solids motion and the effect this has on heat transfer is that of Lehmberg, Hehl, and Schugerl [L4].

2.5 Summary

The discussion in 2.3 and 2.4 is of a general nature intended to outline areas in which a detailed model of the motion of solids in rotating drums may make a useful contribution. The development of such a model was detailed in Section 2.1 where the progression from empirical correlation for mean residence time and hold-up to equations based on the mathematical description of the observed motion is described. The most developed form of these equations is given in the expression of Austin et al for open ended inclined drums, equation 2.34. This is an extension of the equation presented by Austin and Flemmer for horizontal drums. The equation can be summarised in functional form as follows

$$\frac{d\theta_x}{dx} = f(\theta_x, R_d, q, \alpha_d, w, \psi) \qquad (2.49)$$

with boundary condition $\theta_x = \theta_x(0)$ at $x = 0$

Both sets of equations have in them an empirical constant to account for the time a particle spends cascading on the surface. Removal of this limitation by modelling the particle motion in the surface is considered in the next chapter.

The determination of the discharge end filling $\theta_x(0)$ is required before these equations can be used. For open ended drums this has so far been considered as the minimum filling for which the model will hold and for constricted discharge drums the problem has been universally dealt with by empirical correlation. Predicting discharge filling by modelling the solids motion at the discharge end is considered in the next chapter. In addition to these topics Chapter 3 also considers where improvements may be made in the fundamental assumptions of the solids motion.

Investigators	Drum Lengths (m)	Associated Diameter(s) (m)	R_c/R_d Examined	Rotational Speed (% w_c)	Comments
Sullivan et al [S1]	1.52 2.13	.0952 .0762, .1524, .5	1, 0.75	0.5-5	Slopes 1-6°
Gilbert [G1]	.762	.051, 0.0635, .071	1	-	Slope 2.29° Drum rotated by hand
Pickering et al [P1]	3.35	.4254	1	2-7	Rotary kiln - fire-brick lined Slope 2.4°
Kramers & Krookewit [K1]	1.78	.197	1, 0.9, 0.8	2.5-16	Slope 0.5-5°
Vahl & Kingma [V3]	.63	.11	1	8-32	Steel cylinder with "rough surface" Horizontal
Hogg et al [H1] Austin et al [A3]	.248	.095	1, 0.54	67	Lucite drum, Vibratory feeder Horizontal Austin et al - inclined
Abouzeid et al [A4, A5, A9] Karra & Fuerstenau [K3]	.24	.08	1, .875, .75, .625 .56, .44	28	Lucite, Horizontal Vibratory feeder
Karra & Fuerstenau [K2]	.292 .438 .73	.127	-	10, 30, 66, 75	Grate discharge
Mu & Perlmutter [M2]	.406	.102	1	15	

Table 2.1 Experimental Details of Key Past Contributors to the Study of Solids Motion Inside an Unflighted Rotating Drum

Investigators	Material	Bulk Density (kg/m^3)	Angles of Repose (Deg) α_s	α_d	Mass Flow Rates (kg/s)
Sullivan et al [S1]	Ottawa Standard Sand	1480 (?) "typical" of sands	35	-	Up to .01
	30/50 mesh quartz	-	42.5	-	
	Sawdust	-	55.6	-	
Gilbert [G1]	Sand	-	-	-	Equal amounts fed after 1 drum rot.
Pickering et al [P1]	Alumite				
	raw	-	-	41	Up to .08
	calcined	-	-	38	
Kramers & Krookewit [K1]	Sand	1480	-	36°	Up to .0394
	Ground coke	560	-	40°	
Vahl & Kingma [K3]	Sand	1490	33	-	Up to .037
	Rye	710	40	-	
Hogg et al [H1] Austin et al [A3]	35 x 60 mesh Silicon carbide	1460	38	65	.0002-.004
Abouzeid et al [A4, A5, A9] Karra & Fuerstenau [K2]	35 x 48 mesh Dolomite	1300	32	-	.0024 .00153-.00161
Karra & Fuerstenau [K2]	14 x 20 mesh Dolomite	1450	35	-	.00165-.0067
Mu & Perlmutter [M2]	Rice		27	35	.0035

Table 2.2 Physical Properties of Material Used in Apparatus of Table 2.1

CHAPTER 3 - DEVELOPMENT OF AN IMPROVED MODEL FOR SOLIDS TRANSPORT

Introduction

In Section 2.1 the theoretical models developed to date of the transport of solids in a rotating drum were discussed along with their limitations and assumptions. Further development of a theoretical model will be concerned with removing or reducing the limitations of some of these assumptions which in summary are as follows:

1) The bed cross-section has a flat surface of slope α_d with respect to a plane tangential to the lowest point of the drum's circumference.

2) The time spent cascading on the surface is negligible compared to that spent locked in the bed.

3) The thickness of the cascade layer is negligible with respect to the bed depth.

4) All particles re-enter the bed at the same radial distance from which they left.

5) There is no change in the physical properties of the solid material over the length of the drum.

As mentioned in the introduction to this work assumption 5 will be retained. From experimental observation assumption 3 has also been considered reasonable and left unchanged. Of the remaining 3 only assumption 2 has so far received any attention in the literature, as evidenced by the empirically determined constant, intended to take account of the finite time that a particle spends on the surface, included in the most up to date models. The first objective of this work was to remove this empiricism and model the motion of particles on the bed surface, thus determining the time spent in the cascade layer from a theoretical basis. Section 3.1 presents the derivation of an expression for the variation of fractional filling with drum length for both horizontal and inclined drums from which the empirical constant has been removed. The derivation is similar to that for horizontal drums of Hogg et al [H1] (Appendix 2) which was subsequently modified to accommodate inclined drums by Austin et al [A3]. In the present derivation however the time spent cascading on the surface is expressed explicitly throughout and the final equation is correspondingly more complex than its predecessor, (2.34).

The cascade time is determined by considering the motion of the particles in the bed surface. The modelling of this motion is discussed in Section 3.2.

Having removed assumption 2 from the model, Section 3.3 goes on to consider assumption 4 and examines the patterns of particle circulation which give a steady motion of the charge in a rotating drum. The validity of assumption 1, that the bed cross section has a flat surface of slope α_d, is considered next in Section 3.4.

Having reappraised and modified some of the basic assumptions on which the model of solids motion has been based in the literature to date, the solution of the resulting equations is considered in the last sections of this Chapter. As pointed out in Chapter 2, determining the discharge end filling is of key importance and to date this has been achieved by assuming it to be equal to the discharge lip height or by empirical correlation. Section 3.5 presents an alternative theoretical method for determining discharge end filling. Sections 3.6 and 3.7 deal with the solution of the equations for the case of limiting filling and internal weirs respectively. There is a final summary in Section 3.8 of the changes that have been introduced to the model of solids motion and the advantages these introduce over previous work.

3.1 Development of Equation for Filling Along Drum Length in Which Cascade Time is Expressed Explicitly

This derivation follows the form of that of Hogg et al [H1] presented in Appendix 2. The derivation of the axial advance per cascade is the same and it is from this point onwards that the introduction of an expression for the cascade time takes effect. The starting point is taken therefore as the expression for the axial advance per cascade for a particle of path radius r, (A2.3).

$$s(r) = 2r \sin \theta_r \tan \phi \cos \beta \qquad \text{(A2.3)}$$

Where θ_r is the filling angle for the section of bed contained within the particle path of radius r (see Figure 2.3). The expression is used to calculate the axial velocity of the particle by dividing by the time taken to complete a cycle of being locked in the bed and cascading on the surface (the 'cycle time').

$$v(r) = s(r)/\tau(r)$$

Now instead of assuming that $\tau(r)$ is simply equal to the time spent locked in the bed as was done by Saeman, Vahl and Kingma, Kramers and Krookewit and Pickering et al, viz:

$$\tau(r) = 2\theta_r/w$$

or proportional to this time as in Hogg et al [H1] and Austin et al [A3] viz:

$$\tau(r) = 2\theta_r/Bw \qquad \text{(A2.4)}$$

The cycle time is instead expressed as the time spent locked in the bed plus the time spent cascading on the surface

$$\tau(r) = 2\theta_r/w + t_c(r) \qquad (3.1)$$

Where $t_c(r)$ is the time a particle of path radius r spends moving down the free surface of the bed. Combining (3.1) and (A2.3) gives the following expression for axial velocity of the bed element at (r, θ_r)

$$v(r) = \frac{2rw\sin\theta_r \tan\phi \cos\beta}{2\theta_r + wt_c(r)} \qquad (3.2)$$

The volumetric flowrate of this element is obtained by multiplying (3.2) by the incremental area of particle path r,

$$dA(r) = 2r\,\theta_r\,dr$$

which gives

$$dq(r) = \frac{4r^2 w \sin\theta_r \theta_r \tan\phi \cos\beta\, dr}{2\theta_r + wt_c(r)} \qquad (3.3)$$

On integration this yields

$$q = 4w \tan\beta \cos\beta \int_b^{Rd} \frac{r^2 \sin\theta_r \theta_r}{2\theta_r + wt_c(r)}\, dr \qquad (3.4)$$

Where q is the volumetric flowrate of material through the drum and, as before, b is the height from the bed surface to drum axis (minimum radius of particle paths neglecting cascade layer thickness) since b varies with θ_x the integral is a function of θ_x, the filling angle for the whole bed at any distance x along the drum axis from the discharge end. If the integral is denoted by $I(\theta_x)$ then (3.4) becomes

$$q = 4w \tan\phi \cos\beta\, I(\theta_x) \qquad (3.5)$$

The general expression of $\tan\phi$ for inclined drums has been given before in (2.30) (Horizontal drums have $\psi = 0$)

$$\tan\phi = \frac{\cos\alpha_d \sin\beta + \tan\psi\cos\beta}{\sin\alpha_d} \qquad (2.30)$$

when substituted into (3.5) this gives

$$q = 4wI(\theta_x)\, \cos\beta \sin\beta \cot\alpha_d \left(1 + \frac{\tan\psi\cot\beta}{\cos\alpha_d}\right) \qquad (3.6)$$

If the definitions

$$Y = 4w\cot\alpha_d \qquad (3.7)$$
$$C = \tan\psi/\cos\alpha_d$$

are made, and using the identity

$$\cos\beta\sin\beta = \tan\beta/(1+\tan^2\beta) \qquad (2.26)$$

(3.6) becomes:

$$q = YI(\theta_x)\left(\frac{\tan\beta}{1+\tan^2\beta}\right)\left(1 + \frac{C}{\tan\beta}\right) \qquad (3.8)$$

rearranging as a quadratic in tan and extracting the roots yields:

$$\tan\beta = \frac{YI(\theta_x) \pm \sqrt{(YI(\theta_x))^2 - 4q(q-YI(\theta_x)C)}}{2q}$$

$$= \frac{YI(\theta_x)}{2q} \pm \sqrt{\left(\frac{YI(\theta_x)}{2q}\right)^2 - \left(1 - \frac{YCI(\theta_x)}{q}\right)} \qquad (3.9)$$

The negative sign is applicable. As was done in the development of (2.23) $\tan\beta$ may be replaced by $R_d \mathrm{Sin}\theta_x \, d\theta_x/dx$ giving the following equation which relates filling angle θ_x to distance x along the drum from the discharge end

$$\frac{d\theta_x}{dx} = \left(\frac{1}{R_d \sin\theta_x}\right)\left[\left(\frac{YI(\theta_x)}{2q}\right) - \sqrt{\left(\frac{YI(\theta_x)}{2q}\right)^2 - \left(\frac{1-YCI(\theta_x)}{2q}\right)}\right] \qquad (3.10)$$

This is similar in form to (2.34). In this case however $d\theta_x/dx = 0$ when $I(\theta_x) = q/YC$ and the calculation of the filling angle for which transport may be effected with no change in bed height in downward sloping drums is more complex; (3.10) reduces to the form for horizontal drums when $C = 0$. The integration of (3.10) requires that the fractional filling at the discharge be known thus providing a boundary value for θ_x. Integration is then carried out numerically to the end of the drum. This process generates a series of (θ_x, x) pairs from which the bed surface profile may be calculated using the relationship between filling angle and bed height given in (2.12).

$$h = R_d(1-\cos\theta_x) \qquad (2.12)$$

The fractional filling at each point is given by

$$fc = (1/\pi)\,(\theta_x - (\sin 2\theta_x)/2) \qquad 0_x \leq \pi/2 \qquad (2.13)$$

from which the overall filling may be found by integration

$$FC = (1/L) \int_0^L fc(x)dx \qquad (2.14)$$

The determination of discharge end filling is considered in Section 3.5. At present a model of the particle motion in the surface is required since it is necessary to find an expression for the time the particle spends cascading on the surface before (3.10) can be used.

3.2 Particle Motion in the Cascade Layer

It was anticipated that the expressions presented by Mu and Perlmutter [M1] could be used to describe the particle motion on the bed surface. They presented a figure for the general particle trajectory as shown in Figure 3.1.

The postulated motion has three components

1 Ejection from the bed in a parabolic trajectory to point of maximum height above bed.

2 Return to bed surface.

3 Motion down surface with initial velocity gained from (2) and gravitational acceleration down bed transverse surface slopes of α_d with retardation due to inter particle friction.

Mu and Perlmutter's analysis is as follows. The angles used are shown in Figure 3.1.

The particles are assumed to eject from the surface at a tangent to the circular path they follow whilst locked in the bed. The angle of exit (in degrees) with respect to the horizontal is thus,

$$\varphi = 180 - \alpha_d - \theta_r \qquad (3.11)$$

The particles are assumed to rotate at the same speed as the drum whilst locked in the bed thus their initial velocity components in the x and y direction are given by

$$v_x = w r \cos\varphi \qquad v_y = w r \sin\varphi \qquad (3.12)$$

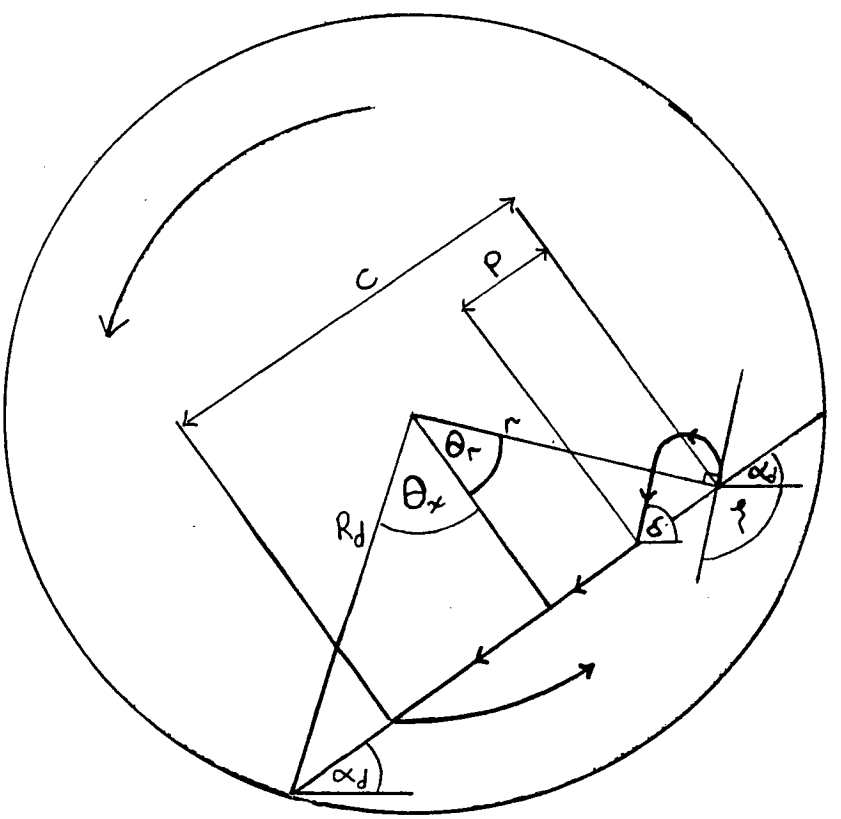

Figure 3.1 - Geometry of Particle Trajectory from Mu and Perlmutter [M1]

The time of travel from ejection to maximum height is

$$t_1 = \frac{wr}{g} \sin \varphi \qquad (3.13)$$

and the time for return from this height to the bed surface is

$$t_2 = \frac{wr}{g}\sqrt{\sin^2 \varphi + 4[\cos^2 \varphi \tan \alpha_d(\tan \alpha_d + \tan \varphi)]} \qquad (3.14)$$

In flight the particle has travelled a distance of P where

$$P = \frac{2}{g}\left[\frac{(wr)^2 \cos^2 \varphi (\tan \alpha_d + \tan \varphi)}{\cos \alpha_d}\right] \qquad (3.15)$$

At the point of return the particle strikes the cascade with a velocity of magnitude

$$V = \sqrt{v_x^2 + (gt_2)^2} \qquad (3.16)$$

at an angle to the horizontal of

$$\delta = \tan^{-1}(2\tan \alpha_d + \tan \varphi) \qquad (3.17)$$

The impact produces an initial velocity component along the cascade surface of

$$V \cos (\delta - \alpha_d)$$

This initial vector is augmented by gravity and simultaneously retarded by friction with the inclined plane of particles forming the cascade surface. The net result is movement through the distance (c-P) over the time interval t_3 where the implicit solution for t_3 is given by

$$V\cos(\delta - \alpha_d)t_3 + \tfrac{1}{2}g(\sin \alpha_d - \mu \cos \alpha_d)t_3^2 = c - P \qquad (3.18)$$

Where μ is the coefficient of inter particle friction in the bed surface and c is the distance travelled transverse to the drum axis by a particle while cascading. This has been considered by Mu and Permutter as equal to the chord length joining the entrance and exit points of the radial element from which the particle has just emerged.

This is one of the limitations of their analysis, if the distance of particle travel in the bed surface is considered equal to that travelled transverse to the drum axis alone the distances c and P will be too short. This could be corrected by replacing c and P with $c/\cos\phi$ and $P/\cos\phi$. As can be seen from (2.30) however any expression for $\cos\phi$ will involve some function of the angle β, thus β will become explicit in the right hand side of (3.10). This would require that an iterative solution for be carried out at each step of the numerical integration of (3.10) significantly increasing the amount of computer time required to effect the integration. This added effort was thought unwarranted since the error in cascade length will be small for small bed surface slopes and factors such as the accuracy of determination of angles α_d, δ and in particular the coefficient of friction μ are likely to have a more pronounced effect on the value of t_3. In addition the difference between α_d, the bed surface slope in transverse section and the true angle of descent of particles along the drum has been neglected.

According to Mu and Perlmutter then, the time spent on the surface of the bed is equal to $t_1 + t_2 + t_3$. An examination of (3.11) however shows that even for the higher end of commonly reported α_d values ($\alpha_d = 40°$) the angle φ is greater than 90° for values of θ_r up to 50°. If θ_r is set equal to θ_x this means that for fillings up to 12% (fc = 0.12) particles are ejected "up" the bed surface in a direction opposite to the flow of the cascade layer. This motion would certainly be predicted for the experiment reported in Part 1 of Mu and Perlmutter's report [M1] ($\alpha_d = 35$ $\theta_x = 50°$ fc = 0.12). In Figure 3.1, a tangent drawn to any of the radial paths as they meet the upper surface of the bed clearly shows this upward direction of the initial trajectory, yet the inference in Mu and Perlmutter's figure is that the trajectory "bends back" on itself and heads down the slope. The upper limit of filling for which this motion would be predicted by (3.11) will increase for lower values of α_d. Such motion has never been observed and suggests that the equations of Mu and Perlmutter do not accurately model the "fracture" or "slipping" process which forms the cascade layer at speeds much less than the critical speed. The contribution of t_1 and t_2 to the time spend on the bed surface have therefore been neglected along with the distance P associated with the parabolic rise and fall. This leaves the following modified version of (3.18) from which the cascade time t_3 may be found.

$$V \cos(\delta - \alpha_d) t_3 + \tfrac{1}{2} g(\sin\alpha_d - \mu\cos\alpha_d) t_3^2 = c \qquad (3.19)$$

The coefficient of t_3 in (3.19) is an expression for the initial velocity of a particle on the bed surface and is the component of the return velocity from a parabolic rise and fall which acts down the slope. Mu and Perlmutter state that, at relatively low rotational speeds the parabolic flight may take only a negligible time interval; however the first term of (3.19) must still be used to account for the initial velocity on the cascade. This may not be the case especially if the cascade layer is formed by a process of continuous slippage. In this instance the initial velocity down the slope will be zero. In order to determine the effect of an initial velocity on the cascade (3.10) was integrated incorporating (3.19), both with and without the coefficient of t_3, to predict the filling in various drums. The value of c, the distance travelled in the transverse direction, was that which has been used in all model building up to now

$$c = 2r \sin\theta_r \qquad (3.20)$$

(another option is considered in Section 3.3). For simplicity no inter particle friction on the bed surface was assumed thus μ was set equal to zero. The discharge end filling from which the integration of (3.10) commences was determined as described later in Section 3.5. The results are shown in Figure 3.2. Both experimental and literature data have been used these are documented in Appendix 4 Tables A4.1, A4.2 and A4.3. It can be seen that there is no significant advantage in either assumption other factors having a more pronounced effect on overall accuracy. It was decided therefore to neglect any initial velocity on the cascade surface, for relatively low rotational speeds this was certainly thought to be more intuitively correct. The final form of the equation for the time spent on the cascade surface is thus

$$t_3 = \sqrt{\frac{2c}{g(\sin\alpha_d - \mu\cos\alpha_d)}} \qquad (3.21)$$

The determination of the value of μ, the coefficient of inter particle friction on the bed surface, is considered in the following section.

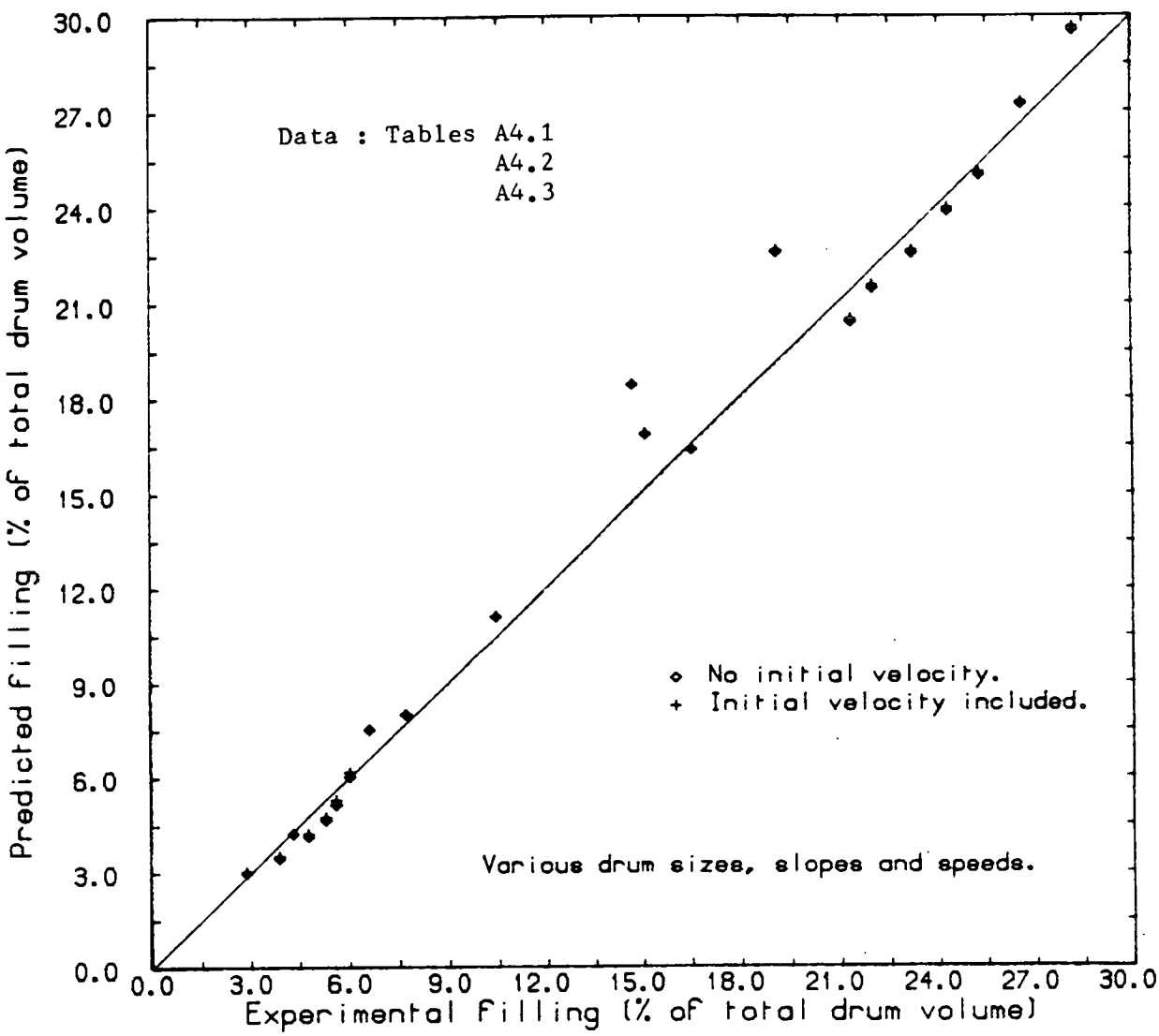

Figure 3.2 - Effect of initial cascade velocity on filling prediction

3.2.1 Coefficient of Surface Friction

Mu and Perlmutter give no indication of how to find μ, the coefficient of interparticle friction in the cascade layer. Back calculation from their results [M2] shows however that they consistently used a value of 0.5. Rather than proceed with this seemingly arbitrary figure the following expressions were considered for predicting the coefficient.

1) $\mu = 0$ (3.22)

This assumes no surface friction and should be applicable if surface friction forces are negligible. This value was adopted by Rogers and Gardner [R4] who also considered the time a particle spends on the surface as an explicit component of the total particle cycle time. They assume the time on the surface as equal to that required for sliding down a frictionless slope of α_d with no initial velocity ((3.21) with μ equal to zero). Rogers and Gardner required an expression for cycle time for incorporation in the solution of the uniaxial dispersion model.

2) The expression for the coefficient of inter particle friction for a stationary cone of material is $\mu = \tan\alpha_s$, where α_s the static angle of repose is the angle of the edge of the cone makes with the horizontal. The equivalent for the dynamic angle of repose of a bed surface was also considered viz:

$$\mu = \tan\alpha_d \qquad (3.23)$$

This turned out to give much too high a value for μ and using this assumption the coefficient of t_3^2 in (3.19) becomes negative for values of α_d >36°. Use of (3.23) was therefore abandoned.

3) Since the tumbling motion in the cascade layer is made up of slipping and rolling of individual particles, the coefficient of friction for the transition from slipping to rolling of a sphere on an inclined plane of slope α_d was also considered. This is as follows

$$\mu = \tan \alpha_d / 3.5 \qquad (3.24)$$

The derivation of this expression for a cylinder is presented by Jaeger [J2]. For a sphere, it simply requires that the appropriate moment of inertia be used in his expression. Spheres were selected as being the best approximation for most bulk granular materials.

4) All of the preceding expressions for the coefficient of inter particle friction on the cascade surface have the effect of increasing μ as the dynamic angle of repose increases. This seems perhaps unreasonable since any increase in α_d is the result of an imposed external torque on the bed and is not a reflection of an increased ability on the part of the particles to hold themselves at this angle due to an increase in μ. It was thought therefore that linking the coefficient of interparticle friction to the static angle of repose may be more appropriate. To this end the coefficient for the transition between sliding and rolling on an incline equal to the static angle of repose was also considered viz:

$$\mu = \tan \alpha_s / 3.5 \qquad (3.25)$$

This implies that no matter what dynamic angle of repose results from drum operating conditions, once free flowing occurs on the surface the coefficient of inter particle friction is constant for a given material.

5) One other angle which it was thought might be appropriate to incorporate into expressions such as (3.21) or (3.22) in place of the dynamic angle of repose was the internal dynamic angle of repose as observed by Franklin and Johanson [F4] (1955). This is the angle of the plane along which the particles re-enter the bed from the cascade layer (see Figure 3.3). Franklin and Johanson studied the flow of material through a circular orifice. They used an enclosed drum of small aspect ratio and considered the internal dynamic angle to be representative of the angle of shear between fast and slow moving particles which "cone" towards an orifice.

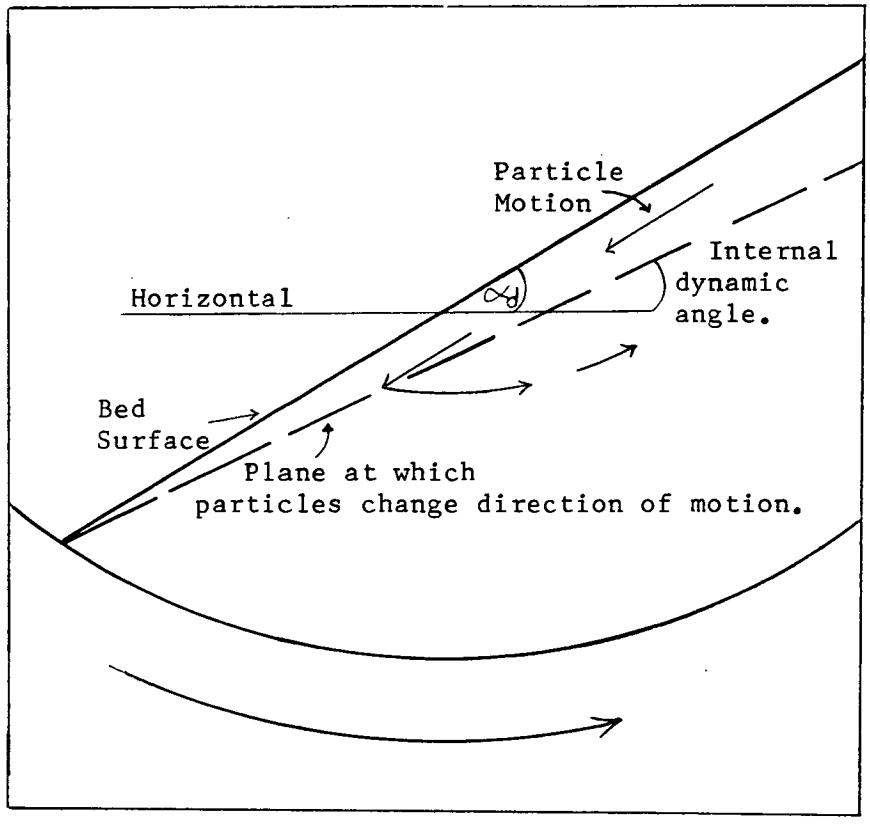

Figure 3.3 - Internal dynamic (kinetic) angle of repose

Franklin and Johanson produced a correlation for internal dynamic angle of repose against static and surface dynamic angles. This was for drum speeds up to 8% w_c and various materials, the internal dynamic angle was observed to be less than the static angle of repose. As Franklin and Johanson point out their correlation is of limited applicability. This and the comparative difficulty in measuring internal dynamic angle of repose as opposed to surface dynamic led to the setting aside of the former for use either to determine the coefficient of surface friction or as a direct replacement for the dynamic angle of repose throughout the model.

There are now three remaining expressions for the coefficient of surface friction (3.22), (3.24) and (3.25). An example of the effect of each of these expressions on the ability of the model, as represented by (3.10), to predict drum filling is shown in Figure 3.4. As would be expected there is an increase in predicted filling as the coefficient of friction increases from zero to the value calculated from the static angle of repose and on to that calculated using the dynamic angle of repose. This reflects the fact that as the coefficient of friction increases the average particle velocity on the surface will decrease, thus the calculated bed cross sectional area must increase to maintain the given volumetric flow rate.

In this instance the experimental results shown in Figure 3.4 and given in Table A4.4, Appendix 4 are best fitted using the assumption of no interparticle friction, the average magnitude of deviation from experiment being 3.9%. The figures for the expressions using static and dynamic angles of repose are however only 0.4 and 0.5% greater than this similar magnitudes of deviation between calculated values using each of the expressions were found for all the experimental data. When all of the available experimental data is taken into consideration however, it was found that (3.25) gave a better fit overall. This was therefore used in (3.21) and the resulting expression below for the time spent cascading on the bed surface was incorporated into the theoretical model and used in all further work.

$$t_3 = \sqrt{\frac{2c}{g(\sin\alpha_d - \tan\alpha_s \cos\alpha_d/3.5)}} \qquad (3.26)$$

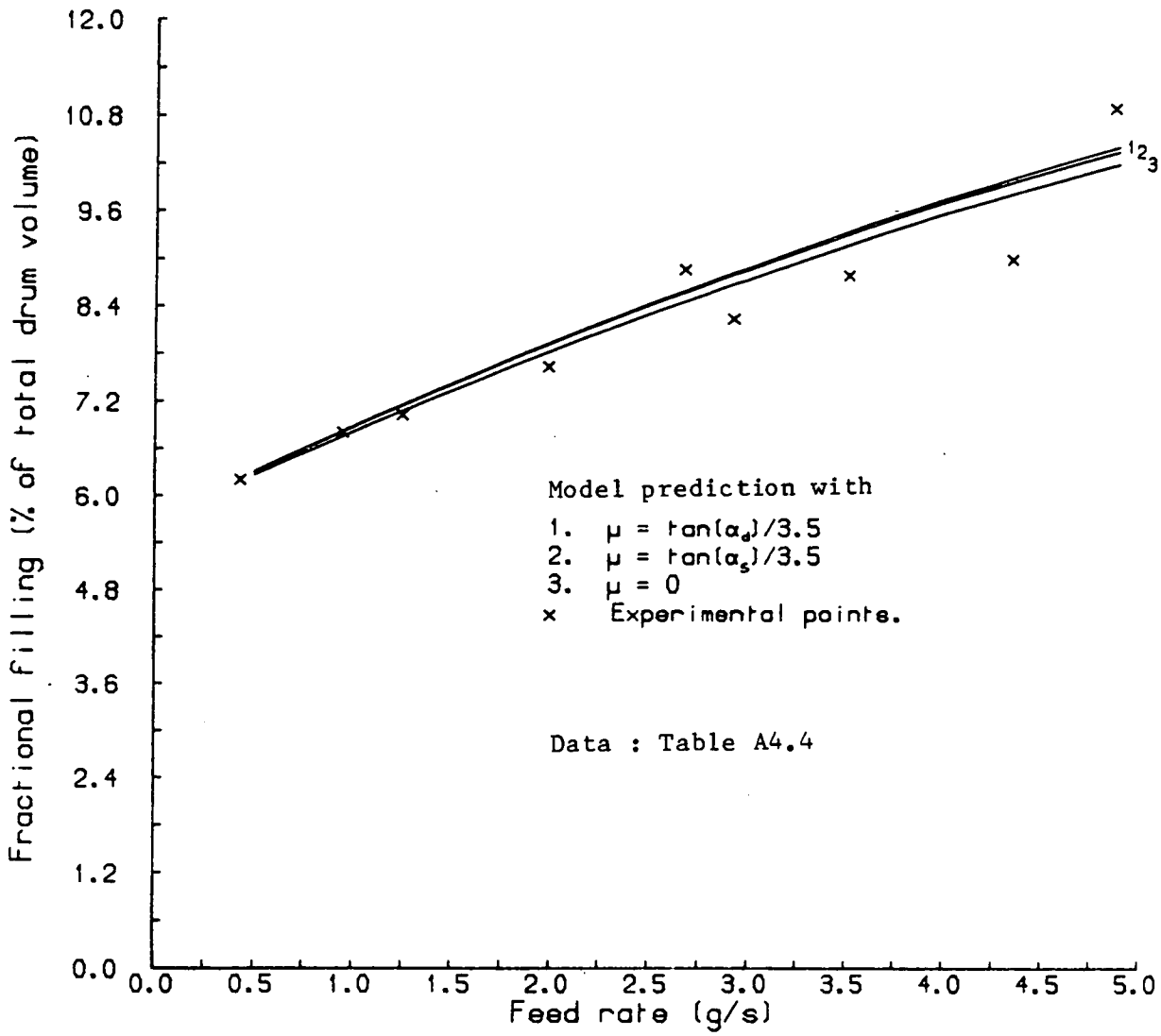

Figure 3.4 - Effect of various expressions for the coefficient of inter particle friction in the bed surface

The finding that the model predicts best for a dynamic system using a fixed value of inter particle friction for each material is in agreement with the results of an investigation by Augenstein and Hogg (1974) [A11] in which the coefficient of inter particle friction was measured for free flow of material on a fixed substrate of the same. The coefficient of friction was found to be independent of particle velocity and surface slope. The existance of an accelerating flow over a range of inclination for powders on a fixed substrate was also found in the later work of Knight (1984) [K5].

The chord length c, defining the transverse distance covered by a particle in the cascade layer is defined in (3.20), the next section in this chapter considers a possible alternative to this expression.

3.3 Particle Path Lengths

Considered up to this point the derivation of the equations which define variation of fractional filling with distance in a rotating drum have all assumed that particles re-enter the bed at the same radial distance from which they emerged (assumption 4 at the start of this chapter). This assumption could only apply to a bed of uniform depth as any reduction in bed surface width (as occurs in drums with decreasing bed height from inlet to discharge) will result in particles re-entering the bed at a radial distance greater than that from which they left. This error will be small for small bed slopes and computational effort required to eliminate it was thought unwarranted when other sources of error in the model and its solution were considered. Mu and Perlmutter [M1] showed that another limiting case in which the particles re-enter the bed at a fixed distance, equal to half the bed surface width, would also result in steady motion of the charge. The transverse distance equal to half the bed surface width, covered by a particle in the cascade layer is thus constant and given by the following expression.

$$c = R_d \sin \theta_x \tag{3.27}$$

The axial transport distance per particle cascade is now no longer a function of the particles radial position

$$s = R_d \sin \theta_x \tan \phi \cos \beta \tag{3.28}$$

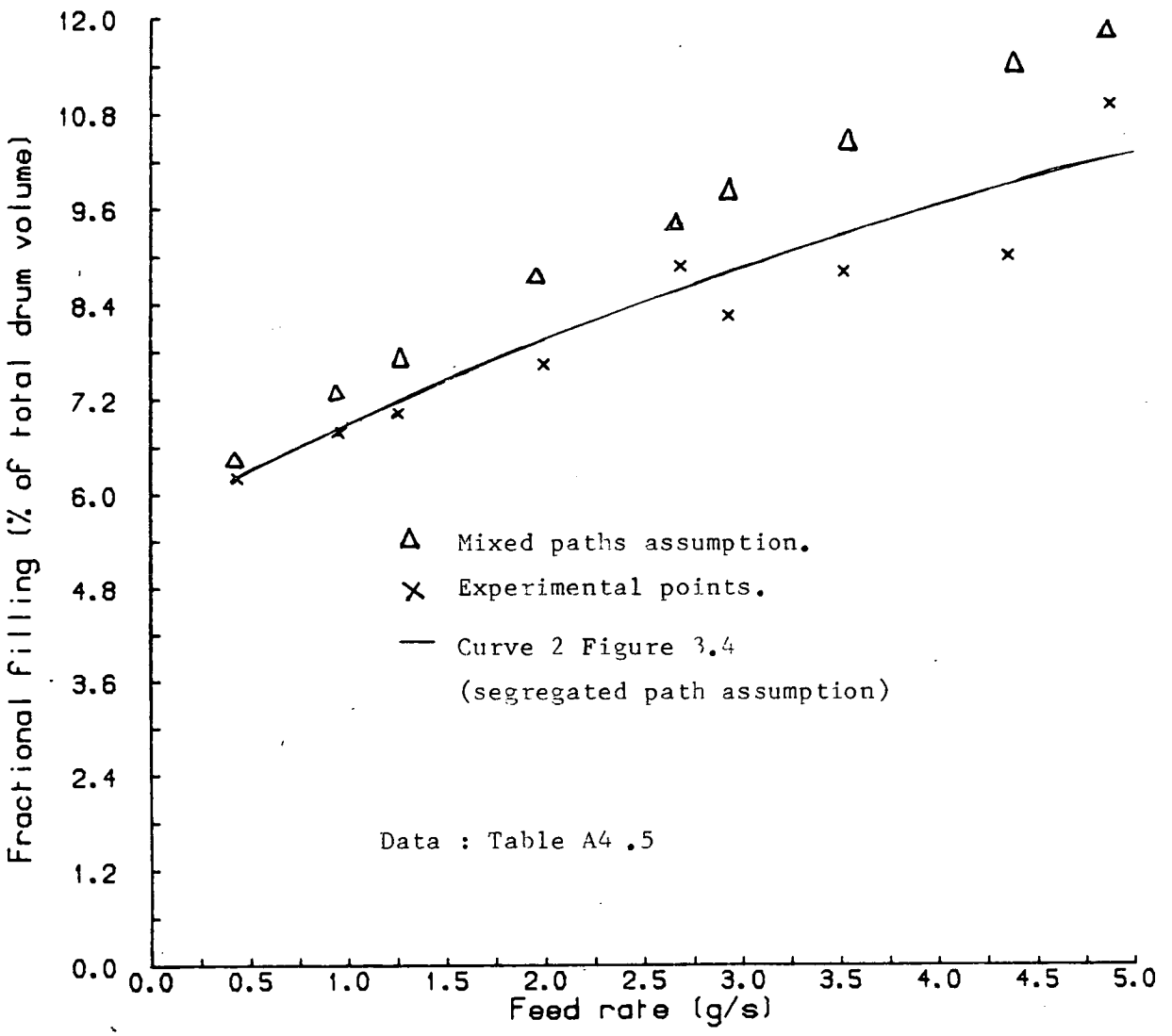

Figure 3.5 - Effect of Segregated vs Mixed Paths for Particles on Surface

If this equation is used in place of (A2.4) and the derivation as detailed in section 3.1 is again performed the resulting equation for the variation in filling with distance is as follows.

$$\frac{d\theta_x}{dx} = \left(\frac{1}{R_d \sin\theta_x}\right)\left[\left(\frac{Y' R_d \sin\theta_x I'(\theta_x)}{2q}\right) - \sqrt{\left(\frac{Y' R_d \sin\theta_x I'(\theta_x)}{2q}\right) - \left(1 - \frac{Y' R_d \sin\theta_x I'(\theta_x) C}{q}\right)}\right] \qquad (3.29)$$

$$\left.\begin{aligned} \text{where } C &= \tan\psi/\cos\alpha_d \\ Y' &= 2w\cot\alpha_d \end{aligned}\right\} \qquad (3.30)$$

$$\text{and } I'(\theta_x) = \int_b^{R_d} \frac{r\theta_r dr}{2\theta_r + w t_c(r)} \qquad (3.31)$$

Equations (3.29)-(3.31) can be compared with their "segregated path" assumption counterparts (3.10) and (3.7) and the definition of $I(\theta_x)$ shown in (3.4) and (3.5).

The cascade time $t_c(r)$ in (3.31) is determined using (3.26) as before, in this instance however with cascade length as defined by (3.27) as opposed to (3.20). The overall filling is determined using (2.13) and (2.14) in conjunction with the (θ_x, x) pairs produced by (3.29) as before.

The fractional filling for the drum used for Figure 3.4 was predicted using the assumption of fixed surface cascade paths and the results are shown in figure 3.5 and Table A4.5, Appendix 4. The fixed cascade length gave consistently higher values for drum filling than the segregated path assumption. The deviation increased with increasing feed rate. It had been thought that the segregated path and fixed cascade path assumptions might provide bounds within which experimental data would lie.

The segregated path assumption however better fitted experimental data and further work with the fixed path length model described in this section was therefore abandoned.

3.4 Bed Transverse Surface Profile

As mentioned in the introduction to this Chapter all of the work to date has assumed that the bed transverse surface profile is linear with a dynamic angle of repose with respect to the drum axis of α_d. In the work of Hogg et al [H1] the bed surface was substantially deformed at relatively high rates of rotation (67% w_c), indeed similar surface deformation was been observed in this investigation and also by Kramers and Krookewit [K1] with sand at relatively low rates of rotation ($\sim$8% w_c). The problems introduced by a non-linear transverse bed surface profile are considered below, first of all however the determination of the dynmaic angle of repose for the many instances in which the assumption of a linear profile holds true is addressed.

3.4.1 Determination of the Dynamic Angle of Repose

Ideally this angle should be measured directly as was done in this investigation but this may often be quite impractical especially where large drums are concerned. In this instance the angle should be measured on a small scale drum/solid system of the same materials rotating at the same fraction of the critical speed to achieve dynamic similarity.

It would be advantageous however to be able to predict the dynamic angle of repose. There appear to have been two expressions presented to date, one empirical and the other theoretically based. The empirical relation of Bachmann [B3] is given below and presented in Johnstone and Thring [J3] which was cited as its source by Cross [C2]

$$\alpha_d = \alpha_s + w/w_c \qquad (3.32)$$

where α_d and α_s are measured in radians. This expression was found to give reasonable results up to around 5% w_c, beyond this the rate of increase in dynamic angle of repose observed experimentally was much lower than the $0.6°/\%w_c$ predicted by (3.32). This expression was found to over predict for both experimental and literature data. The degree of over prediction varied depending on the drum/solid system considered and was thought to be due to the effect of slip at the drum/solid

interface. This factor is very difficult to quantify and is considered further in the next section on non linear surface profiles.

The only theoretically based expression for predicting dynamic angle of repose seems to be that of Suzuki and Tanaka [S7]. In this case the solid material is treated as a Bingham plastic and the motion in the rotating cylinder considered as creeping flow in a rectangular vessel whose walls move in the direction of rotation of the drum with the same speed as the drum. The dimensions of the rectangle are chosen such that it has the same height as the maximum bed depth and a width which gives it the same cross sectional area as the bed. Equations for the stream functions along the rectangular boundaries are developed and used to solve the expression for the torque imparted to the fluid as given by the integral of the shear stress at the wall over the wetted periphery. This torque is then equated to that imparted by the mass of the bed considered to act on a lever arm from the drum axis to its centre of mass. The following expression results.

$$\rho g A R_g \sin\alpha_d = \frac{4\mu R_d^2 w}{h}\left\{3R_d(3-3(h/R_d)+(h/R_d)^2)+\frac{2-(h/R_d)}{2L}(3hL+h^2-3LR_d)\right\}+R_d S\tau_y \qquad (3.33)$$

h is the bed depth and g is the gravitational constant.

2L is the width of the rectangle. R_g is the radial distance to the bed centre of mass. A is the bed cross sectional area. S is the contact arc length between bed and drum, τ_y is the yield stress of the fluid and μ the apparent viscosity of the solid. It can be seen that (3.33) defines a linear relation between $\sin\alpha_d$ and w. τ_y and μ are calculated from the intercept and slope respectively. When w=0 (3.33) reduces to

$$\sin\alpha_d = \frac{R_d S}{\rho g A R_g}\tau_y \qquad (3.34)$$

In this situation with the drum stationary α_d can be replaced by α_s and the yield stress determined. It is not immediately obvious, but (3.34) for a material with uniform static angle of repose, predicts that the yield stress will change with filling in the drum and also with the size of the drum used, this can be seen as follows. For a drum with a given fractional filling the radius of the centre of mass will be the same fraction f of the drum radius

$$R_g = fR_d \tag{3.35}$$

The area of the charge will be given by

$$A = fc\,\pi\,R_d^2 \tag{3.36}$$

and the "wetted periphery" by

$$S = 2R_d\theta_x \tag{3.37}$$

Where θ_x is the filling angle corresponding to a fractional filling fc for any drum size. If the degree of filling is the same then f, fc, and θ_x will remain unchanged. If these expanded forms of the terms in (3.34) are substituted back into the original the following expression results.

$$\sin \alpha_s = \frac{2\theta_x}{\rho g fc\,\pi\, fR_d}\,\tau_y \tag{3.38}$$

α_s is observed to be a constant for any given solid and will have the same value in any size drum for a fixed fractional filling. All the terms in (3.38) apart from R_d (and consequently τ_y if α_s is to remain constant) would remain unchanged for any size drum with uniform filling. Equation (3.38) thus predicts that τ_y will change with drum size.

Once a figure for τ_y has been determined this is used along with a drum speed w for which the corresponding angle of repose α_d is known to determine μ, the apparent viscosity of the powder. According to the theory this is also dependent on filling and drum size. This is inconsistent with the behaviour of a Bingham Plastic and coupled with the need for measured data in the above analysis led to (3.38) being excluded as a predictor of dynamic angle of repose.

3.4.2 Non Linear Bed Transverse Surface Profile

A non linear profile introduces areas of discrepancy between model and experiment. The nature of the motion in the bed surface is unlikely to be modelled accurately by the equations developed for the linear profile. This will affect the model's ability to predict the rate of increase in bed height through the drum. Even if the rate of increase in mean bed height is predicted, the model computes

filling by integrating the area under a linear bed surface and would require a knowledge of the surface shape to compensate for other profiles.

The problems of dealing with a geometry other than linear for a bed transverse surface profile has either been ignored by those concerned with transport through rotating drums or else an effective linear profile and dynamic angle of repose have been assumed. The latter has much to recommend it in that it requires no modification of the transport model, it does however introduce a degree of arbitrariness since an effective dynamic angle of repose is more difficult to define. It may be possible to define it as that which gives the same bed cross sectional area as the deformed bed surface, but this again requires that the shape can be predicted at least for geometrical manipulation if not for modelling the motion.

Bed surface shape has been considered for batch devices such as rotating drum mixers and ball mills [O2, K6, H4] all of which generally operate with much higher fillings and rates of rotation than drums in which transport is effected. The earliest work was carried out by Davis (1919) [D2] who determined the locus of points for which particles of different radial paths were in equilibrium under the influence of centrifugal and gravitational forces (the so called "Davis Circle"). He plotted parabolic trajectories with initial vectors tangential to the particles radial path. There was assumed to be no slip between particles or between particles and the drum wall. The resulting equation required that particles be carried up past the x-axis (if the centre of the drum is considered as the origin) before commencing a return trajectory, irrespective of filling or particle frictional properties. Barth (1930) [B4] extended the work of Davis by considering particles at the surface to be in equilibrium between the forces due to gravity, rotation and inter-particle friction (but all particles are assumed to rotate at the same speed as the drum). The derivation as presented by Rose and Sullivan (1958) [R6] is unclear but the final equation for the "equilibrium surface" has been widely used by those investigating rotating drum mixers [H4, K6], it takes the form

$$R_b = C_b \, e^{\Psi_b \tan\alpha_s} \qquad (3.39)$$

Where C_b is a parameter which is related to the degree of filling in the mill and R_b and ψ_b are polar coordinates of a general point on the surface. The origin for the polar coordinates is situated a distance g/w^2 above the centre of the drum which is in fact the diameter of the Davis circle. Though this equilibrium surface exists the particles are still required to penetrate the Davis circle before projection can occur.

The work of Henein et al (1983) [H5, H6] on the transverse motion of solids in rotary kilns was concerned primarily with the phenomena of slipping and slumping which occur at relatively low rotational speeds. Their data shows that such motion progresses to a rolling motion at speeds greater than 5% w_c except in the case of very low bed/wall friction for which bulk bed slipping lasts much longer. They did consider 'cascading' but defined this as occurring when the bed surface, with a linear surface profile projected into the 1st quadrant. Their model is based on bulk bed rotation and requires many empirical measurements - once 'cascading' is established they consider the particles to adopt parabolic trajectories.

Since none of the above adequately represented what was observed to happen in this investigation in which curved bed surfaces were present for very low fillings an attempt was made to derive a force balance for particles at each point of their journey while locked in the bed. It was hoped to include the effects of slip between particles and the wall and between each other and thus determine the nature of the locus of points at which particles cascade down the surface. The force on any particle tangential to its radial path is proportional to the normal force upon it. If slip exists the normal force will vary as the particle rotates with the drum and is subject to varying depths of particles above it. This indicates that an iterative solution, in which a surface profile is assumed and subsequently confirmed or not by a point to point force balance is required. The added computational effort and complexity was thought unwarranted when there existed the possibility of accounting for non linear profiles by some measurement which might be made on the experimental system. As discussed in Chapter 5 Section 5.1, this has not been possible and the prediction of bed surface profile is worthy of further attention.

3.5 Modelling of Drum Discharge Both Open and Constricted

The development in the preceding sections of an expression for the time a particle spends cascading on the surface allows attention to be focussed on determining the filling at the discharge end which is all that remains to be found before (3.10) may be integrated. Previous methods for determining discharge filling in open ended and constricted drums are discussed in Chapter 2. For constricted discharge drums the discharge end filling has been determined solely by empircial correlation [A4, H1]. For open ended drums however one theoretical solution has been presented in which the expression for volumetric flowrate through a rotating drum as developed by Austin et al [A3] was rearranged to give filling angle as the independent variable. This expression was then minimised by using the remaining 'free' variable bed surface slope β. For horizontal drums the minimum filling arises when $\beta = 45°$ (this was shown previously though the working was not given, by Austin and Flemmer [A2]).

It seems unlikely that all beds will discharge with an angle between their surface and horizontal of 45° since most bulk materials have static angles of repose well below this figure and any dynamic effect might be expected to reduce rather than increase them. If then, the bed is assumed to collapse at the discharge end at its static angle of repose (as was also suggested by Saeman) a discharge filling may be determined as follows.

Figure 3.6 shows the proposed discharge geometry in which the bed collapses out of the discharge end down a slope of angle, E, to the drum axis. For horizontal drums E will be equal to the static angle of repose α_s and for inclined drums it will equal α_s minus the slope of the drum ($E = \alpha_s - \psi$). In both cases the bed surface axial slope with respect to the drum axis, β, is equal to E. The discharge 'slope' is of course hypothetical since the material will fall under the effect of gravity upon leaving the drum. It is assumed however that the initial velocity on this 'slope' will be representative of that with which the solid leaves the drum.

The bed surface slope, β, has been the independent variable in the volumetric flowrate expression thus far, which has been used to determine the relationship between filling and distance along the drum. If β is now specified at the discharge end another variable may be selected from the volumetric flowrate expression and this will

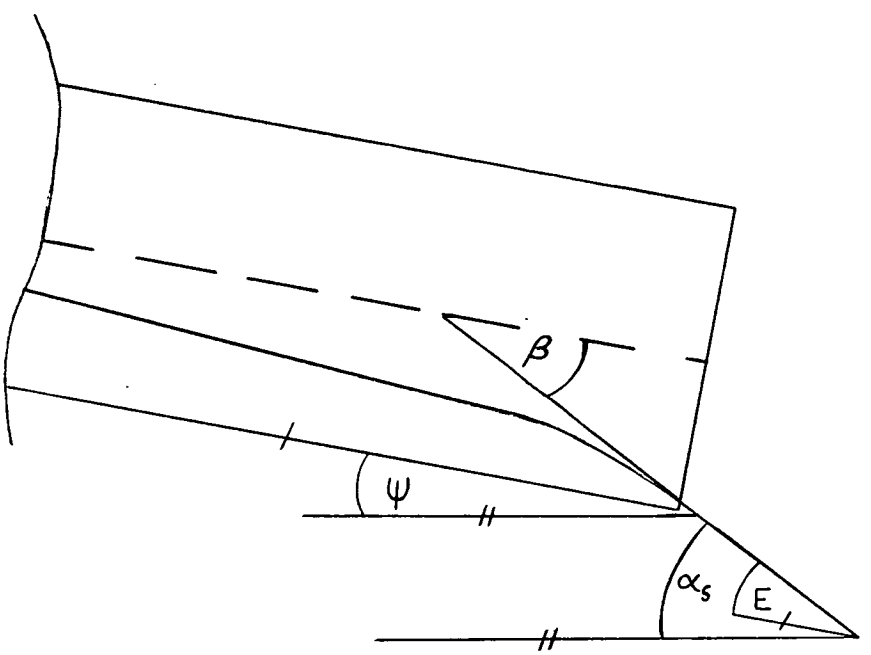

Figure 3.6 - Side elevation of drum discharge showing bed surface discharge at angle α_s to the horizontal

enable the filling at this point to be determined. Returning to the expression for volume flow as given by (3.6) with ($I(\theta_x)$ written out in full,

$$q = 4w\cos\beta\sin\beta\cot\alpha_d\left(1 + \frac{\tan\varphi\cot\beta}{\cos\alpha_d}\right)\int_b^{Rd} \frac{r^2\sin\theta_r\theta_r}{2\theta_r+wt_c(r)}\,dr \qquad (3.40)$$

The independent variable is now chosen to be b, the lower limit of integration of $I(\theta_x)$. With a known flowrate through a drum and a specified β, (3.40) can be solved for b and the discharge end filling then determined from

$$\theta_x = \cos^{-1}\left(b/R_d\right) \qquad (3.41)$$

In a constricted discharge drum it was thought that it might be appropriate to consider the bed height at the constriction equivalent to that which would exist at the discharge end of a drum of uniform radius equal to that of the constriction.

The method of determining discharge end filling described above is again applicable, in this instance however the constriction radius, R_c, is used as the upper limit of integration in (3.40). The value of b determined is again combined with the drum radius, R_d, to determine the discharge end filling angle using (3.41).

3.6 The limiting filling case

Limiting filling in which transport may be effected with no change in bed height has been considered generally in the early part of 2.1. This phenomenon can only occur in inclined drums. The solution of (3.10) for limiting filling conditions will now be considered for both open ended and constricted discharge drums.

3.6.1 Open ended drums

The solution of the differential equation for filling is quite straightforward in this case. Limiting filling for which $d\theta_x/dx = 0$ can be seen from (3.10) to occur if $I(\theta_x) = q/YC$, which in full is

$$\int_b^{Rd} \frac{r^2\sin\theta_r\theta_r}{2\theta_r+wt_c(r)}\,dr = \frac{q\sin\alpha_d}{4wtan\psi} \qquad (3.42)$$

This can be solved for b and the value of limiting filling angle θ_{lim} determined using (3.41).

Since for open ended drums the discharge end filling is the lowest in the drum numerical integration of (3.10) in increments of θ_x will always approach θ_{lim} from below thus the integration can be carried out close to θ_{lim} (the integral is indeterminate for $\theta_x = \theta_{lim}$) and from the point along the drum at which this occurs up to the drum inlet can be considered to have uniform filling of angle θ_{lim}. An open ended drum with limiting filling is thus composed of two regions as shown in Figure 3.7. The cumulative filling up to θ_{lim} is determined using (2.13) and (2.14) as before and the filling over the rest of the drum using (2.13) with $\theta_x = \theta_{lim}$. Each "filling section" is then multiplied by the fraction of the drum length over which it applies and the results summed to give the overall filling in the drum.

3.6.2 Constricted discharge drums

The solution of (3.10) for constricted discharge drums is accomplished by numerical integration starting from a discharge filling which is found as explained in Section 3.5, subsequently if a limiting filling is approached as the bed builds up along the drum, the procedure for open ended drums in the same situation is adopted. The problem arises for drums whose constrictions are such that they force the discharge end filling to be higher than the limiting filling for the drum. This results in bed profiles as shown in Figure 2.6 curves b and c.

Since Kramers and Krookewit [K1] there has been no literature dealing with the prediction of holdup in inclined constricted discharge drums from a theoretical basis. They took what is essentially a simplified form of (3.10), derived on the basis of a less rigorous model than that described in Section 3.1 and used it above the limiting filling value. This requires that the integration variable be reduced from the known value at the discharge toward the limiting filling value which is thus approached from "above". It seems inappropriate to use equations based on the assumption that bed height reduces from feed to discharge with respect to the horizontal, to solve for a situation in which bed height increases towards the discharge end. This is reflected in the fact that Kramers and Krookewit's agreement between theory and experiment is worst for this situation. In order to rectify this

apparent gap in the theoretically based prediction of drum filling the following analysis for inclined drums with discharge end fillings greater than the limiting filling for the drum was developed.

Though the motion behind a constriction is undoubtedly more complex than that considered up to this point, the bed profile is simple in form and analogous to that which would occur for a liquid flowing from the feed to discharge end of the stationary drum. It seemed appropriate then to consider the discharge mechanism to be unaltered in this situation, thus allowing the discharge end bed height to be determined as described in 3.5, and then to determine the filling from geometrical considerations alone.

Once the discharge end bed height has been determined it is assumed to remain unchanged with respect to the horizontal on moving up the drum. This height will either meet the limiting filling bed height at some distance x along the drum (figure 2.6b) or reach the inlet of the drum before doing so (figure 2.6c). In both instances the distance along the drum, x, to which the horizontal surface line extends is given by

$$x = (H_d - H_{lim})\tan\psi \qquad (3.43)$$

Where H_d is the bed beight at discharge found from the solution of (3.40) with R_c as upper limit of integration and H_{lim} is the height of limiting filling in the drum found by solving (3.42) for b, ($H = R_d - b$). Once x is determined it can be used to determine whether profile 2.6b ($x<L$) or 2.6c ($x>L$) is appropriate. If there is limiting filling alone over part of the drum (2.6b) then the calculation of filling in the drum is split into two parts. The filling in the conic section is determined by integrating the filling equation over the range in filling angle delimited by H_d and H_{lim} as outlined by (2.12), (2.13) and (2.14). The latter will apply from o to x in this instance. The remainder of the drum has uniform filling found using (2.12) with $\theta_x = \theta_{lim}$. The total filling is found by multiplying the two components by the fraction of the drum length over which they apply and summing their respective contributions. In the case of the whole of the drum being occupied by a bed in the form of a conical section then (2.12), (2.13) and (2.14) are applied over the whole drum length, the inlet bed height being determined by solving for H_{lim} with $x = L$ in (3.43).

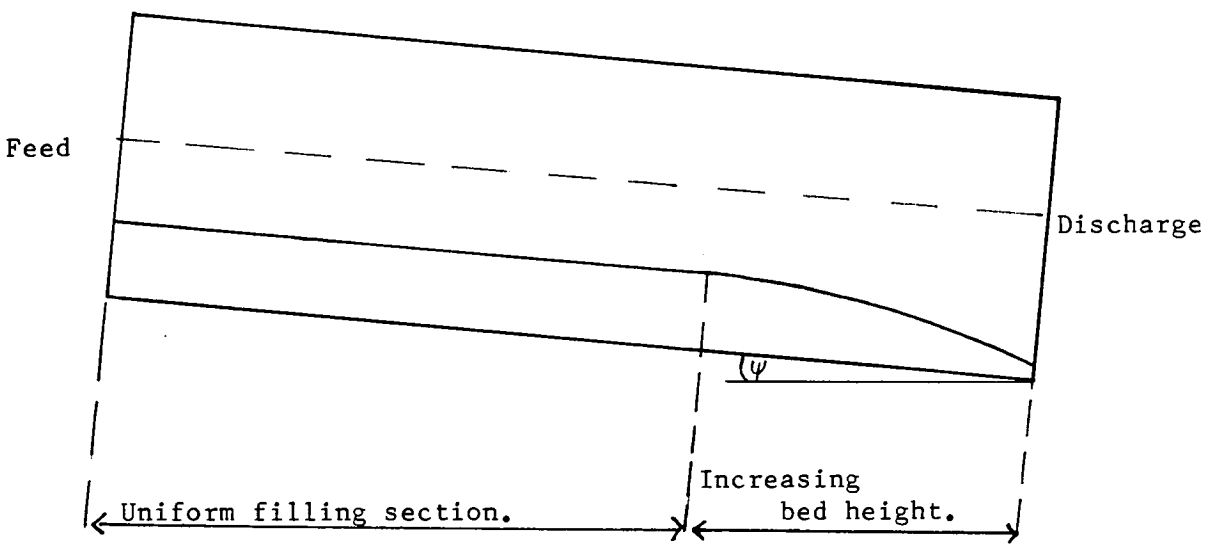

Figure 3.7 – Open ended drum in which limiting filling is attained part way up the drum

3.7 Internal Constrictions

Internal constrictions are considered to split the drum up into sections which can be dealt with as individual drums. The discharge end filling is thus determined as previously discussed and (3.10) is integrated until the x coordinate matches the distance in from the discharge end of the location of the first internal weir. At this point the bed height over this weir is determined as for the discharge constriction, if this height is less than that already reached by integration of (3.10) then the latter is used, otherwise it becomes the starting point for integration from here to the next internal weir. This procedure is repeated until the drum inlet is reached at which point the filling in each section is multiplied by the fractional length of that section and summed with the other values to give the overall filling in the drum. If limiting filling occurs in any of the drum sections delimited by weirs then this is dealt with as for a limiting filling drum which has been discussed.

3.8 Summary

The equations which have been developed in this chapter are based on the model of the solids motion in rotating drums as postulated and first mathematically analysed by Vahl [V2] and Saeman [S2].

Earlier workers were limited by mathematical approximations introduced to simplify both the development of equations describing the solids motion and their subsequent solution. Later workers removed most of these limitations but still retained a constant of proportionality for the time a particle spent cascading on the surface which had to be determined by fitting the model to a variety of experimental results. In addition, for constricted drums, the boundary condition at the discharge end which is needed for the solution of the equations of motion was determined empirically. Both of these requirements have been removed in this chapter, the model has no longer any need for fitted constants. It still remains however, as for any fluid or solid conveying system, that the physical properties of the conveyed medium be determined. Of these the interaction of the bulk solid/drum system as reflected in the dynamic angle of repose is the most difficult to ascertain and to meaningfully represent within the model. The problems associated with

measuring this property, the errors introduced by slip at the drum wall and deformation of the bed surface have been considered in this chapter and are further discussed in Chapter 5.

In addition to removing existing empirical limitations the assumption in the model that particles re-enter the bed at the same radial distance from which they left was investigated and shown to give a better description of the motion than an alternative in which particles re-enter the bed after travelling a fixed distance down the cascade surface.

A general solution for determining the height over a weir has been developed in this chapter. This and the fact that it is no longer necessary to fit constants for the model has allowed a general solution technique for drums of any size with one or more weirs at any point along their length to be developed. The solution is effected using a digital computer, the flowsheet for this process is given in Figure 3.8.

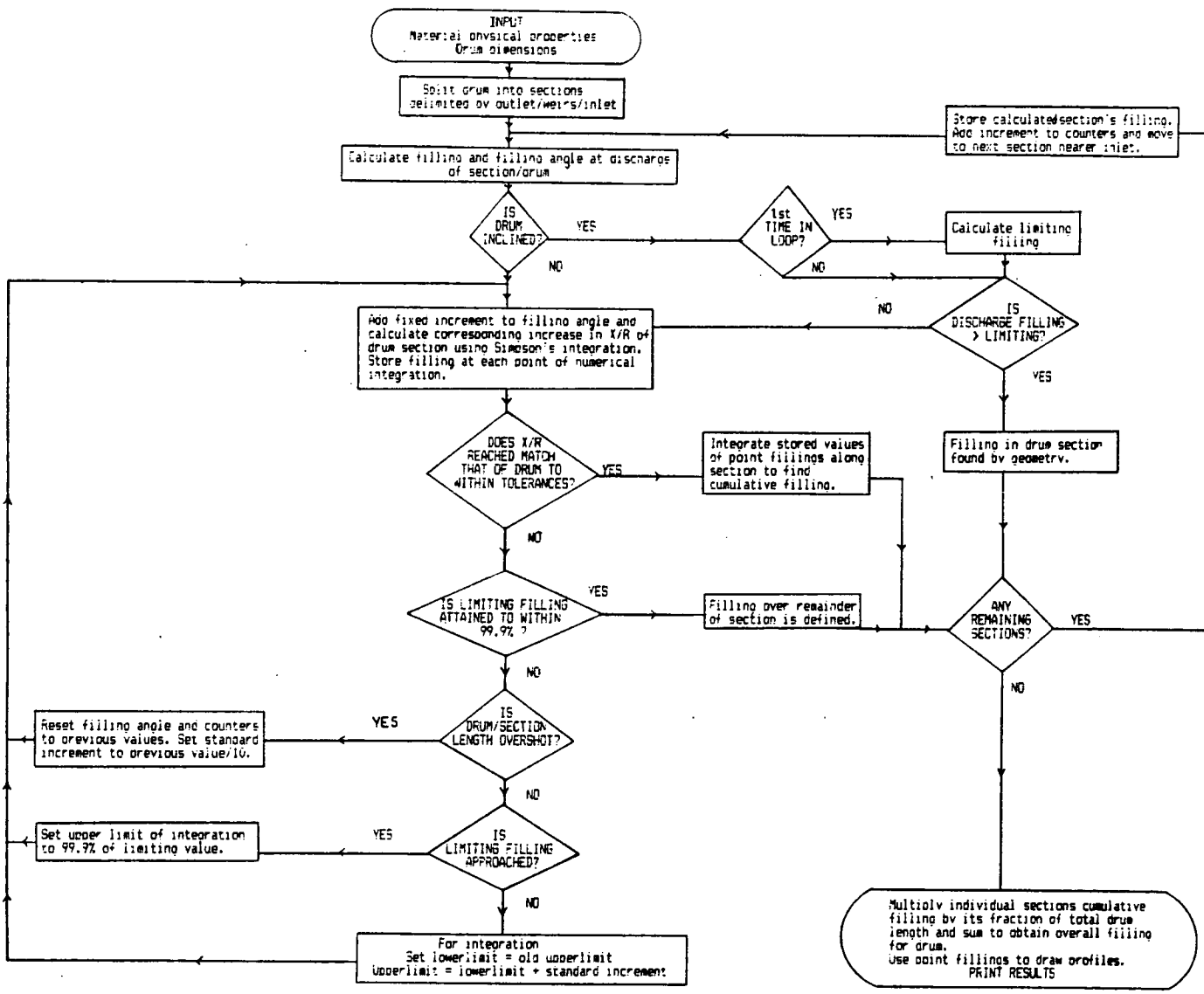

Figure 3.8 Flowchart for Solution of Equations of Motion for Solids in a Rotating Drum

CHAPTER 4

Experimental Equipment and Technique

Introduction

This chapter gives details of the experimental methods and equipment used in this investigation. Section 4.1 deals with measurements associated with the bulk solids used. Techniques for measuring bulk density and angles of repose are discussed along with their associated errors. Feed systems for the rotating drums are considered in Section 4.2. Section 4.3 discusses the experimental drums employed, their detailed design and drive system are described in 4.3.1 and 4.3.2 respectively. The method of discharged solids collection and sampling is given in section 4.4. Finally the experimental technique is described in Section 4.5.

4.1 Determination of the Properties of the Bulk Solids

The bulk solids used for flow-through experiments in this investigation were Grade 3 Glass Ballotini and Grade 15 Garside sand. Particle size distributions are given in Appendix 5. The other physical properties of interest for these materials are as detailed below.

4.1.1 Bulk Density

The bulk density for the materials was measured using a 250 cm^3 measuring cylinder and a known mass of bulk solid. For Ballotini the test weight was 400 grams and for sand 350 grams. The solid was introduced to the cylinder through a funnel and the volume occupied was noted. The cylinder top was then covered and the cylinder slowly inverted then replaced, this allowed the solid to adopt alternative packing configurations. The process was repeated until the mean and limiting values for bulk density were established (10 inversions were adequate). The errors associated with the weight and volume measurements were less than 1%. The variation due to packing gave the following results for bulk density.

Ballotini 1.78 $g/cm^3 \pm 6\%$

Sand 1.47 $g/cm^3 \pm 4\%$

4.1.2 Static angles of repose

The static angles of repose were measured using the "tilting box" and "natural fall" methods. For this a perspex box as shown in figure 4.1a was constructed. This was pivoted along one end and rested upon a laboratory scissor jack which had been modified so that the box's point of support was tangent to a cylindrical bar to ensure a smooth motion as the box was raised. The "tilting box" method as its name suggests involved slowly raising the free end of the box until slip occurred at the free surface. At this point the angle of inclination of the box was measured and taken as representative of the material's static angle of repose (see figure 4.1b). The base of the solid containing box section was made of rough porous sintered metal plate, this and the plenum chamber beneath it was incorporated in the box design in anticipation of the need for information on the variation of static angle of repose with

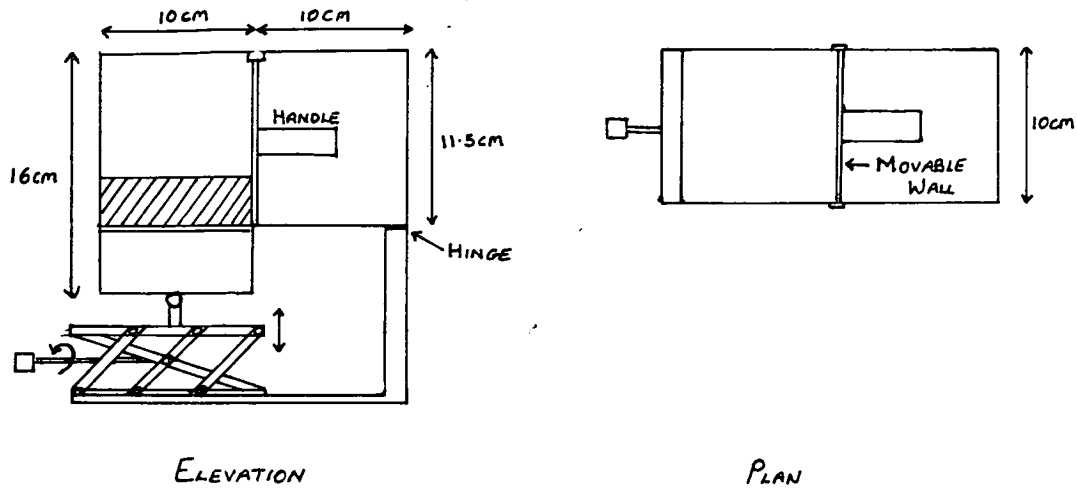

Figure 4.1a - General dimensions of static angle of repose measuring device

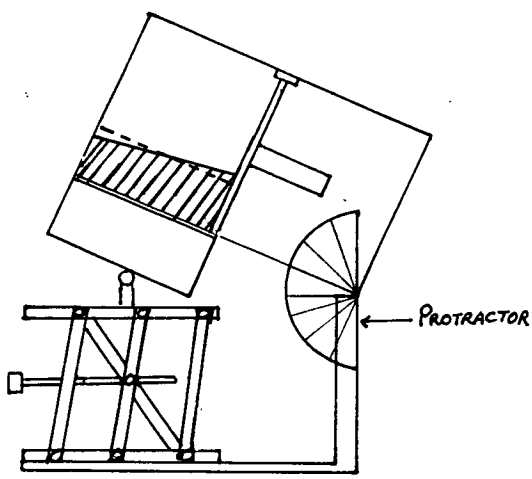

Figure 4.1b - Tilted box after surface slip has occurred

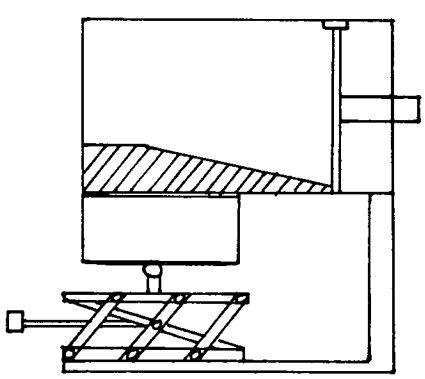

Figure 4.1c - Profile of charge after slow withdrawal of moveable wall

fluidisation or air flow through the charge. In the event this variation was not investigated.

The "natural fall" measurement of angle of repose utilised the movable wall shown with handle in figure 4.1a. The box and its enclosed solid charge were levelled and then the movable wall was steadily withdrawn until no further collapse of the charge occurred (see figure 4.1c). The angle of the free surface to the horizontal was taken as a measure of the materials static angle of repose.

There was no difference in result for both of the above methods when using ballotini. This had a value for the static angle of repose of 24.5° $\pm$ 0.5°. This is in keeping with Train's [T1] observation on the angle of repose of spherical particles. For sand however the "box tilt" method gave a value of 35° for α_s and the "natural fall" method 34°, the value for sand was taken as 34.5°.

4.1.3 Dynamic angle of repose

This is widely recognised to be very difficult to measure with solid material issuing from the discharge end of a drum, the most accessible point for measurement. It was decided therefore to measure dynamic angle of repose indirectly using a photographic technique. For this the use of video with its ease of processing and "on line" analysis was adopted.

Two scales were arranged parallel to the front face of the drum, one on each side of the discharge opening. The video camera was aligned so that the scales bounded the edge of the picture on the monitor and the centre of the screen was occupied by the mid point of the bed surface. This configuration allowed a straight edge (a thin strip of paper) to be placed across the screen in line with the image of the bed surface. This edge extended beyond the drum walls in the picture and intersected the scales on either side of the discharge constriction (figure 4.2). The scales were calibrated in centimetres and the difference between the points of intersection gave a value for the 'y' coordinate which when combined with the known distance between the two uprights, 'x', allowed the dynamic angle of repose to be determined from the inverse tangent of y/x. The potential for parallax error was minimised by using two parallel perspex plates etched with a 1 centimeter square grid (figure 4.3). These were placed at the discharge point on the drum drive table and

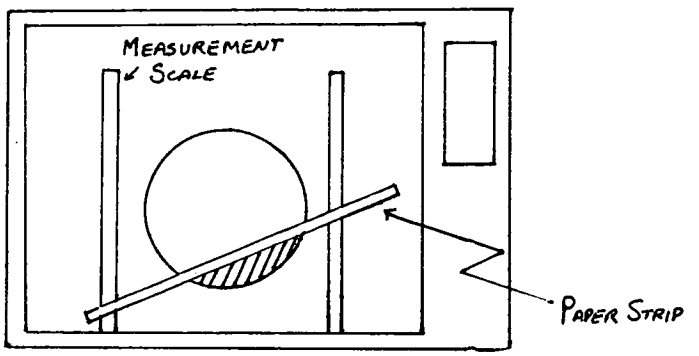

Figure 4.2 - Configuration of drum discharge, vertical scales and paper measurement strip on video monitor

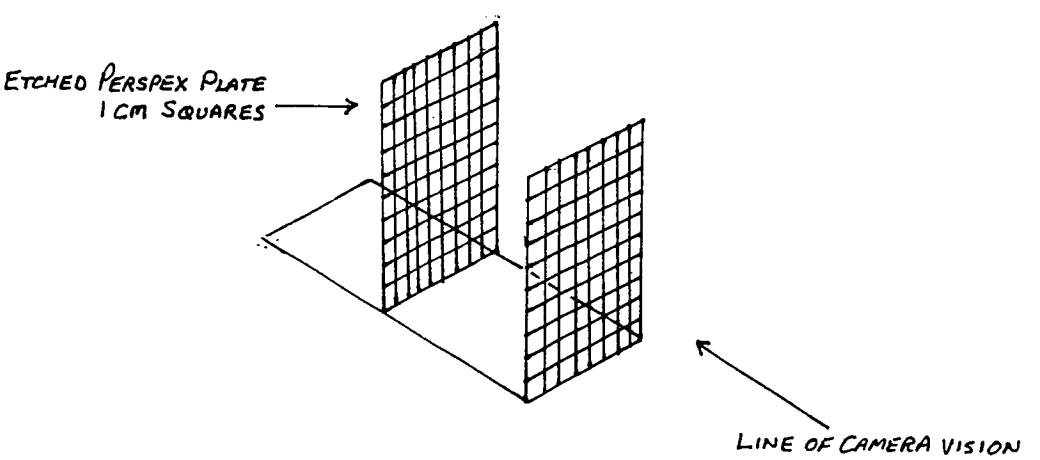

Figure 4.3 - Parallax test grids

by selecting the grid lines which covered the area which would be occupied by the bed surface the camera could be arranged so that the horizontal and vertical lines on the front plate exactly obscured those on the back plate in the region of interest.

During an experiment once the system was running at steady state the motion at the discharge end was recorded for a period of approximately twenty seconds and the run number added to the sound track. Noting the position on the tape counter allowed the data to be readily extracted from the recording at a later stage. The maximum error in the measurements used to determine the trigonometric ratios was $\pm$ 1.5% arising for the lowest angles measured. Over the filling ratios used in this investigation a sensitivity analysis showed that variations of up to 10% in α_d had a maximum effect on the magnitude of the filling of 40% of the magnitude of variation in α_d. Thus the error in α_d measurement will affect the computed filling's value by $\pm$ 0.6% at most.

4.2 Feed Systems

Two methods of feeding bulk solid material to the rotating drum were employed. In the first a small vibratory feeder was used. This was found to require a constant head of solid in order to achieve uniform feed rates. A constant head was maintained using two concentric cylinders. The inner fed the vibratory feeder directly while being topped up itself with a flow rate of solids greater than that removed from its base. The surplus cascaded over the top and back to a reservoir from which the circulating flow was taken using a compressed air "riser" arrangement (figure 4.4). It was also found that a cylindrical discharge nozzle gave steadier feed rates than the standard "chute" supplied with the feeder. For this a unit which had previously been fabricated for feeding pigments was used (figure 4.5). The system overall, shown in figure 4.6, had an upper feed rate limit of 5 g/s beyond which the cylindrical discharge became choked. Rather than attempt to modify the system and enlarge its bulk material capacity it was decided to use a screw feeder which allowed much larger feed rates (limited only by the gearing to the drive shaft) and included a large capacity feed hopper (figure 4.7). This unit was coupled to a variable speed gearbox and gave uniform feedrates over the whole range of rotational speeds. Uniformity of feed rate was considered achieved if the feed system consistently delivered amounts of material which when collected over

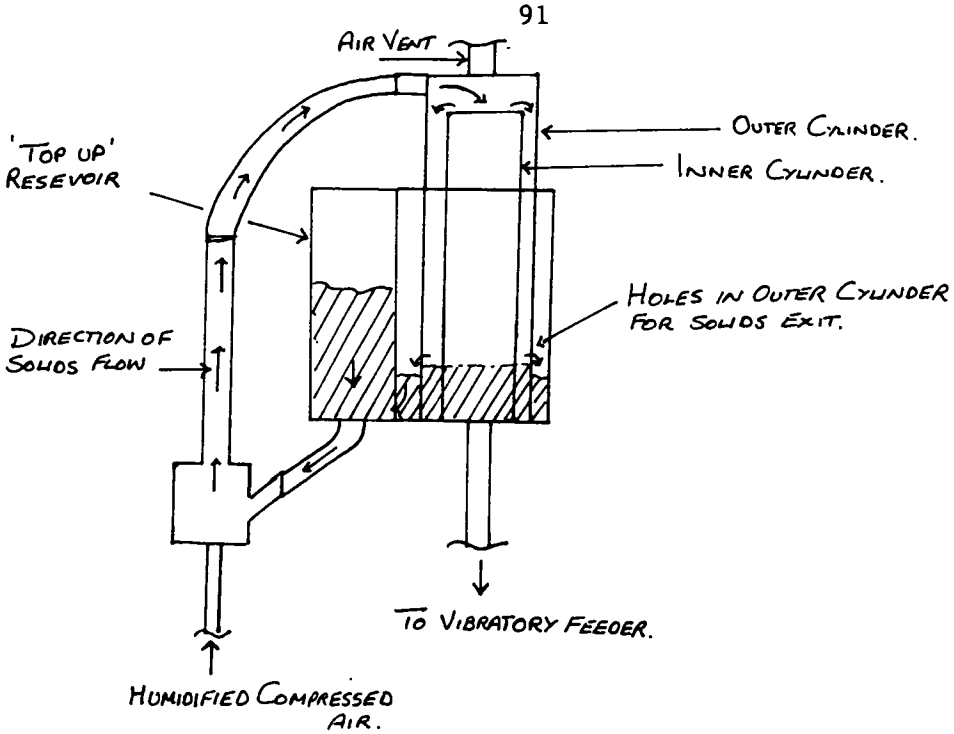

Figure 4.4 - Recirculating solids flow arrangement for maintenance of constant head above vibratory feeder

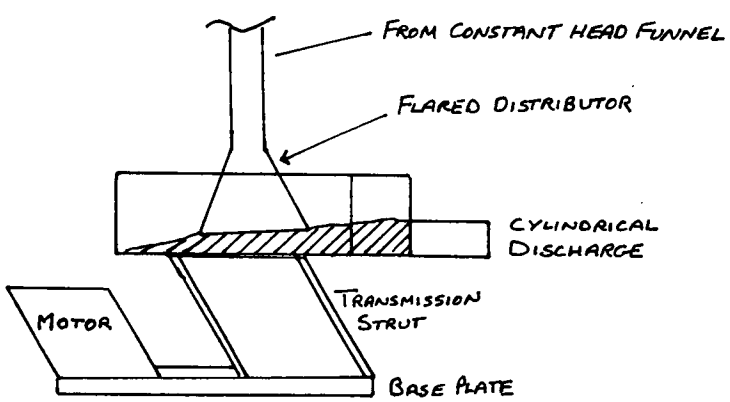

Figure 4.5 - Modified vibratory feeder arrangements

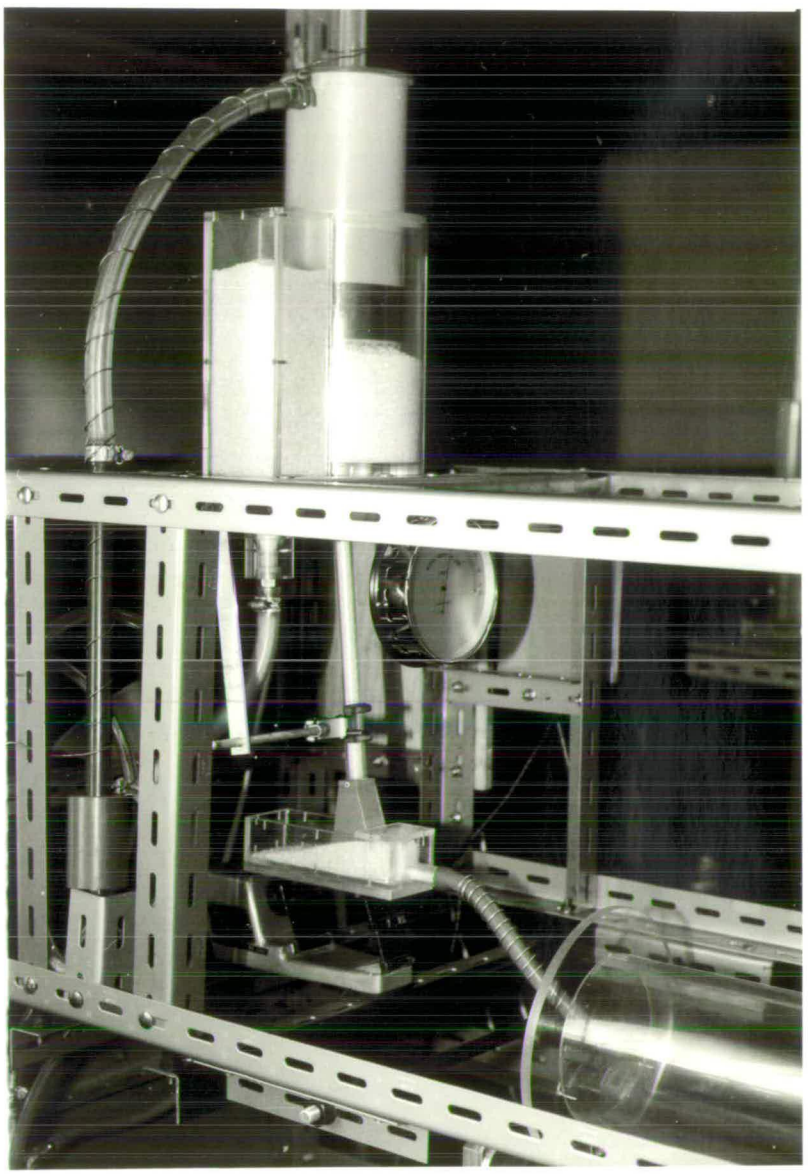

Figure 4.6 - Photograph of overall vibratory feeder system

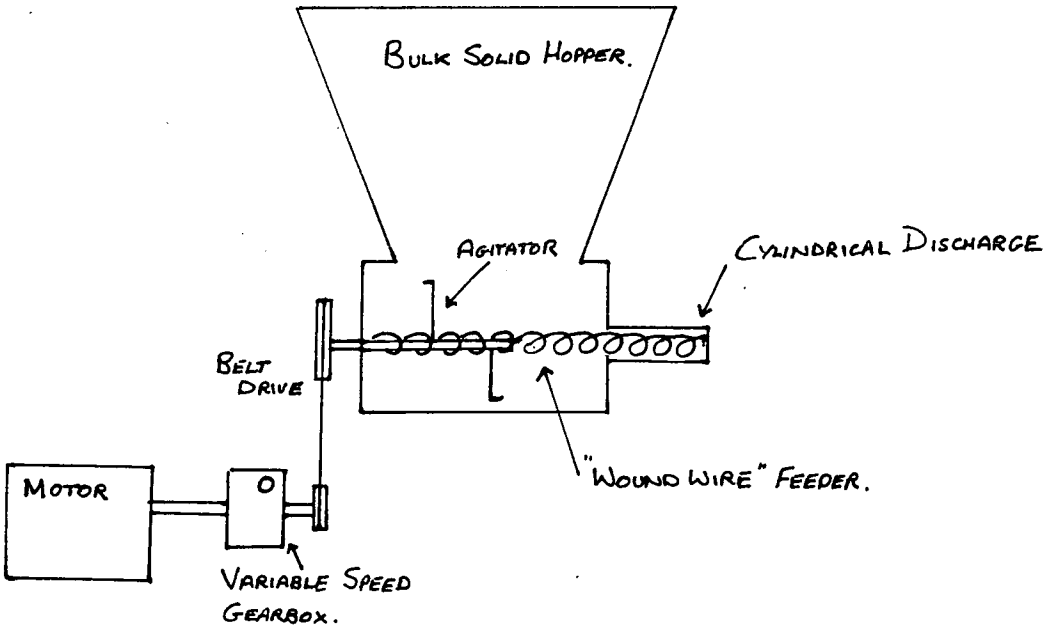

Figure 4.7 - Arrangement of screw feeder

a fixed time (in this case 1 minute) did not vary in weight outside the bounds of experimental error associated with the measurement technique. The latter was around 3.5% decreasing with increasing feed rate as the fixed error in weighing became less significant with increasing sample size.

4.3 Drum and Drum Drive

The objectives in designing this system were to provide the ability to drive drums of various dimensions over a wide speed range and various inclinations. To this end a drum drive table able to receive drive and locate the discharge end of different drums was constructed. The drums themselves were constructed to minimise the degree of table adjustment required.

4.3.1 Drum Design

The drums were constructed using PVC tubing. The tubing was machined to ensure that the bore was uniform and of accurately known size. It was decided to run the drums on "roll rings" similar in concept to the "tyres" on commercial kilns, these were arranged to be the end flanges of the drums. The discharge end flanges also provided the means of varying the discharge opening. They were made removable and each had a central hole machined as shown in figure 4.8. The flanges were sufficiently thick to ensure rigid support of a fully loaded drum. As it was desired to have a thin discharge lip the central hole was essentially countersunk into the thick flange, the resulting taper assisted solid discharge without bouncing on what would otherwise be a ledge. The flanges were all machined to a uniform diameter and fixed to the ends of the drums using screws.

For experiments with internal constrictions a drum was fabricated which consisted of two halves joined together using flanged faces. One flange was made "proud" of its associated drum wall face. This allowed discs with central holes of varying diameter to be inserted into the recess (figure 4.9) to form an internal weir on the joining of the two drum halves.

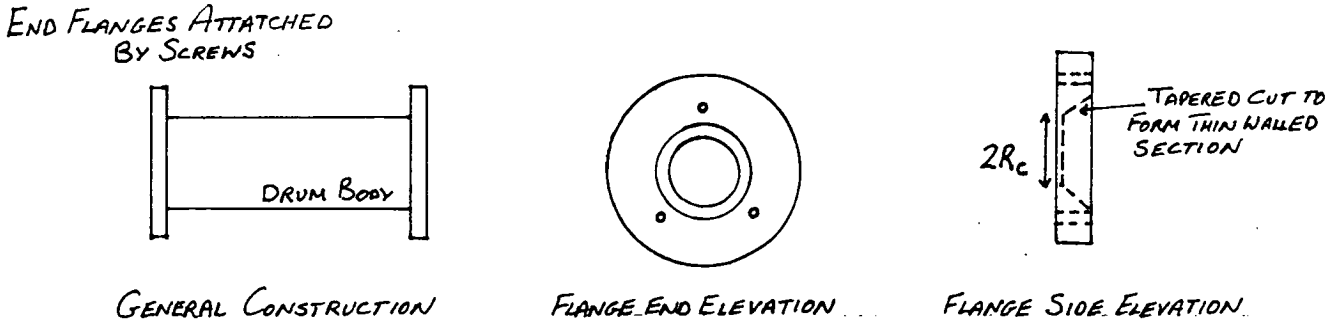

Figure 4.8 - Details of drum construction and end flanges

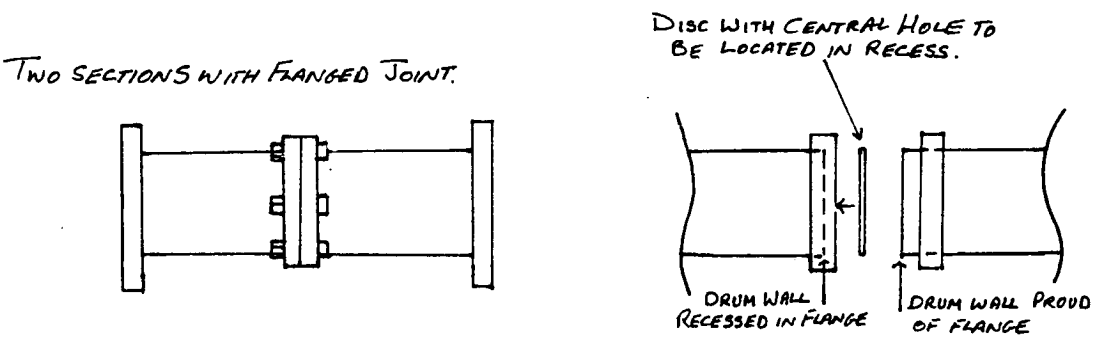

Figure 4.9 - Drum construction with internal weirs

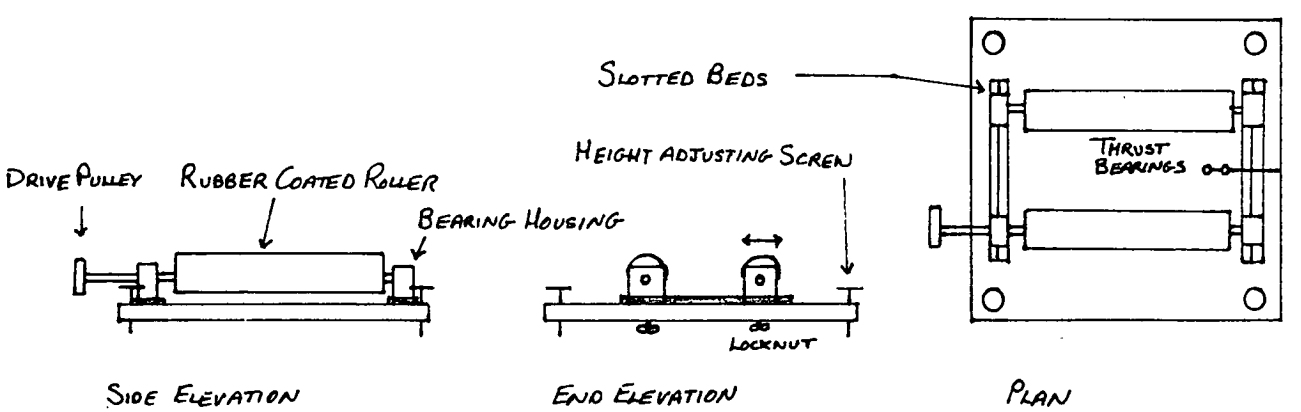

Figure 4.10 - General arrangement of drum drive table

The dimensions of the drums and constrictions used were detailed at the point of presentation of the results obtained from them in Chapter 5.

4.3.2 Drum Drive Table

This was made from a rectangular section of chipboard. Two slots were cut into opposite ends and metal slide beds were inserted. This allowed the bearing housings for the drum roller shafts to be adjusted to cope with drums of varying width (figure 4.10). Each corner of the drive table was fitted with a height adjusting screw. These were used, along with a clinometer, to set the slope of the table and thus the slope at which the drum would operate. The drum was held in position axially using two thrust bearings which could be located one on either side of the rear flange of the drum.

The drive shafts were made of 4.8 cm diameter rubber coated hollow aluminium tubing. End pieces with central shafts of 1 cm diameter connected the hollow shafts to the bearings within the housings attached to the drive table. One small diameter shaft was extended through its bearing housing and a vee belt pulley was attached to its protruding end. This pulley was coupled with another fixed to a variable speed gearbox and motor assembly. The latter was mounted on scissor jacks to accommodate the vertical displacement of the drive shaft when the drum drive table was inclined.

The drum drive system was located in a "Dexion" framework which also housed the feed and collection systems. The four points of contact between the drive table and the frame were hemispherical impressions machined from flat aluminium alloy bars which received the rounded points of the jacking screws. These bars were rubber mounted and provided virtual mechanical isolation of the drive table from the frame. By measuring the rate of rotation of the drum drive shaft and of the drum itself using a digital tachometer it was possible to confirm that the speeds varied by the ratio of their radii and thus there was no slip between the rubber coated rollers and the drum flange.

4.4 Solids Collection

Once discharged from the end of the rotating drum the solids fell onto a high sided sheet metal chute which led down at an angle of

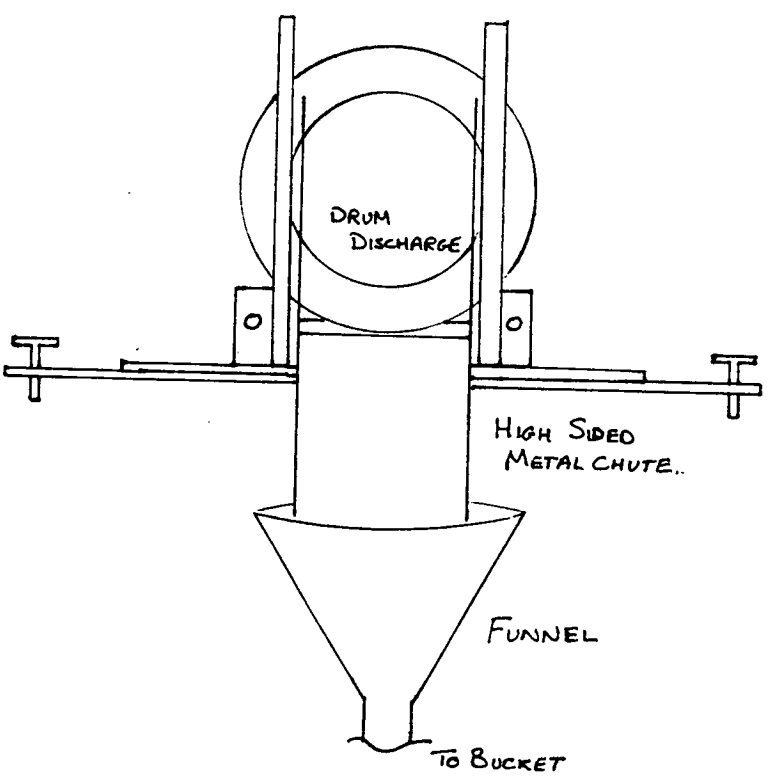

Figure 4.11 - General arrangement of solids discharge and collection

45° from the drum for 20 cm. The chute led into a wide necked funnel through which the solids were led vertically down to a large volume basin. Sufficient space was left at the discharge of the funnel to allow a sampling beaker to be inserted for collecting solids over a fixed time period. The general arrangement is shown in figure 4.11.

4.5 Experimental Technique

The following section details the experimental procedure used when determining the fractional filling in a drum of any given configuration.

Once the particular drum which was to be investigated had been assembled from the various bodies and discharge flanges available it was placed on the drive table and the rollers adjusted to ensure positive drive to the drum. The latter was checked by selecting the required rate of rotation on the motor's gearbox and then measuring the rotational speed of the drive rollers and of the drum using an optical tachometer.

Once the configuration of the drum and drive system was established attention was turned to measuring the dynamic angle of repose. The distance between the vertical scales on the roller end bearing housings was measured and noted. Next the parallax grids were placed at the mid-point between the rollers with the front face in the plane of the drum discharge. The camera could then be positioned so that the lens was in line with and parallel to the discharge of the drum. The drum was next replaced on the rollers and the discharge chute and feed chute connected. The final stage of preparation was to note the relative humidity and temperature in the laboratory.

An experiment was started by setting the drum in motion, the feed to the drum was next started. After the bed level in the drum had built up and the flow of solid from the discharge had become established the discharging solid was collected over 1 minute intervals. When the weight of three consecutive samples was in agreement within the bounds of experimental error the system was considered to be at steady state. At this point a video recording was taken over a fixed time interval with the details of the run simultaneously dubbed and a note made of the tape counter settings.

Once this had been carried out the feed to the drum was stopped at the same time a plug was placed in the funnel at the base of the discharge chute. This procedure was adopted in an effort to avoid the error which would arise if the discharge was stopped at the same time as the feed by switching off the drum. The drum would not come to rest immediately and would continue discharging during this "run down" period.

The material contained in the drum and plugged funnel was then weighed and the filling in the drum calculated using the measured bulk density of the material.

CHAPTER 5 - RESULTS AND DISCUSSION

Introduction

This chapter examines the model's predictive ability; its performance for various drum configurations, solid materials and operating conditions is analysed. Both experimental data from the literature and those obtained using the equipment described in Chapter 4 have been used, (the results are presented graphically and on each graph is the number of the table which contains the results and experimental details pertaining to the figure is given. The tables are collected together in Appendix 4.)

Attention was initially focussed on the mathematical modelling of the motion and its implementation on the computer. To this end it was expedient to use experimental results from the literature. The limited amount of suitable data and lack of properly reported physical properties led to the initiation of an experimental program. The results of this were intended to both complement and verify those already found. No attempt was made to provide a comprehensive empirical anaylsis of the relationship between hold-up and drum operating conditions as this had already been achieved in the experiments of Abouzeid and Fuersetenau [A4]. The aim was to provide a quantity and quality of data which would confirm that the model followed the observed patterns and allow the accuracy with which this was achieved to be determined.

The first section in this Chapter deals with the variation in filling with feed rate, this includes subsections on the effects of slip at bed/wall interface and the effect of different bulk materials. Sections 5.2, 5.3 and 5.4 deal with variations in filling with drum speed, inclination and discharge opening respectively. Section 5.5 considers internal weirs and 5.6 the dimensionless comparison of results. The final section provides an overview of the results in Chapter 5.

5.1 Variation of Fractional Filling with Feed Rate

The general behaviour observed experimentally and predicted by the model in which the filling increases with increasing feed rate was as had been found previously [A4, H1]. Initially the data of Abouzeid and Fuerstenau [A4] and Karra and Fuerstanau [K3] were used to test the model's ability to predict fractional filling. An example is given in Figure 5.1 in which Abouzeid and Fuerstenau's Figure 3 is reproduced along with that predicted by the model. Abouzeid and Fuerstenau considered that the relationship was linear "except possibly at the very low feed rate (below 0.5 g/sec in this system) where the rate of increase of hold-up appears to decrease slightly as feed rate increases." Despite this statement Figure 8 in Abouzeid and Fuerstenau's paper shows the same data as in their Figure 3, this time as one of a family of curves, for drums of different inclinations, all of which show a decreasing rate of increase of filling with feed rate. The curve is again presented in their Figure 9 where it has once more a region of rapid increase in filling with feed rate followed by a region of constant slope. A region of relatively high rate of increase of filling with feed rate followed by a much larger region in which the rate of increase is constant but lower was predicted by the model for all filling versus feed rate data. The angles of repose for Abouzeid and Fuerstenau's bulk solid (35 x 48 US mesh Dolomite) were not given and the dynamic angle has been taken from a later investigation into residence time distribution [A10] carried out on the same system. The static angle of repose for 14 x 20 US mesh Dolomite was reported by Karra and Fuerstenau [K2] and has been used. It should be noted that [A4] defines fractional filling as the fraction of the drum volume, minus the volume of a "core cylinder" with the radius equal to that of the discharge constriction, which is occupied by the solid bed, though this is never stated explicitly.

As mentioned in Chapter 2 Abouzeid and Fuerstenau used Hogg et al's equation (2.35) to calculate overall filling in the drum. This equation is particularly sensitive to the value of discharge end filling fc(0). None of the groups suggested in [A4, A5] when used with the method outlined there was found to give values of fc(0) anywhere near the given experimental points. This is surprising since they report only small deviations between experiment and theory using the values of the fitted constants given. This could not be confirmed and thus no "theoretical" curve from this work

included. The equations of Hogg et al [H1] for constricted discharge horizontal drums are inapplicable here as the constants they contain have been fitted for drums rotating at much higher speeds.

In Figure 5.1 the initial rate of increase in filling with feed rate is due to the need for the bed to build up a "driving head" between outlet and inlet. This becomes established over a relatively short feed rate range and thereafter increasing the feed rate results in a uniform addition to bed depth over the drum, the average axial bed surface slope remaining unchanged. The model accurately predicts the slope of the constant rate section for Abouzeid and Fuerstenau's data.

The similarities between the apparatus of Abouzeid and Fuerstenau [A4] and Hogg et al [H1] are evident in Table 2.1. A drum of similar dimensions was also used in this investigation. End plates were constructed which matched the constriction to drum radius ratio of Abouzeid and Fuerstenau and matched the largest in the range of Hogg et al. To achieve dynamic similarity the drum was rotated at the same fraction of its critical speed as previous investigations. Figure 5.2 shows the variation of fractional filling with feed rate for both discharge end constrictions. The experiments were carried out over a much wider feed range than used by Abouzeid and Fuerstenau, their curve is included in the figure and will be used when discussing the dimensionless comparison of results in Section 5.6. Here again the model predicts regions of different slope with a short transition range joining them.

Comparison of the slopes of the model prediction and the results from the experimental drum suggest that at lower feed rates the postulated mechanism of motion accurately matches the bed behaviour, as feed rate increases however the bed appears to pass material more rapidly than is predicted by the model. This is considered to be due to slip between the wall of the drum and bed and is discussed below, this topic was also considered when examining non linear bed profiles in Chapter 3.

5.1.1 The Effect of Slip at the Wall of the Drum

Hogg et al [H1] and Abouzeid and Fuerstenau [A4] were concerned with the movement of solid beds in unflighted drums as in this investigation, they did however have longitudinal lifters fitted to their experimental drums. In the case of Hogg et al these consisted

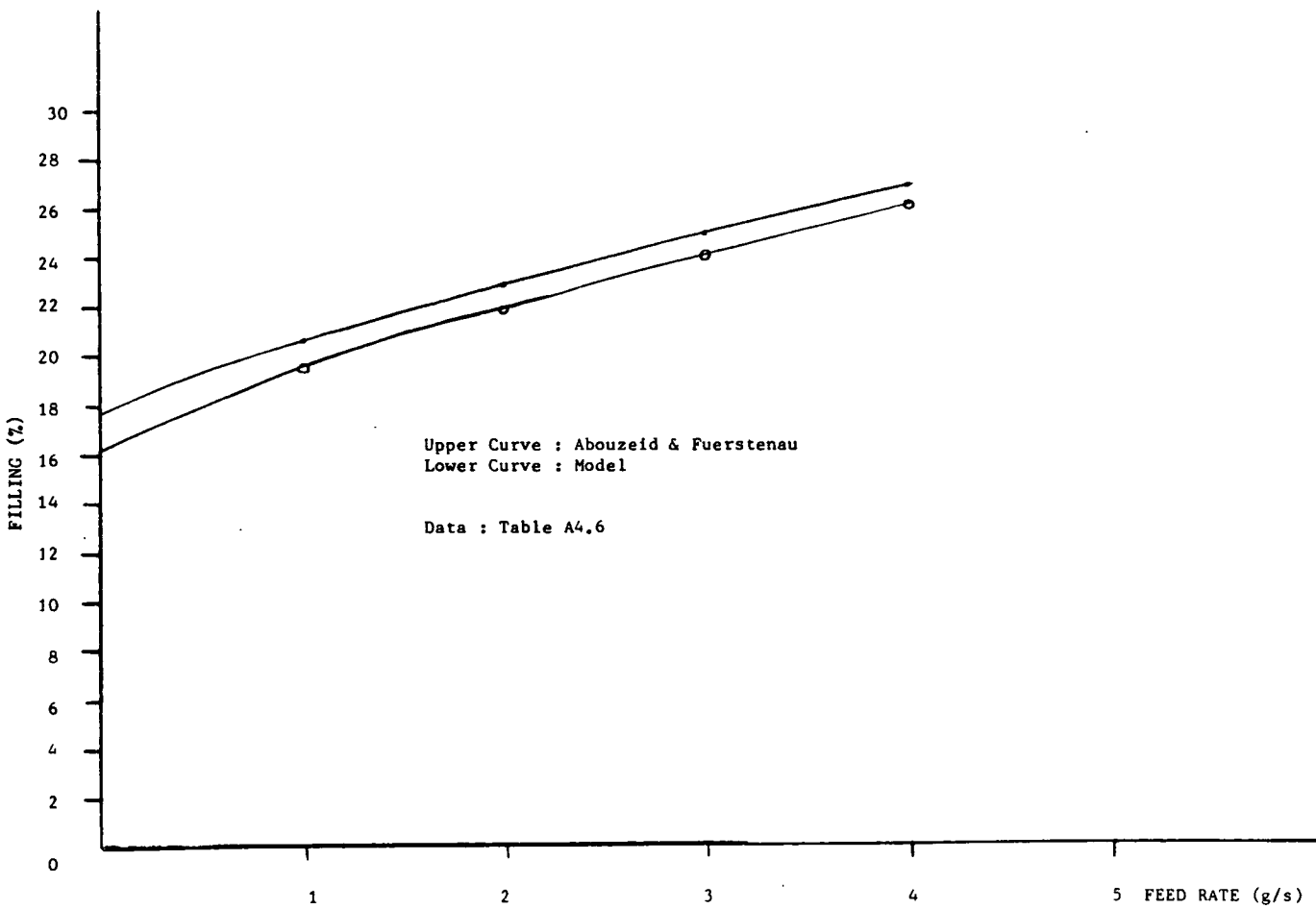

Figure 5.1 Comparison of Model with Data of Abouzeid and Fuerstenau [A4]

of eight lengths of 1/16" steel wires and for Abouzeid and Fuerstenau eight semi-circular cross section bars of 0.3 cm diameter. These lifters take up 3.3% and 3.8% of the drum radius respectively, much less than the fraction taken up by flights which is usually a minimum of 10%. Indeed the purpose of the lifters was not to carry up and shower particles through the drum cross section but to minimise slip at the wall and ensure "proper flow". It was recognised that such devices would have an effect, however small, on the motion of particles beside them when these particles were just about to cascade (see for example the photographs in Mu & Perlmutter [M2]), and so they were not used in this investigation. The drums initially available were made of plain PVC tubing as described in Chapter 4. The motion of the charge in these drums appeared steady and comprised the two sections of bulk bed movement and cascade layer expected. It was anticipated that the main effect of any slip at the wall would be reflected in the dynamic angle of repose and suitably accounted for in the model by the variation of this parameter.

There is indeed a variation in dynamic angle of repose of the beds in the drums with differing discharge constriction. The drum with the larger filling had an average dynamic angle of repose of 28° while the lesser filled drum had only 24.2°. It appears at first as though the model has responded to this difference appropriately and a good overall match is obtained for both cases. If however the shape of the curves is examined another effect of slip for which the model does not compensate becomes evident.

The lower curve of Figure 5.2 had an average value for α_d of 24.2° and the experimental values were randomly distributed about this mean. The magnitude of deviation has been considered in Chapter 4. The experimental points on the upper curve however had an increase of 1.5° in α_d over the feed rate range. This resulted in it having more of a continuous decrease in slope over its range. The observation that an increase in α_d in this instance resulted in a decrease in filling is contrary to what is predicted by the model. This can be seen as follows. The equation which defines the angle at which a particle rolls down the surface of a bed is given below for horizontal drums

$$\tan\phi = \frac{\cos\alpha_d \sin\beta}{\sin\alpha_d} \qquad (2.20)$$

As is shown in the derivation in Appendix 2 the axial advance per cascade is proportional to ($\tan \phi \cos \beta$). Thus if α_d increases, β must also increase to maintain the same axial advance per cascade and so the model predicts that for a fixed feed rate the hold-up in the drum increases with increasing α_d. The need to increase β will be offset by the decrease in cycle time which will result from particles cascading down a steeper slope, the model however predicts that overall, the effect of increasing α_d, all other factors remaining constant, is to increase drum hold up. The opposite behaviour observed experimentally is thought to have the following explanation. As the feed to the drum is increased there is a corresponding build up in bed depth. If there is bed/wall slip present in the system the increased depth of material will tend to reduce its effect and narrow the velocity difference between the drum wall and particles adjacent to it. This also results in an increase in dynamic angle of repose but contrary to the further increase in bed depth which the model predicts as necessary to maintain throughput the reduced cycle time is compensation enough. The model assumes that all particles locked in the bed move with the same speed as the drum wall and considers changes in α_d as due to changes in material properties rather than drum/solid interaction.

Any attempt to quantify the degree of slip is difficult due to the variation of the forces along the bed/wall contact arc as discussed in 3.4.2. In an effort to minimise the effect of slip the drum was lined with sandpaper, this had greatest effect on drums with low filling and the effect on the lower curves of Figure 5.2 can be seen in Figure 5.3. The sandpaper caused the ballotini to adopt a steeper slope with an average angle of repose of 27.2°. Using this value the model predicts higher fillings than for the 24.2° slope of the unlined drum. Empirically however the filling was observed to decrease. Despite the divergence of the model and experiment as the motion in the drum is made to approximate the model's "ideal" more closely the agreement is still good.

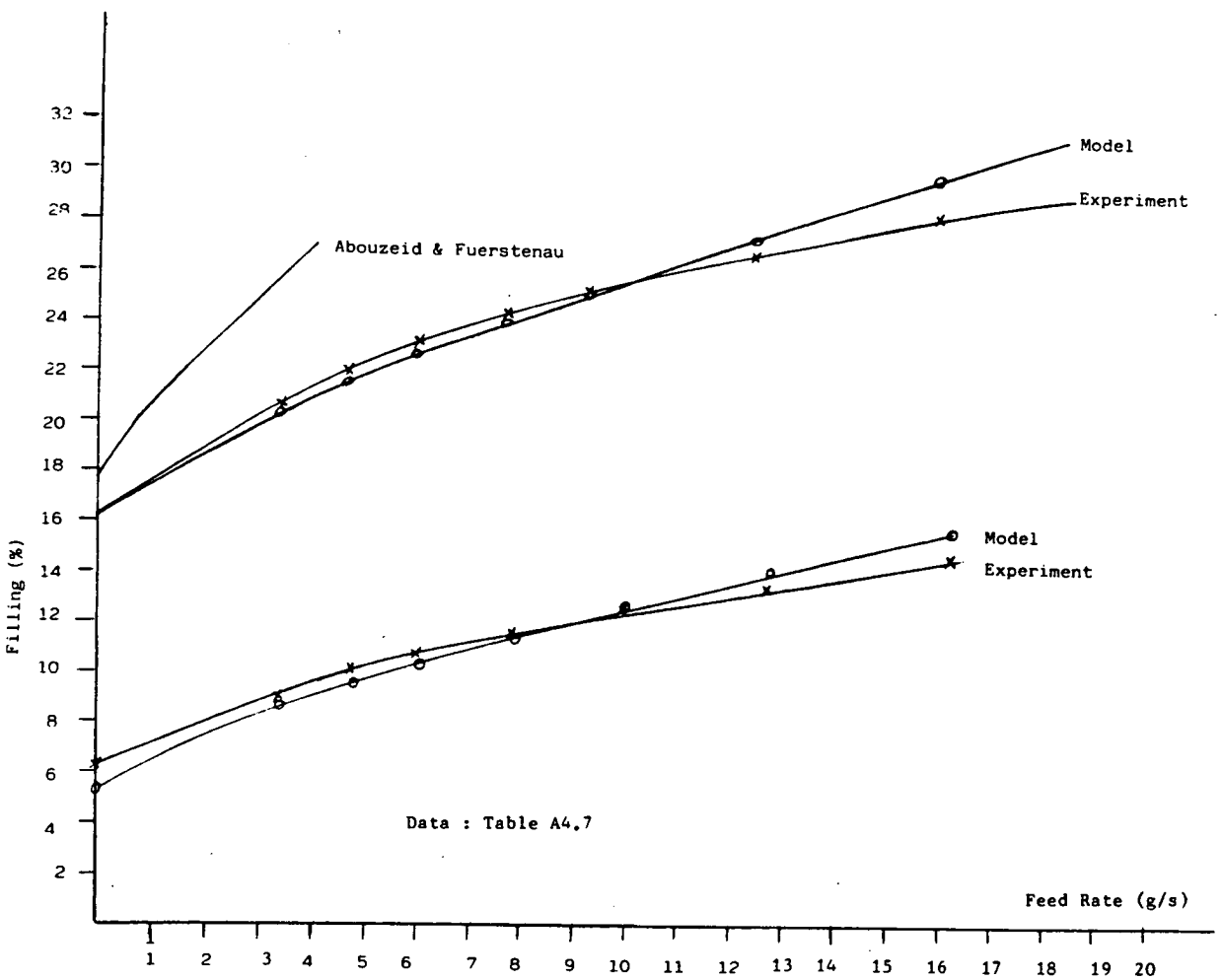

Figure 5.2 Variation in Fractional Filling with Feed Rate for Different Degrees of Discharge Constriction

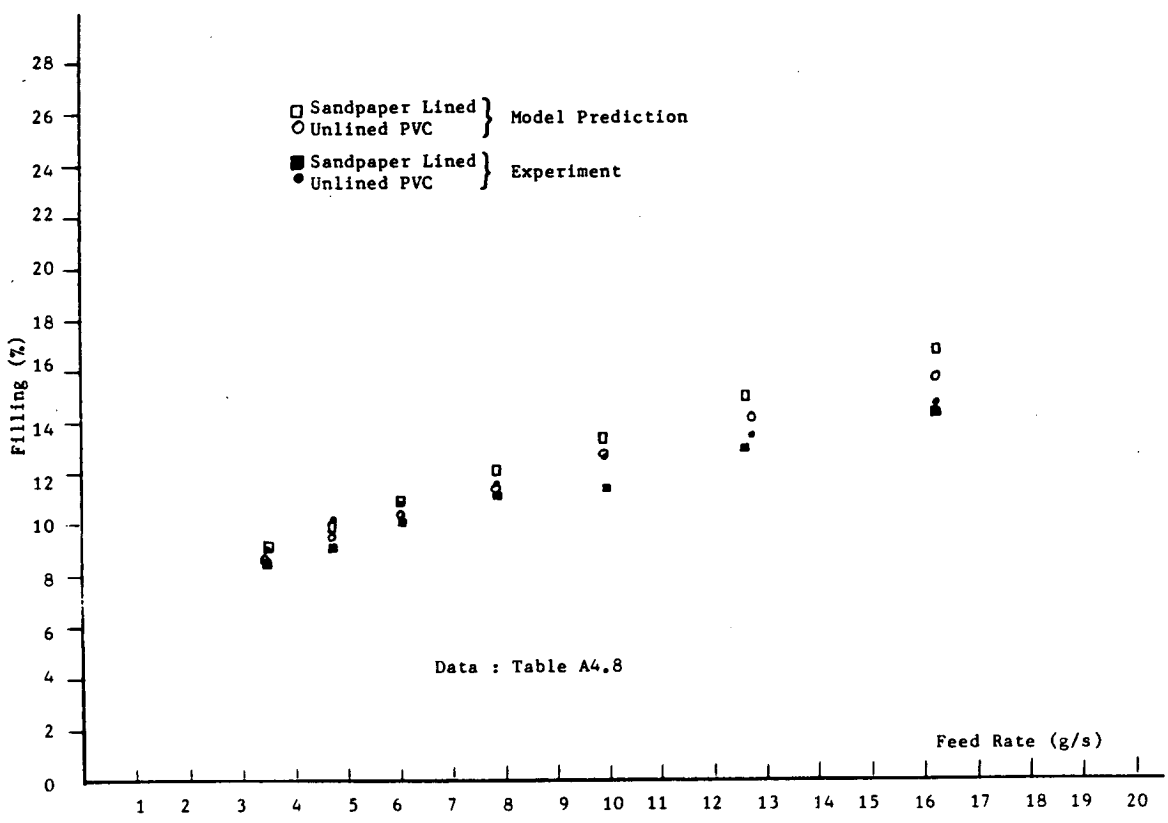

Figure 5.3 **Variation in Predicted and Observed Filling Between Lined and Unlined Drums**

The nature of the material will affect the degree of slip at the wall and may also introduce other effects as described below.

5.1.2 Comparison of Sand versus Ballotini

Prior to lining the drum with sandpaper the experiments whose results are shown in Figure 5.2 were repeated using sand as bulk material (ρ = 1470 kgm^{-3}, α_s = 34°). The results are shown in Figure 5.4 with the ballotini curves included for comparison. The hold up is much larger for sand which is consistent with the fact that it has a much higher static angle of repose than ballotini. The effect of slip, as reflected in the dynamic angle, is the opposite to that observed for the ballotini. The effective dynamic angle of repose (angle of repose was difficult to measure due to bed surface distortion) was observed to decrease as filling increased. Briscoe et al [B5] used fragmented silicates of a similar size range in their investigation and noted that for this material the increment of frictional coefficient (the ratio of frictional force, measured via torque readings on a rotating drum, to particle weight) produced by each particle-wall contact was "not very sensitive to the load on that particle". Since as filling increases the bed volume increases more rapidly than bed/wall contact area, the fact that the torque "transmission efficiency" remains constant results in the drum supporting the bed at a lower dynamic angle of response. The ballotini particles were of a much larger size than the sand and very smooth. In situations in which slip is present (unlined drums) an increase in bed volume also increases the coefficient of bed/wall friction due to its locking the particles more tightly together, preventing inter particle slip and rotation.

One further area of contrast between sand and ballotini in their behaviour in a rotating drum is in the nature of their transverse surface profile over the whole range of conditions investigated. For Ballotini there was some "deformation" at high rotational speeds (greater than 50% w_c). One or two layers next the wall were carried past the point of intersection of the bulk bed surface line and the drum wall. It is likely that the round smooth nature of the Ballotini does not provide sufficent inter particle friction to allow the bed surface to become grossly deformed by the "carry past", to a lesser and lesser extent, of particle layers progressively nearer the centre of the drum as was observed for sand. The latter exhibited an "S" or "kidney" shaped

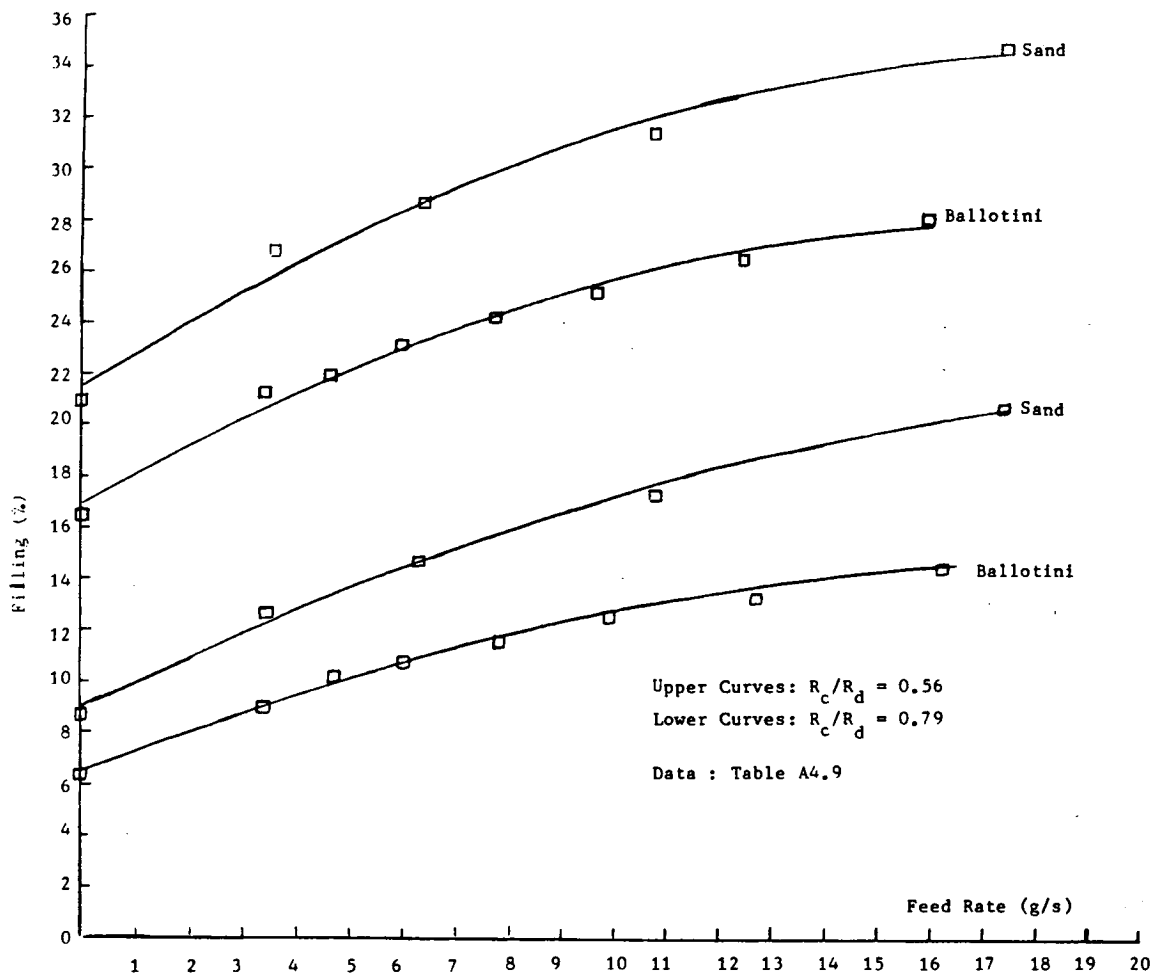

Figure 5.4 Variation of Fractional Filling with Feed Rate. Comparison of Sand and Ballotini

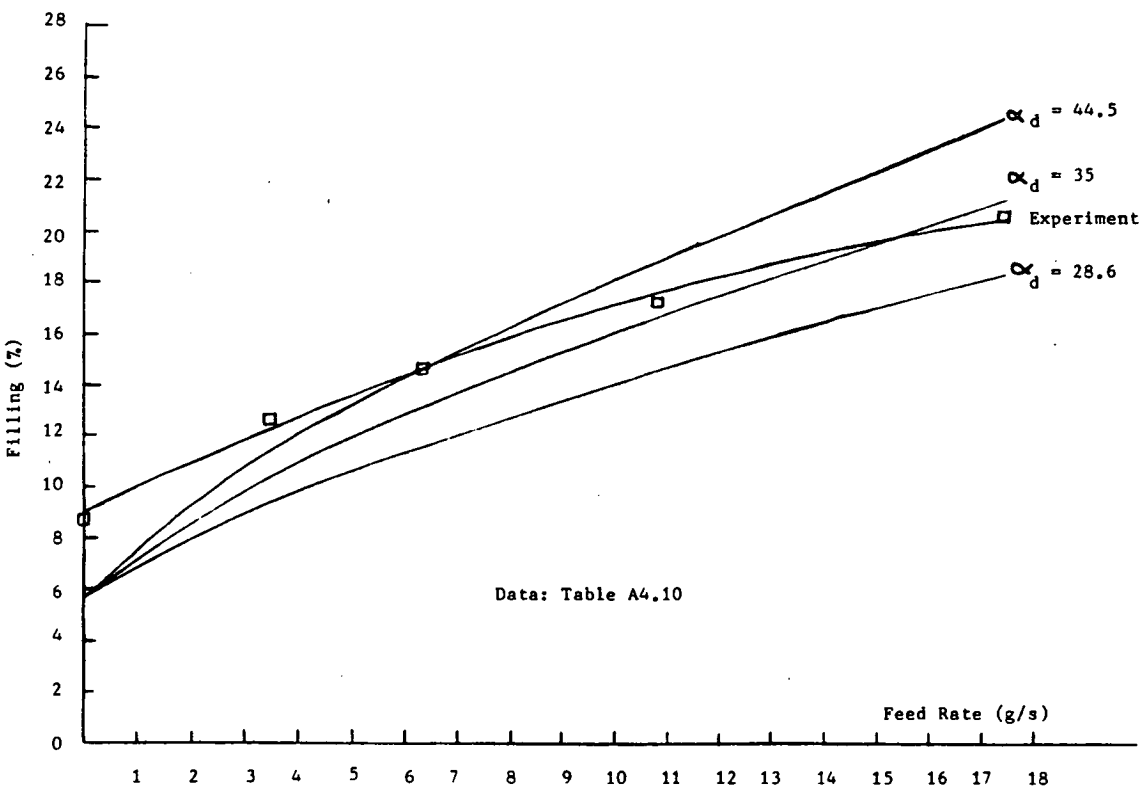

Figure 5.5 Effect of Dynamic Angle of Repose on Model Prediction

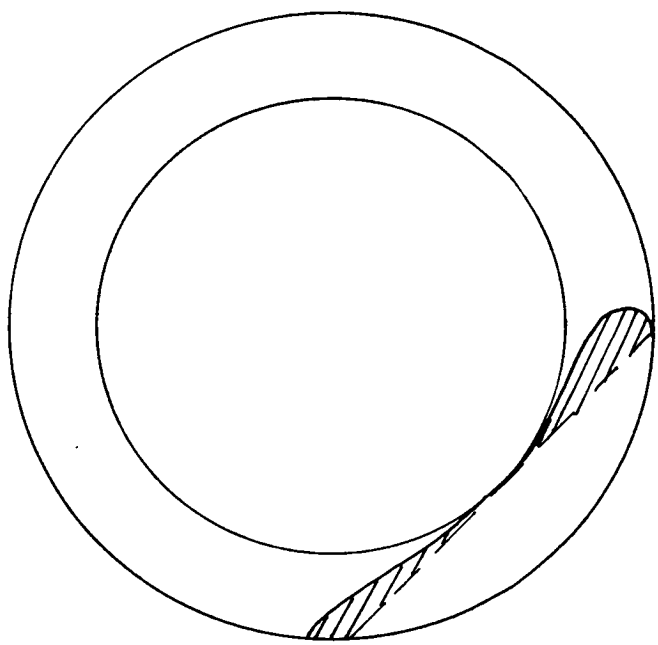

Figure 5.6 Additional Holdup (Shaded) at Zero Feed Rate Due to Bed Surface Deformation

profile which is sometimes reported in the literature and which has been mentioned in Chapter 3. Such a profile makes it difficult to determine an effective angle of repose. In addition since the model as it stands computes overall filling by integrating point fillings along the drum length which are calculated on the basis of a linear profile it cannot hope to match the filling in a drum which has a deformed bed surface over the whole feed rate range. This is illustrated in Figure 5.5 in which the experimental sand curve is shown along with the model curves calculated using the upper dynamic angle of repose exhibited by approximately the upper half of the cascade layer, the lower dynamic angle of repose exhibited by that portion of the cascade layer in which the particles re-enter the bed and the average of the two. It is immediately evident that the point of maximum discrepancy between predicted and actual filling is for the case of zero feed rate. At this point the model computes the filling by assuming no axial bed surface slope and a linear bed surface profile which is tangential to the circular discharge opening, the filling may then be found from geometry. The nature of the deformation is such that it will allow a portion of the bed to be tangential to the discharge opening while maintaining an additional "hold up" above the tangent line as shown in Figure 5.6. Since this extra hold up is not accounted for by the model a dynamic angle of repose which causes the model to match the rate of increase in filling with feed rate results in a constant difference between theory and experiment as in the lower curve of Figure 5.5.

Without altering the theoretical model, all that can legitimately be adjusted is dynamic angle of repose and as can be seen in the upper curves of Figure 5.5 this may indeed improve the overall agreement between theory and experiment over the range but at the expense of accuracy in matching the rate of increase of filling with feed rate. Underprediction at low feed rate and over prediction at higher rates was reported by Kramers and Krookewit [K1] who also used sand and noted a deformed surface profile. Predicting the nature and occurrence of a deformed surface is far from simple and though the model copes to some extent using angle of repose further work is required to improve its accuracy for this situation. The majority of the results discussed below are for ballotini in a sandpaper lined drum for which the transverse bed surface profile was linear.

5.2 Variation of Filling with Drum Speed

For a horizontal drum with fixed feed rate Abouzeid and Fuerstenau [A4] noted three distinct regions in the variation of filling with drum speed. Up to 15% w_c there is a sharp decrease in filling, thereafter it remains essentially constant until around 45% w_c where it increases. Their curve is shown in Figure 5.7 along with curves computed using the model with fixed dynamic angle of response and also using equation (3.32) which predicts an increase in α_d with drum speed as follows:

$$\alpha_d = \alpha_s + w/w_c \qquad (3.32)$$

It can be seen that with an unvarying dynamic angle of repose the effect of increasing drum speed in the model is to produce a decrease in filling the rate of which also decreases as drum speed increases.

Abouzeid and Fuerstenau did not report any value for α_d in their paper and gave no indication of any variation with speed. The fact that the dynamic angle of repose does vary with speed has been observed experimentally. Equation (3.32) does not accurately predict the observed angle of repose beyond around 5% w_c. When included in the model however it does indicate that a continuous increase in α_d with drum speed eventually counteracts the effect of the drum speed on axial velocity and produces an increase in filling with increasing speed. This is the cause of the increase observed by Abouzeid and Fuerstenau at higher speeds. The effective dynamic angle of repose was increased and there was an increasing contribution to hold up from a progressively deformed bed surface as the particles tended towards cataracting (motion in which particles are carried almost completely round with the drum wall before detaching and showering through the open area of the drum cross section). Filling decreases with increasing speed at low drum speeds because as drum speed increases so too does the rate at which particles are carried to the point from which they cascade down the surface. This, for a fixed feed rate, allows the axial distance traversed per cascade to be reduced which is achieved by lowering the axial bed surface slope resulting in a smaller bed build up from discharge to inlet. The decrease in filling continues until a minimum filling for the given feed rate is attained. The filling then remains essentially constant over a range of increasing speeds until the progressive deformation of the bed surface at higher speeds takes effect.

Abouzeid and Fuerstenau showed that as drum inclination increased so too did the rate of decrease in filling at low drum speeds. Figure 5.8 shows the fractional filling versus drum speed curve for an inclined drum for which the variation in angle of repose with speed was recorded. The model using these values follows the empirical curve quite closely. The region of largest deviation between the two is in the low feed rate range, this was also a region of larger discrepancy in Figure 5.7. The rapid decrease in filling with drum speed in these regions means that even if the slope of the curve is well matched slight displacements of the curve on the x axis result in large discrepancies between observed and predicted filling. Not only is the decrease in filling more rapid for inclined drums it also endures for longer with increasing slope. This is due to the fact that for inclined drums the fixed axial slope imparted to the bed by the drum can allow the bed surface slope with respect to the drum axis to reduce to zero. This allows the decrease in filling to progress further for inclined drums than for horizontal. The decrease is more rapid since, for similar reductions in axial bed surface slope a greater proportion of the bed volume is removed for inclined drums.

The rate of increase in filling at higher speeds is observed to decrease with increasing drum inclination. This is explained when it is considered that for a horizontal drum cataracting particles are carried up the drum wall in a path which is transverse to the drum's longitudinal axis and during free flight back to the surface of the bed they maintain this attitude and thus do not travel axially. In inclined drums however the distance travelled with respect to the drum's axis during the free flight of a particle which has been lifted, again transverse to the axis, contributes to the solid's transport through the drum.

The ability of the model to match the variation in filling with drum speed is best in the region of approximately constant filling between 15 and 50% of the drum speed. At the lower end of the speed range the effects of any error introduced by slip or bed deformation will be most pronounced due to the rapid change in filling. Above 50% w_c the model does not allow for the progression of particles towards cataracting.

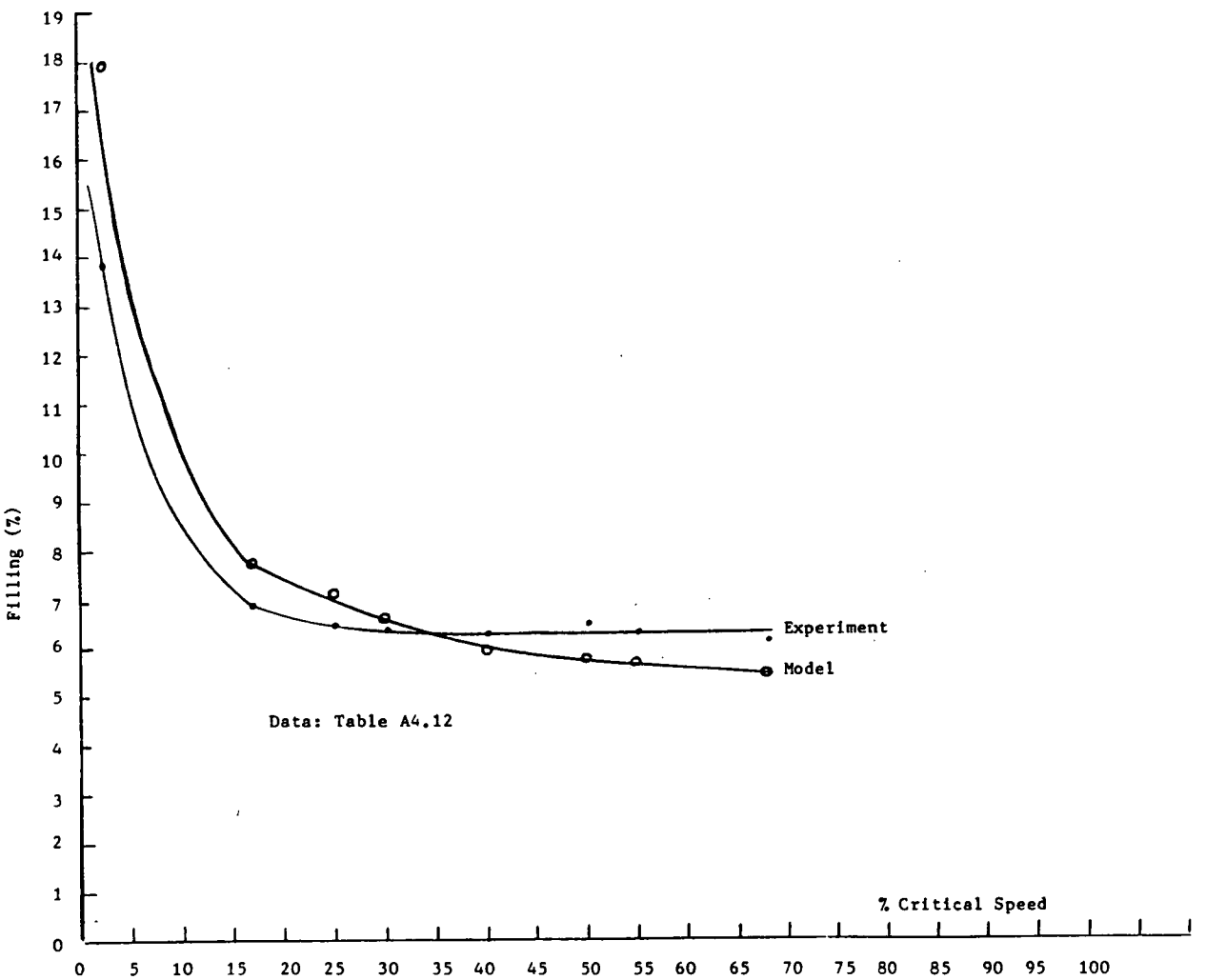

Figure 5.8 Match Between Model and Experiment for Increasing Drum Speed - Inclined Drum

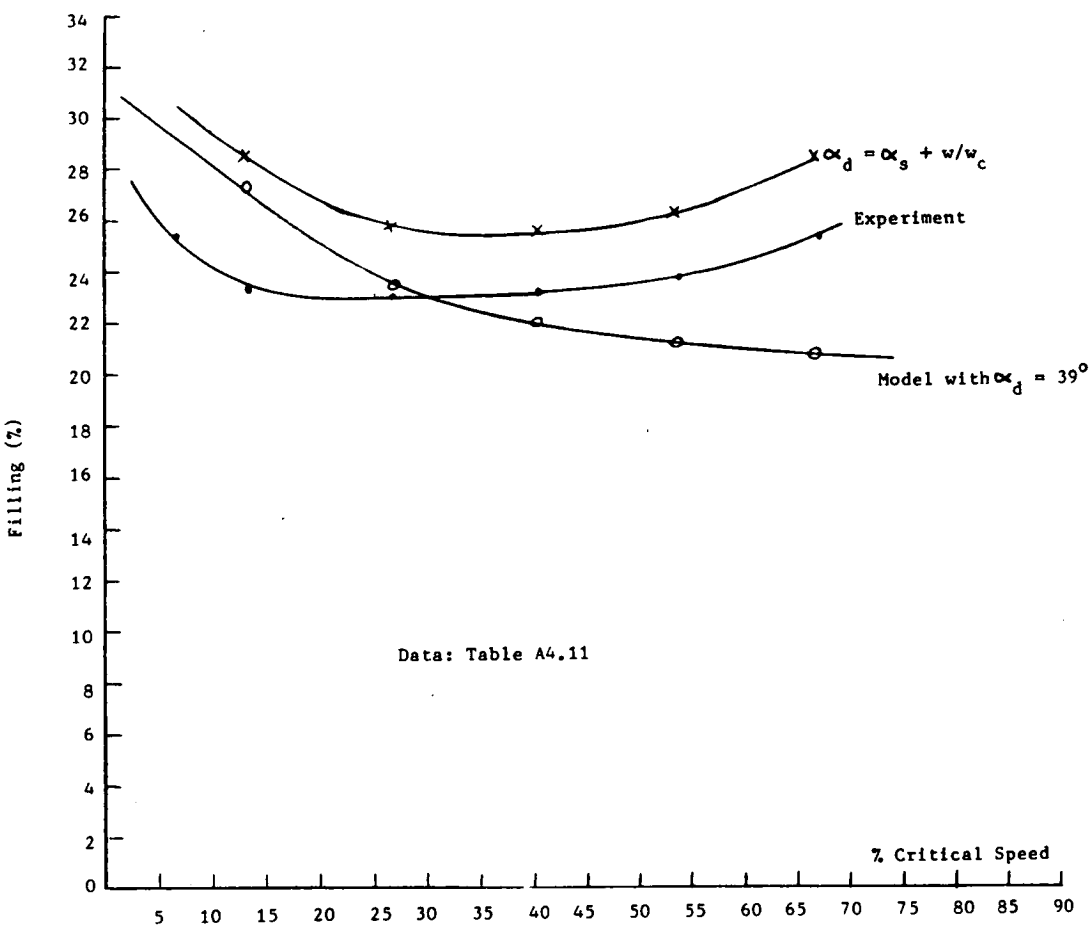

Figure 5.7 Model Prediction with Fixed α_d and α_d Increasing with Speed

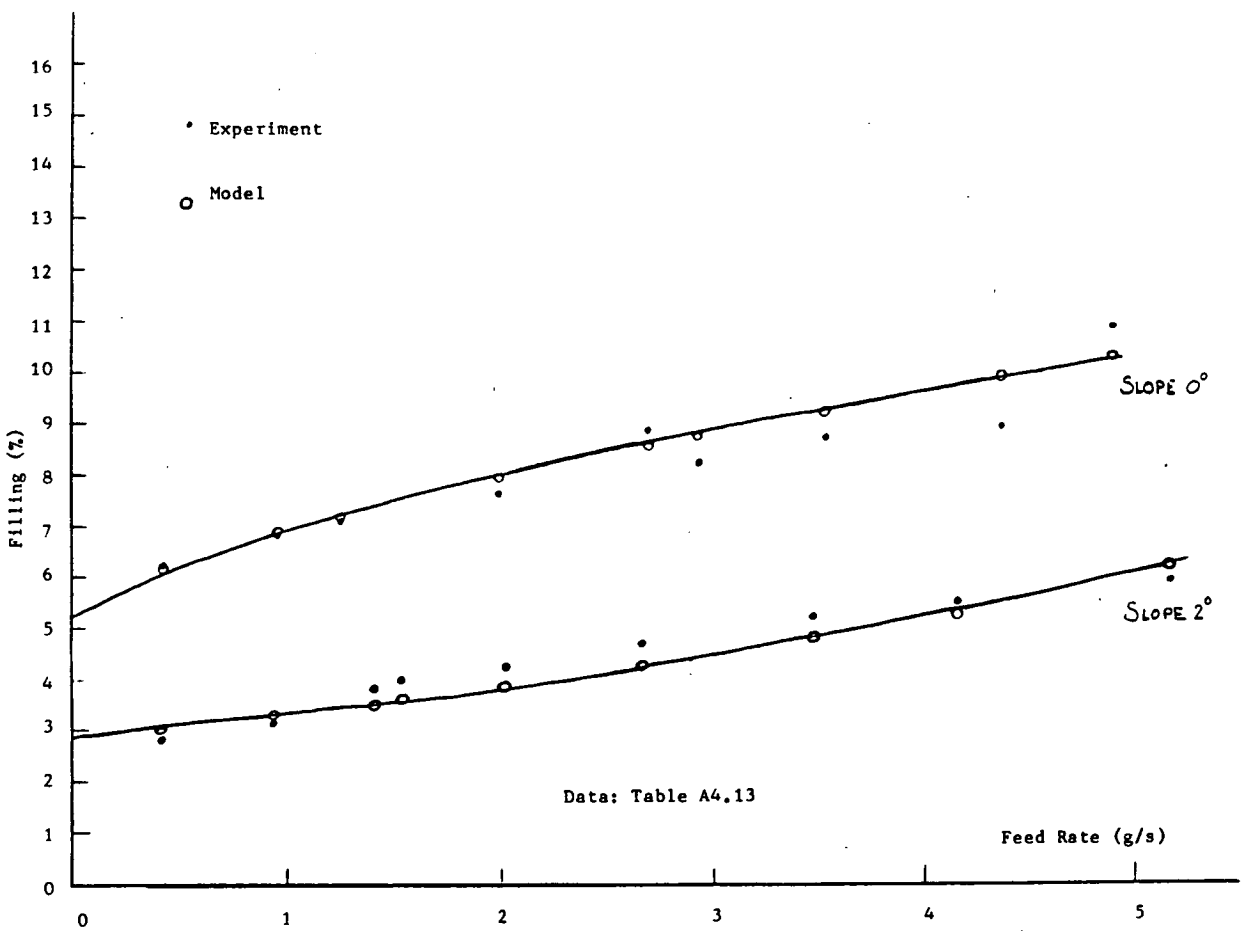

Figure 5.9 Comparison of Model with Experiment for an Inclined Drum

5.3 Variation of Filling with Drum Inclination

The variation of filling with feed rate and drum speed which have been considered in the preceding sections are all modified to some extent as drum inclination increases. The effect of drum inclination on the variation of filling with drum speed was discussed in Section 5.2. The effect of inclination on the variation of filling with feed rate is shown in Figure 5.9. Over most of the feed range the curves are similar in slope and shape. There is however a difference in behaviour at the lower feed rates. This is because of the inclined drum's ability to transport material with a bed height which is less than the discharge constriction height which has been discussed previously in 2.2 and 3.2.6 when considering "limiting filling" in inclined drums. The net effect is that as feed rate is reduced, from a point at which the bed was required to increase in height from discharge to feed end to a point at which the maximum bed height required is below the discharge consticting, the curve of filling versus feed rate reduces as for a horizontal drum. It then passes through a transition point and reduces much less rapidly due to the introduction of hold up behind the weir which is in addition to that necessary for transport. The fillings for the situation in which the discharge lip is higher than the maximum required bed height are determined by geometry as described in Section 3.6.2.

The main effect of an inclination is to allow the bed to transport a given flowrate of material with a much lower depth of material than for a horizontal drum passing the same flow. Figure 5.8 shows the model's ability to match the observed effect on filling of inclining a drum with fixed feed rate.

5.4 Variation in Filling with Discharge Opening

The relationship between filling and discharge opening for a horizontal drum with fixed feed rate, running at 27% w_c is shown using the data of Karra and Fuerstenau [K3] in Figure 5.10. This shows a good agreement between literature and theory bearing in mind that the angles of repose for this system have been gleaned from more than one source and the magnitude of deviation varies with feed rate. There is an approximately constant percentage deviation between the curves over the range. Included in Figure 5.10 are two points for the constrictions used with the small drum in this investigation, these are also for a horizontal drum rotating at 28% w_c. The rate of decrease in filling is similar to that observed for the literature data but the match between theory and experiment is better.

5.5 Drums with an Internal Weir

As discussed in Chapter 3, the model deals with an internal weir by considering the main drum to be composed of two smaller drums, one with discharge at the end of the whole drum and inlet the internal constriction, the second is considered to have its discharge as the internal constriction and inlet that of the main drum. This is readily extended to the case of multiple weirs.

Flow in an internally constricted drum can result in three separate situations viz the bed height on the discharge side of the internal constriction lies below, just matches or is greater than the height necessary for transport across the lip. Table 5.1 shows the results of experimental and model prediction for each of these situations for an extended version of the previously used drum rotating at 8% w_c in the horizontal position. These conditions gave good correlation between theory and experiment thus any error introduced by the asusmption concerning the internal weir should be evidenced by differences in accuracy of filling prediction between discharge and inlet drum sections. The drum dimensions are given in the form

length x diameter x discharge diameter x internal constriction diameter

The internal weir was located 24.5 cm from the discharge end, the drum was unlined PVC.

TABLE 5.1

Dimensions (cm)	Feed Rate (g/s)	Fillings (%)					
		MODEL			EXPERIMENTAL		
		Inlet Section	Discharge Section	Overall	Inlet Section	Discharge Section	Overall
50 x 9.4 x 7.4 x 5.25	1.72	22.6	11.0	16.9	23.0	11.8	17.6
50 x 9.4 x 7.4 x 5.25	5.00	30.8	17.9	24.5	31.3	17.9	24.7
50 x 9.4 x 7.4 x 7.4	4.95	32.3	19.0	25.8	29.8	18.0	24.0

The longitudinal bed profiles for the above experiments were drawn using the computed results and are shown in Figures 5.11, 12, 13.

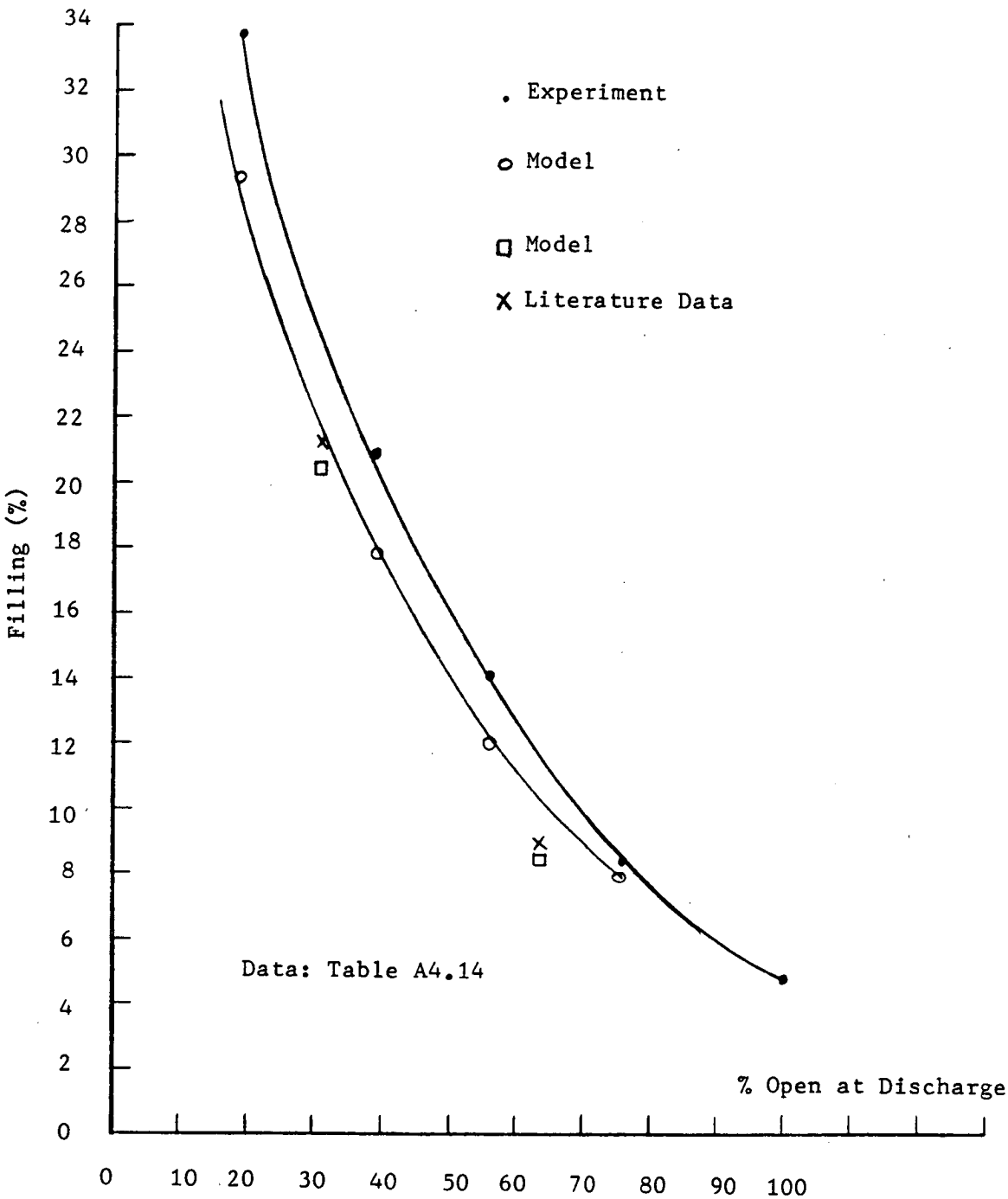

Figure 5.10 Model Prediction for Increasing Open Area at Discharge

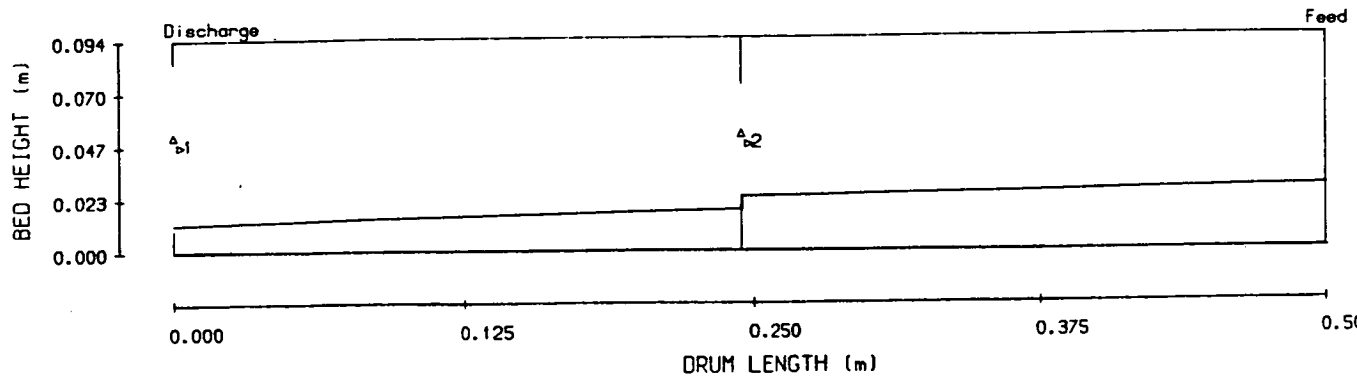

Figure 5.11 Computer Predicted Profile for 1st Data Set of Table 5.1

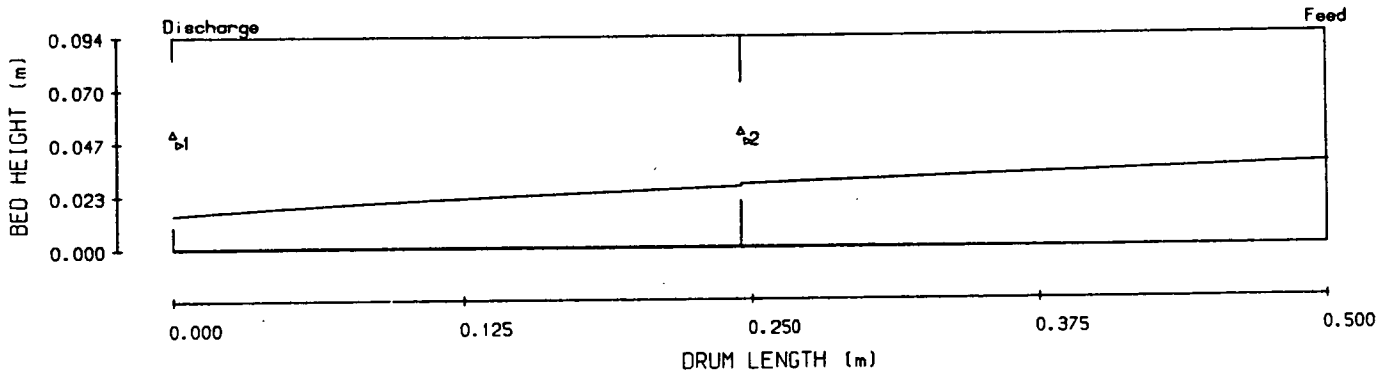

Figure 5.12 Predicted Profile for Data Set 2 Table 5.1

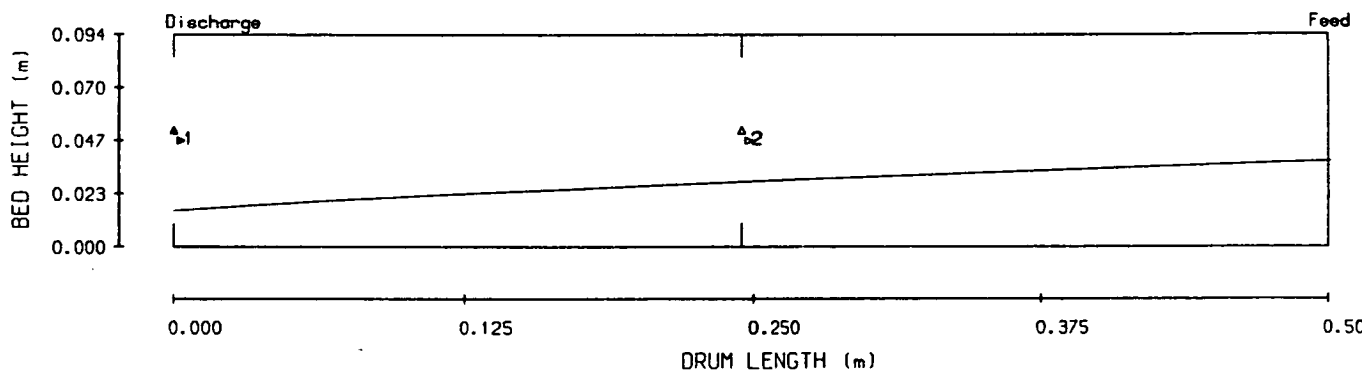

Figure 5.13 Predicted Profile for Data Set 3 Table 5.1

The bulk material was sand, density 1470 kgm^{-3} α_d 34.5°. The dynamic angle of repose for 8% w_c was not significantly different from the static value.

In all three cases the assumption that the internal weir merely introduces a bed height boundary condition which may or may not be significant appears vindicated by the agreement between theory and experiment.

5.6 Dimensionless Comparison of Results

The curve of Abouzeid and Fuerstenau [A4] was included in Figure 5.2 for comparison with the results of this investigation. The drums were only slightly different in size, the one used in this investigation had a 10% shorter length and 18% larger diameter but both drums had the same fraction of their discharge area constricted and were rotated at the same fraction of their critical speed. The differences between the literature data and the present work are quite marked, the literature curve has a much steeper slope and extends over only a fraction of the feed rate range. If however the curves are plotted using the dimensionless feed rate parameter Ψ as abscissa, (as defined by Abouzeid and Fuerstenau [A5]) Figure 5.14 shows that both drums are operating over a similar range. The ability of the parameter Ψ to place results for drums of different dimensions on a common base is further illustrated by Figures 5.15 and 5.16. These figures use data generated by the model for two drum diameters with different body lengths. Both have the same fraction of their discharge constricted and are rotating at the same fraction of their critical speed. When the filling is plotted against feedrate the curves for different drum diameter and different L/D lie in separate regions of the graph space (Figure 5.15). If however the parameter Ψ is used the curves for different diameter but same L/D become coincident. There remains however a distinction between curves of varying L/D. This is contrary to the figures presented by Abouzeid and Fuerstenau [A5] in which the curves for all L/D are coincident and the relationship between feedrate and filling is presented as linear. The drums used there spanned a relatively small L/D range of 2-6 and in their Figure 2 there is an evident discrepancy between points for L/D=2 and the others. Very few of the curves presented include points which span the L/D range. It has proved impossible to back calculate from figures in the text to find out what feed rate range was used. All

attempts result in answers orders of magnitude too large. If however the range reported in a previous paper using drums of similar dimension [A4] is used then Abouzeid's data would extend as far as the line shown on Figure 5.16. With such a short L/D and ψ range it can be seen how a linear relationship with all L/D points coincident could be achieved. It is obvious however that

$$\psi = \frac{FL}{\text{Cot}\alpha_d \rho w D^4}$$

cannot be used as a universal scale up parameter as claimed by Abouzeid and Fuerstenau. An improved correlation was found using the following expression for

$$\psi = \frac{F}{\text{Cot}\alpha_d \rho w D^3} \left(\frac{L}{D}\right)^{0.75}$$

The effect of defining ψ in this way can be seen in Figure 5.17.

It is evident from the shape of the upper curves in Figure 5.15 that it will not be possible to find a parameter ψ which will allow all the curves to be coincident over their whole length. Figure 5.17 shows greatest discrepancy for low L/D drums at high fillings. Abouzeid and Fuerstenau noted that their predictive ability diminished as drum size and L/D increased, they recommended that the largest available drum be used to fit the constants for their model to ensure accuracy at larger sizes. This illustrates again the advantage of the model developed in this work in its ability to predict drum behaviour over a wide range of operating conditions without being "tied" to constants fitted using experimental scale equipment.

5.7 Summary of Discussion

It has been shown that the wholly theoretical model derived in Chapter 3 correctly predicts the nature of the relationships between filling and feed rate, drum speed, inclination and dimension for constricted drums both horizontal and inclined. This is a considerable improvement over previous wholly theoretical models.

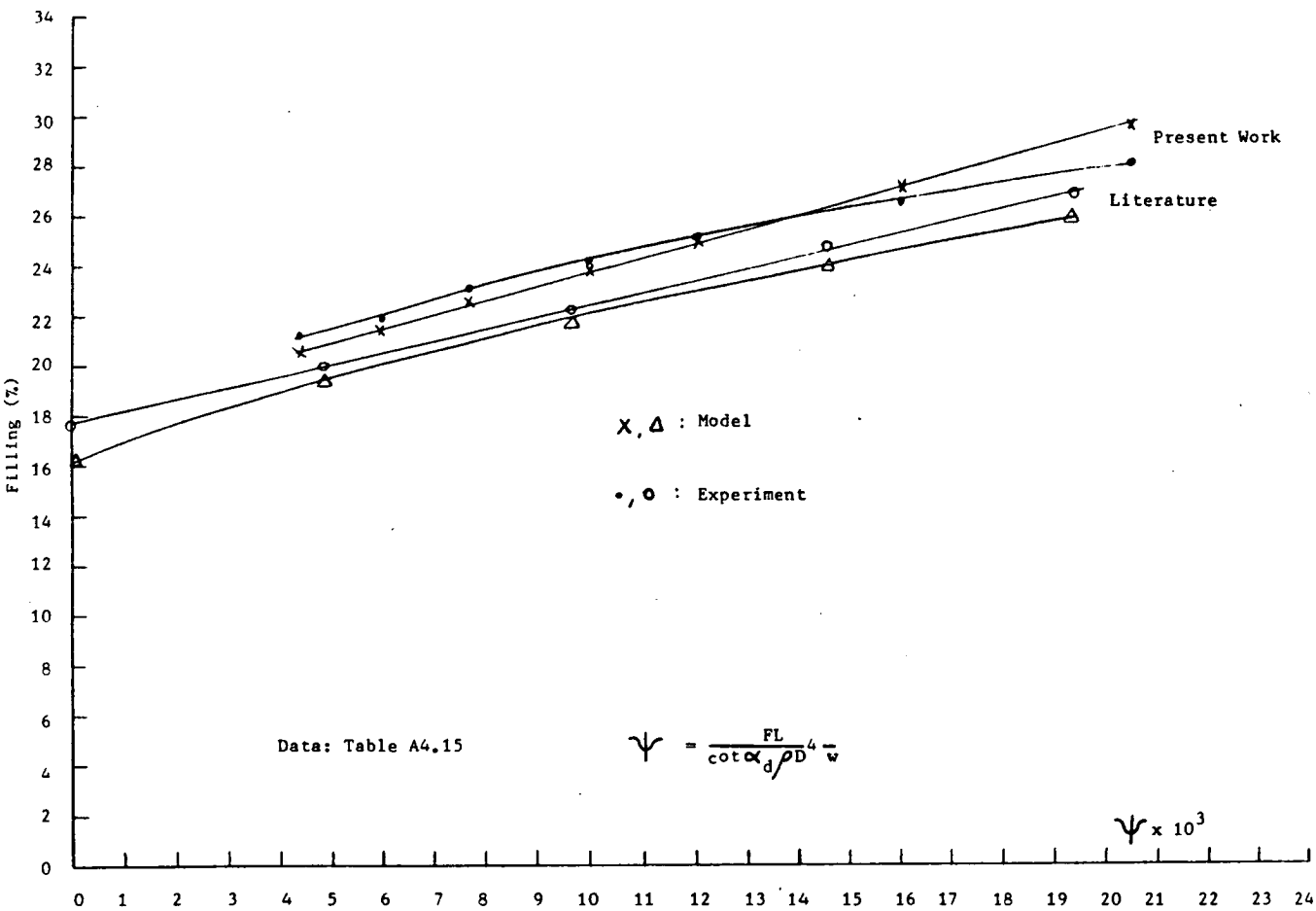

Figure 5.14 Comparison of Literature and Experimental Data from Figure 5.2 on a Dimensionless Basis

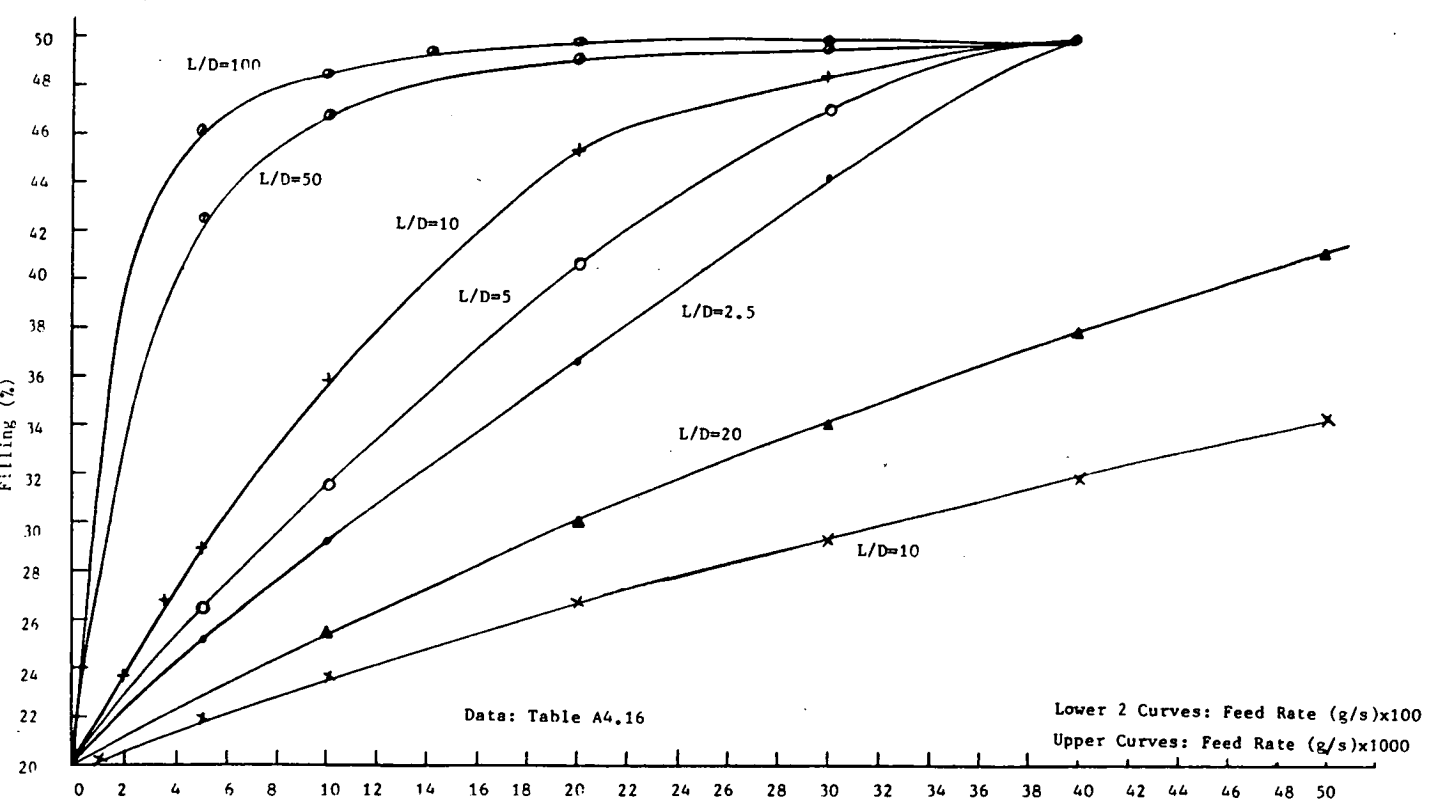

Figure 5.15 Model Prediction of Filling Versus Feedrate for Various Drum L/D

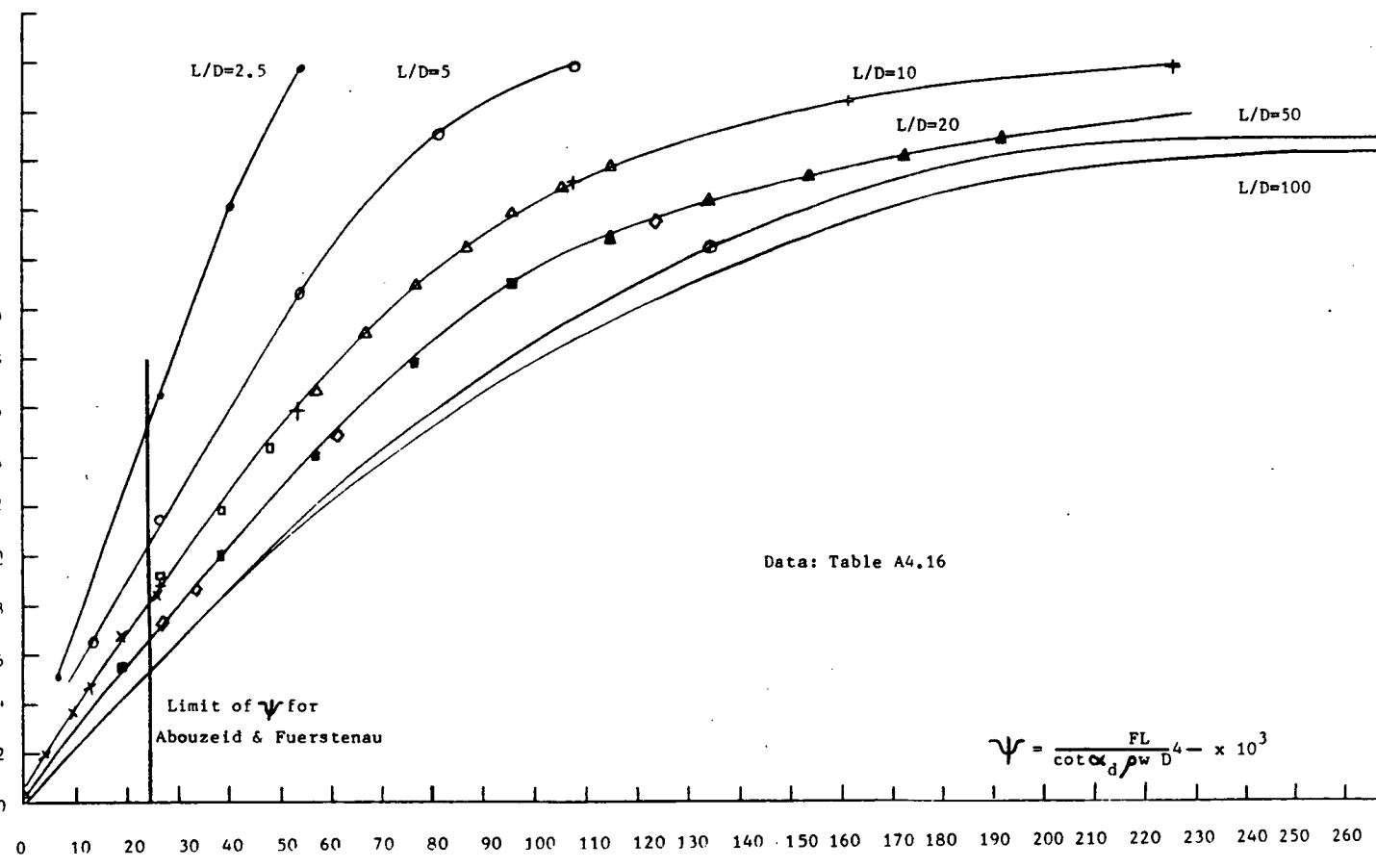

Figure 5.16 Comparison of Data from Figure 5.15 on a Dimensionless Basis

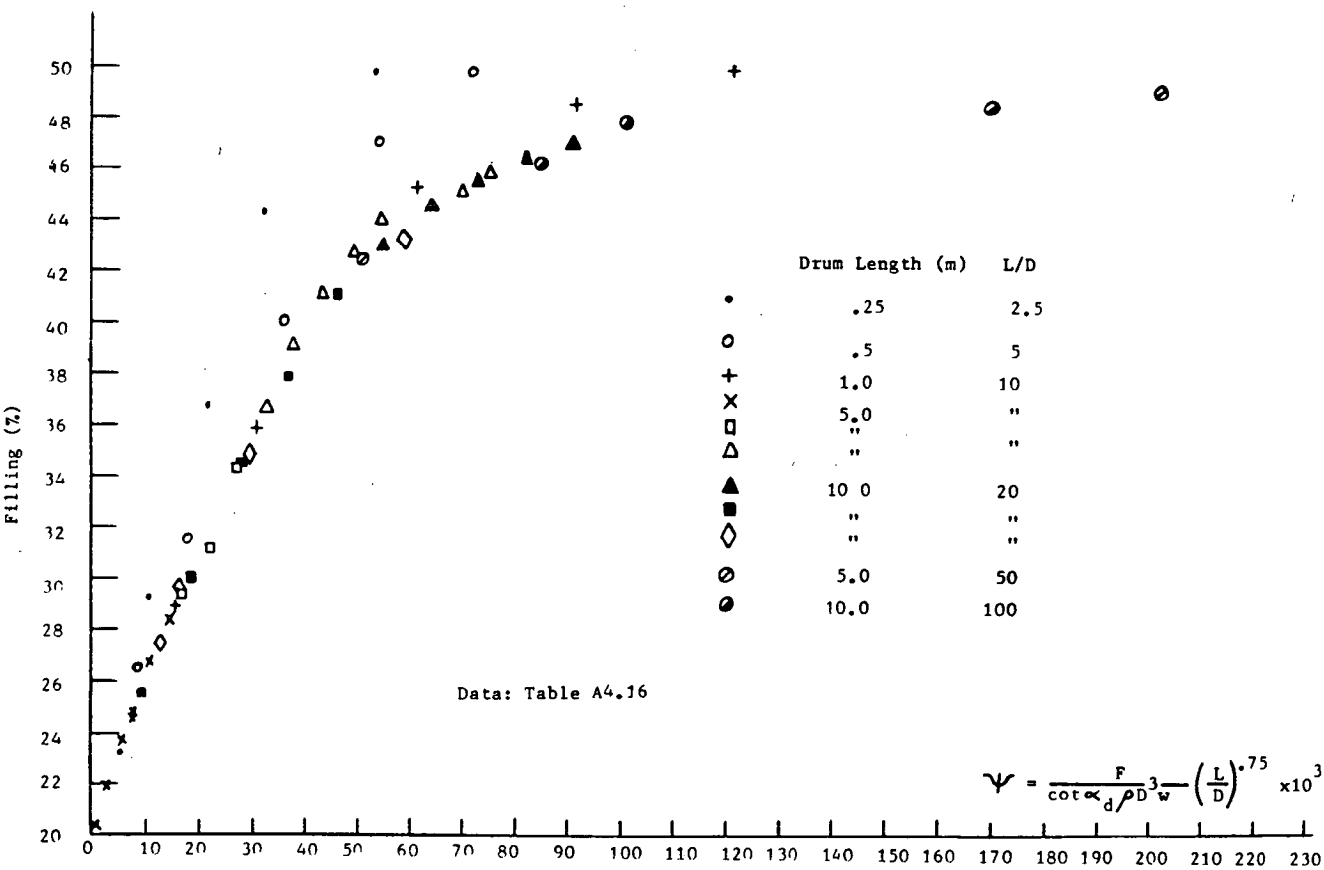

Figure 5.17 Comparison of Data from Figure 5.16 Using Modified Dimensionless Parameter

The accuracy of the predictions has been identified as being influenced by the extent to which slip between the solid bed and drum wall exists. This is particularly difficult to quantify from first principles.

The model's ability to cope with drums containing an internal weir has been established and it had been used to indicate that a dimensionless parameter previously accepted as allowing drums of various dimensions to be compared is only applicable over a very limited range. The requirement for dynamic similarity and similar fractional area constricted remains unaltered but a revised grouping allows drums of various dimensions to be compared over much wider feed rate ranges.

CHAPTER 6

CONCLUSIONS AND RECOMMENDATIONS

Achievements

The main objective of this work has been to acquire an understanding and to develop a model of the motion of solid particles inside an unflighted rotating drum. This would enable the filling and bed profile for drums both horizontal and inclined, with or without constrictions at any point along their length to be predicted. In particular it was the intention to produce a model based on the fundamental properties of the solids without parameters whose value has to be determined by "best fitting" to a series of experiments. This model would thus have a much greater range of applicability and greater ease of use than hitherto.

This objective has been achieved and the model matches empirical data to within 15% over a wide range of operating conditions. Situations for which agreement is worse can be identified in advance when components of bed motion which the model does not accurately describe are present. This approach was not possible hitherto as areas in which the mathematical description of the motion is inaccurate were compensated for or masked by the constants and expressions in previous models which were fitted to experimental data.

In addition to achieving the main objective of this work, advances have also been made in the following areas:

1 **Modelling the Effect of Constrictions**

The current model allows the height above an annular constriction at any point along a drum to be predicted. This value could previously be predicted, for discharge constrictions only, and then only by empirical correlation. Previous work is also limited to considering only constricted discharge drums which are horizontal. The present model can deal with annular constrictions within both horizontal and inclined drums. Solutions for inclined constricted drums in which "limiting filling" exists are also provided.

2 Scale Up

The model can be applied to drums of any size. It is not restricted by having parameters fitted from small scale equipment. In addition it has been shown that previously suggested scale up parameters are only useful for comparing drum data on a dimensionless basis over a limited range of conditions. The current model has been used to derive a modified scale up parameter allowing comparison of drum data over a much wider range of operating conditions.

Limitations

Two areas which affect the agreement between the model and experiment are:-

(a) The occurence of a non linear bed surface profile, and
(b) The occurance of slip at the bed/wall interface.

The first of these violates the first assumption on which the model of motion is based viz the bed cross section has a flat surface. Previous models could attain a reasonable match with experiment by suitable choice of empirical constant. The current model requires that the occurrence of bed surface deformation and the motion which results be fundamentally explained. Initial attempts to describe them using an effective dynamic angle of repose have met with limited success and further work is required. Non linear bed surface profiles can arise at very low drum speeds (less than 10% w_c) for some drum/solid systems. For these the model should be used with care, most however begin to deform at speeds greater than 50% w_c; this is recommended as the upper limit of applicability for the current model.

The occurrence of slip at the bed/wall interface affects the accuracy with which the model calculates particle cycle times. Various expressions for the effect of interparticle friction on surface velocity have been examined and optimised as have expressions for surface cascade lengths. When locked in the bed however the particle is simply assumed to move with the same velocity as the drum. The presence of slip may be identified, for example in systems whose rate of increase in filling with feedrate decreases as feedrate increases,

its effect is however influenced by operating conditions, primarily the degree of filling. This can lead to variation in the accuracy of prediction as operating conditions change. The ability to account and compensate for this is seen as an important area for future extension of this work.

Further Fundamental Work

One possible solution to the problem of describing bed surface deformation would be to carry out an incremental face balance on a particle as it moves around the drum and thus calculate its position at all times in its cycle. An initial study of this method indicated that it would be computationally complex. Pursuit of this approach would also require that the second limitation discussed above, the tribology of the system, be more thoroughly investigated and described.

Development and Use of the Model

The solution technique for the model, stepwise numerical integration of the equations of motion along the drum length, lends itself to incorporating changes in parameters with distance. Further development of the model should not be restricted therefore to refining those aspects of motion which are not fully described at present but should also look to incorporate the wider phenomena of varying physical properties with distance which can arise from the effects of reaction, gas evolution and heat transfer. Models of these could be built into the framework provided by the model of solids motion in a rotating drum.

Conclusion

A general model for the motion of solids inside an unflighted rotating drum with one or more weirs along its length has been developed. The use of a computer has allowed the mathematical description of the motion to be more detailed than hitherto. The model matches empirical data to within 15% over a wide range of operating conditions. Areas for which agreement is worse can be identified in advance.

Appendix 1

Derivation of the equation for volumetric flow rate in a rotating drum proposed by Saeman.

Saeman [S2, S3] developed the following equation for the axial advance of a particle whilst rolling on the surface of the bed in an inclined drum.

$$s = c(\tan\Psi + \tan\beta \cos\alpha_d)/\sin\alpha_d \qquad (A1.1)$$

Where s is the axial transport distance per cascade, c is the transverse distance covered by a particle whilst rolling on the surface, equal to the length of chord connecting the entrance and exit points of radial element from which the particle has just emerged (see Figures 2.2 and 3.1) and β is the angle between the surface of the bed and the drum axis. The equation is also later used by Kramers and Krookewit [K1] in their model development.

Saeman simplifies A1.1 further by approximating $\tan\Psi$ and $\tan\beta$ by their radian angles. For horizontal drums $\Psi = 0$ and (A1.1) reduces to

$$s = c \tan\beta \cot\alpha_d \qquad (A1.2)$$

which is the equation used by Vahl [V2] in the derivation of his results as reported by Vahl and Kingma [V3]. For an inclined drum with uniform bed depth throughout $\beta = 0$ and (A1.1) becomes

$$s = c \tan\Psi / \sin\alpha_d \qquad (A1.3)$$

This is a relatively simple geometry to verify (see Appendix 2) yet in addition to simplifications previously mentioned in the main text Pickering et al [P1] have incorrectly expressed s as

$$s = c \sin\Psi / \sin\alpha_d \qquad (A1.4)$$

Though this will not have a significant effect for low values of drum slope.

It should be noted that equation A1.1 does not define exactly the axial distance covered per cascade but in fact the distance travelled in the surface of the bed. This could be corrected by multiplying by $\cos\beta$ to relate the surface advancement to an equivalent distance along the drum axis. In all probability however this correction was deliberately omitted

to reduce the complexity of the resulting equations, a prime objective in pre-digital computer days. Equations A1.1 and A1.2 are thus only accurate for small values of β as noted by Vahl and Kingma.

The time spent locked in the bed is calculated per revolution of the drum. The number of cascades for any radial element per revolution are defined as:

$$N_{CR} = \pi/\theta_r \qquad (A1.5)$$

where θ_r is half the angle subtended at the centre of the drum for any radial position r (Figure 2.3).

If the rate of rotation N (rpm) is multiplied by the number of cascades/revolution the time per cascade is given by:

$$\tau = N\pi/\theta_r \qquad (A1.6)$$

The axial tranport velocity $v(r) = s/\tau$ is thus given by:

$$v(r) = \frac{cN\pi(\tan\psi + \tan\beta \cos\alpha_d)}{\sin\alpha_d \theta_r} \qquad (A1.7)$$

at this point the equation may be simplified for low filling uniform bed depth drums ($\beta = 0$, $\theta_r \simeq c/2r$, $r \simeq R_d$) as previously discussed in the main text and be used as denominator with the drum length to obtain a mean residence time. For larger fractional fillings (A1.7) is extended to a volumetric basis by multiplying both sides by the incremental area associated with the radial path r.

$$dA = 2r\theta_r dr \qquad (A1.8)$$

Equation (A1.7) multiplied by (A1.8) and simplified gives

$$v(r)dA = \frac{2\pi rcN(\tan\psi + \tan\beta \cos\alpha_d)}{\sin\alpha_d} dr \qquad (A1.9)$$

c may be expressed as a function of the path radius by:

$$c = 2(r^2 - b^2)^{\frac{1}{2}} \qquad \text{(A1.10)}$$

where b is the distance from the bed surface to the drum axis, assumed equal to the minimum radius of any particle (neglecting the thickness of the cascade layer). Thus (A1.9) becomes:

$$v(r)dA = \frac{4\pi N(\tan\psi + \tan\beta \cos\alpha_d)(r^2 - b^2)^{\frac{1}{2}}.r\, dr}{\sin\alpha_d} \qquad \text{(A1.11)}$$

The average volumetric flowrate is now obtained by integrating the above from r = b to r = R_d giving:

$$q = \frac{4\pi N}{3}\left(\frac{\tan\psi + \tan\beta \cos\alpha_d}{\sin\alpha_d}\right)(R_d^2 - b^2)^{3/2} \qquad \text{(A1.12)}$$

This is equation (2.9) of the main text.

Appendix 2

Using the notation of Figures 2.2 and 2.3 the derivation of equation (2.19) as presented by Hogg et al [H1] is given below.

During one circulation of the bed a particle moves from A to C along the bed surface. If the distance moved along the drum axis is denoted by s it is clear that

$$s = l(x) \tan \phi \cos \beta \qquad (A2.1)$$

where $l(x)$ is the width of the bed surface at distance x along the drum axis.

Equation A2.1 is not completely correct because as the bed surface slopes downwards it decreases in width and the point at which a particle at the bed edge re-enters the bed at the wall will be closer to the centre of the drum. BAC is not therefore a right angle, the error introduced assuming that it is however, will be small for small β and significantly smaller than that introduced by terms included in the final expression for feedrate.

Hogg et al develop the derivation as follows:

Considering the motion of particles in the transverse plane, it is apparent that particles must enter the surface region at all points along the upper half of this plane. Similarly particles are being removed from the surface region at all points along the lower half. Furthermore to maintain the steady motion of the charge all particles must, on the average, re-enter the bed in the same radial element from which they emerged. Consider particles in some radial element at (r,θ). Each of these particles must move a distance $l(r)$ in the surface region where they undergo an axial displacement $s(r)$ given by

$$s(r) = l(r) \tan \phi \cos \beta \qquad (A2.2)$$

But from the geometry of the system, $l(r) = 2r\sin\theta_r$
so that

$$s(r) = 2r \sin \theta_r \tan \phi \cos \beta \qquad (A2.3)$$

If it is assumed that the time spent by each particle in the surface region is negligible compared with that spent in the bed itself, the time τ taken for one complete circulation can be determined from $\tau(r) = 2\theta_r/w$, where w is the angular velocity of the cylinder. A similar result can be obtained through the use of the less restricting (but more arbitrary) assumption that the total circulation time is **proportional** to the time spent in the "static" region of the bed. In this case, the circulation time is given by:

$$\tau(r) = 2\theta(r)/Bw \qquad (A2.4)$$

where B is an unknown constant.

Since particles in the element at r receive an axial displacement s(r) in time $\tau(r)$, the axial velocity v(r) of these particles is given by:

$$v(r) = s(r)/\tau(r)$$

Substitution for s(r) and $\tau(r)$ from equations (A2.3) and (A2.4) respectively yields:

$$v(r) = \frac{w}{\theta_r} Br \sin\theta_r \tan\phi \cos\beta \qquad (A2.5)$$

The volume axial flow rate dq(r) of particles at r is $dq(r) = v(r)dA$, where dA is the cross-sectional area of the element given by $dA(r) = 2r\theta_r dr$, so from the equation (A2.5):

$$dq(r) = 2Bwr^2 \sin\theta_r \tan\phi \cos\beta \, dr \qquad (A2.6)$$

Since $\cos\theta_r = b/r$, where b is the perpendicular distance between the surface of the charge and the centre of the cylinder, equation (A2.6) can be rewritten as:

$$dq(r) = 2Bwr^2\left(1 - \frac{b^2}{r^2}\right)^{1/2} \tan\phi \cos\beta \, dr \qquad (A2.7)$$

The overall volume flow rate q is obtained from:

$$q = 2Bw \tan\phi \cos\beta \int_b^{R_d} r(r^2 - b^2)^{\frac{1}{2}} dr \qquad (A2.8)$$

where R_d is the radius of the cylinder. Integration gives:

$$q = 2/3wBR_d^3\left(1 - \frac{b^2}{R_d^2}\right)^{3/2} \tan\phi \cos\beta \qquad (A2.9)$$

The quantity b/R_d is related to the "filling angle" θ, defined as half the angle subtended, at the centre of the cylinder, by the intersection of the surface of the bed with the shell, through the relation $\cos\theta = b/R_d$. Hence:

$$q = 2/3wBR_d^3 \sin^3\theta_x \tan\phi \cos\beta \qquad (A2.10)$$

For steady state operation, the mass flow rate across any transverse section must be constant and equal to the feed rate of particles into the cylinder. Thus the mass flow rate F of particles is given by:

$$F = 2/3wB\rho_b R_d^3 \sin^3\theta_x \tan\phi \cos\beta \qquad (A2.11)$$

where ρ_b is the bulk density of the feed material.

Appendix 3

Development of the Equation for the Angle which gives the Line of Steepest Descent for a Particle Cascading on the Bed Surface

Consider first the simple case of a drum with uniform bed depth along its length. In being carried from its initial point of entry, A, to its point of exit, B, from the bed the particle is lifted in a plane perpendicular to the drum axis a distance h_1 (see Figure A3.1).

$$h_1 = 1 \sin\alpha_d \tag{A3.1}$$

where 1 is the chord length connecting entrance and exit points for one bed circulation. Since the drum is inclined at some angle ψ to the horizontal the vertical displacement of the particle is given by h_{1v} (see Figure A3.2)

$$h_{1v} = 1 \sin\alpha_d \cos\psi \tag{A3.2}$$

The vertical distance between the initial point of entry to the bed, A, and the point of re-entry to the bed, C, is h_{2v} (see Figure A3.3).

$$h_{2v} = 1 \tan\phi \sin\psi \tag{A3.3}$$

The angle of descent in the bed surface ϕ will be such that the total vertical drop $h_{1v} + h_{2v}$ is a maximum.

If the angle between the horizontal and the line of descent m is considered as Γ then:

$$\sin\Gamma = \frac{h_{1v} + h_{2v}}{m} \tag{A3.4}$$

from which

$$\sin\Gamma = \frac{1\sin\alpha_d \cos\psi + 1 \tan\phi \sin\psi}{1/\cos\phi} \tag{A3.5}$$

which gives

$$\sin\Gamma = \cos\phi \sin\alpha_d \cos\psi + \sin\phi \sin\psi \tag{A3.6}$$

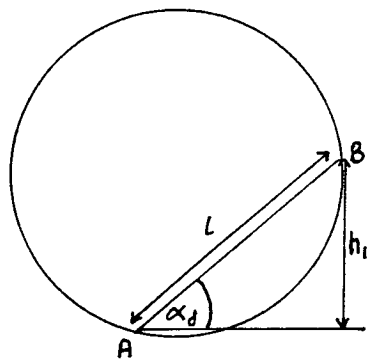

Figure A3.1 Elevation of Particle in Plane Perpendicular to Drum Axis

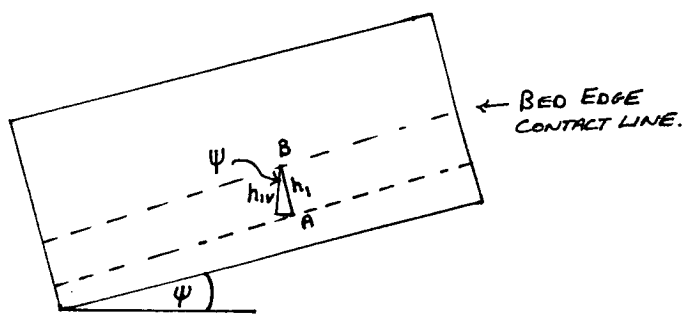

Figure A3.2 Equivalent Displacement of Particle in Vertical Plane

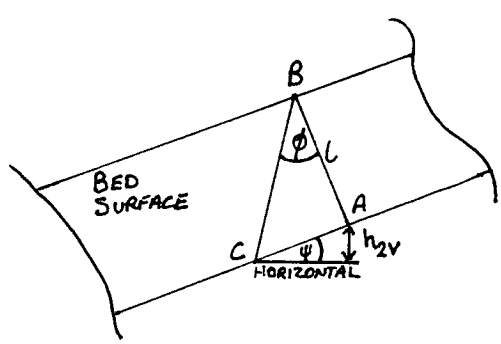

Figure A3.3 Particle Path in Bed Surface and Vertical Displacement between Initial Point of Entry and Point of Re-entry

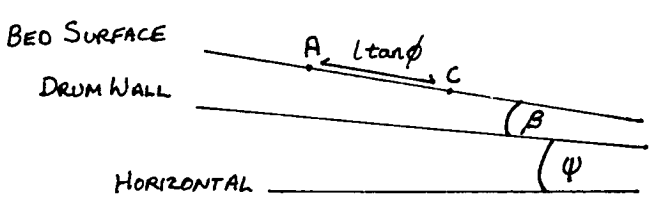

Figure A3.4 View of Bed Edge at Base of Particle Cascades

We seek to maximise the vertical drop with therefore look for

$$d \sin \Gamma / d\phi = 0$$

$$\frac{d \sin \Gamma}{d\phi} = - \sin \phi \sin \alpha_d \cos \psi + \cos \phi \sin \psi \qquad (A3.7)$$

If this equals zero then

$$\cos \phi \sin \psi = \sin \phi \sin \alpha_d \cos \psi \qquad (A3.8)$$

from which

$$\tan \phi = \frac{\tan \psi}{\sin \alpha_d} \qquad (A3.9)$$

This is the equation linking angle of descent to drum slope and dynamic angle of repose of the solid.

If now an inclined drum in which the bed surface varies in depth along its length and makes angle β with the drum axis is considered, a similar analysis may be made (β is considered constant over the cascade length). In this case the bed surface slope β gives an additional contribution to the overall vertical displacement as a particle exits and then re-enters the bed. The initial height gained during circulation remains unchanged.

$$h_{1v} = 1 \sin \alpha_d \cos \psi \qquad (A3.2)$$

If we look "edge on" to the bed in line with the points of initial entry, A, and re-entry, C, (see Figure A3.4) the distance between these points is $1 \tan \phi$ and the vertical displacement assoicated with bed surface slope is

$$h_{3v} = 1 \tan \phi \sin \beta \cos \alpha_d \cos \psi \qquad (A3.10)$$

Similarly there is a displacement due to the drum inclination, h_{2v}

$$h_{2v} = 1 \tan \phi \cos \beta \sin \psi \qquad (A3.11)$$

The angle between the horizontal and the line of descent in the bed surface now becomes

$$\sin \Gamma = \frac{h_{1v} + h_{2v} + h_{3v}}{m} \qquad \text{(A3.12)}$$

from which

$$\sin \Gamma = \frac{1 \sin \alpha_d \cos \psi + 1 \tan \phi \cos \beta \sin \psi + 1 \tan \phi \sin \beta \cos \alpha_d \cos \psi}{1/\cos \phi} \qquad \text{(A3.13)}$$

which gives

$$\sin \Gamma = \cos \phi \sin \alpha_d \cos \psi + \sin \phi (\cos \beta \sin \psi + \sin \beta \cos \alpha_d \cos \psi) \qquad \text{(A3.14)}$$

again seeking $d \sin \Gamma / d\phi = 0$.

$$\frac{d \sin \Gamma}{d\phi} = - \sin \phi \sin \alpha_d \cos \psi + \cos \phi (\cos \beta \sin \psi + \sin \beta \cos \alpha_d \cos \psi) \qquad \text{(A3.15)}$$

from which

$$\cos \phi (\cos \beta \sin \psi + \sin \beta \cos \alpha_d \cos \psi) = \sin \phi \sin \alpha_d \cos \psi \qquad \text{(A3.16)}$$

and

$$\tan \phi = \frac{\cos \alpha_d \sin \beta + \tan \psi \cos \beta}{\sin \alpha_d} \qquad \text{(A3.17)}$$

This is the equation linking angle of descent to drum slope, dynamic angle of repose and bed surface slope with respect to the drum axis.

Appendix 4

Details of Experimental Data Used

Table A4.1 : Data for Figure 3.2 Model(1)=Initial velocity on surface. Model(2)= No initial velocity For both μ=0
Drum : PVC. Material : Ballotini

Feed Rate (Kg/s)	Density (Kg/m3)	Dynamic Angle of rep. (Deg)	Static Angle of rep. (Deg)	Slope (Deg)	Length (m)	Drum Rad. (m)	Constriction Radius (m)	Drum Speed (RPM)	% Critical Speed (-)	Filling Exper.(%)	Model(1) (%)	Model(2) (%)
0.00000	1780	28	24.5	0	0.216	0.0465	0.0262	38.5	27.9	16.39	16.39	16.39
0.00337	1780	28	24.5	0	0.216	0.0465	0.0262	38.5	27.9	21.55	20.09	20.27
0.00460	1780	28	24.5	0	0.216	0.0465	0.0262	38.5	27.9	22.00	21.44	21.79
0.00593	1780	28	24.5	0	0.216	0.0465	0.0262	38.5	27.9	22.20	22.51	22.42
0.00769	1780	28	24.5	0	0.216	0.0465	0.0262	38.5	27.9	24.20	23.84	23.77
0.00926	1780	28	24.5	0	0.216	0.0465	0.0262	38.5	27.9	25.30	24.96	24.85
0.01240	1780	28	24.5	0	0.216	0.0465	0.0262	38.5	27.9	26.90	27.21	27.00
0.01590	1780	28	24.5	0	0.216	0.0465	0.0262	38.5	27.9	28.20	29.57	29.24

Table A4.2 : Data for Figure 3.2 Model(1)=Initial velocity on surface. Model(2)= No initial velocity For both μ=0
Drum : Sandpaper lined PVC. Material : Ballotini

Feed Rate (Kg/s)	Density (Kg/m3)	Dynamic Angle of rep. (Deg)	Static Angle of rep. (Deg)	Slope (Deg)	Length (m)	Drum Rad. (m)	Constriction Radius (m)	Drum Speed (RPM)	% Critical Speed (-)	Filling Exper.(%)	Model(1) (%)	Model(2) (%)
0.00041	1780	28	24.5	2	0.216	0.0465	0.037	34.5	24.9	2.87	3.00	3.03
0.00141	1780	28	24.5	2	0.216	0.0465	0.037	34.5	24.9	3.87	3.46	3.51
0.00269	1780	28	24.5	2	0.216	0.0465	0.037	34.5	24.9	4.77	4.16	4.22
0.00347	1780	28	24.5	2	0.216	0.0465	0.037	34.5	24.9	5.0	4.68	4.72
0.00415	1780	28	24.5	2	0.216	0.0465	0.037	34.5	24.9	5.6	5.16	5.23
0.00516	1780	28	24.5	2	0.216	0.0465	0.037	34.5	24.9	6.0	6.03	6.07

Table A4.3 : Data for Figure 3.2 Model(1)=Initial velocity on surface. Model(2)= No initial velocity For both μ=0
Data from Kramers & Krookewit [K1] : Runs with coke.

Feed Rate (Kg/s)	Density (Kg/m3)	Dynamic Angle of rep. (Deg)	Static Angle of rep. (Deg)	Slope (Deg)	Length (m)	Drum Rad. (m)	Constriction Radius (m)	Drum Speed (RPM)	% Critical Speed (-)	Filling Exper.(%)	Model(1) (%)	Model(2) (%)
0.00182	560	40	35	0.57	1.78	0.0985	0.079	5.10	5.4	10.4	11.11	11.11
0.00233	560	40	35	0.77	1.78	0.0985	0.079	9.42	9.9	7.7	8.00	8.00
0.00971	560	40	35	0.77	1.78	0.0985	0.079	14.28	15.0	15.1	16.86	16.89
0.01290	560	40	35	1.32	1.78	0.0985	0.079	9.42	9.9	19.1	22.57	22.63
0.00338	560	40	35	1.32	1.78	0.0985	0.079	9.42	9.9	6.6	7.53	7.53
0.00369	560	40	35	1.86	1.78	0.0985	0.079	14.28	15.0	4.3	4.24	4.26
0.01680	560	40	35	3.10	1.78	0.0985	0.079	8.46	8.9	14.7	18.42	18.45

Table A4.4 : Data for Figure 3.4 Models (1),(2) & (3) Correspond to curves of the same number
Drum : Sandpaper lined PVC. Material : Ballotini

Feed Rate (Kg/s)	Density (Kg/m3)	Dynamic Angle of rep. (Deg)	Static Angle of rep. (Deg)	Slope (Deg)	Length (m)	Drum Rad. (m)	Constriction Radius (m)	Drum Speed (RPM)	% Critical Speed (-)	Filling Exper.(%)	Model(1) (%)	Model(2) (%)	Model (3) (%)
0.00043	1780	28	24.5	0	0.216	0.0465	0.037	34.5	24.9	6.20	6.18	6.17	6.14
0.00095	1780	28	24.5	0	0.216	0.0465	0.037	34.5	24.9	6.80	6.85	6.83	6.77
0.00125	1780	28	24.5	0	0.216	0.0465	0.037	34.5	24.9	7.02	7.18	7.17	7.10
0.00199	1780	28	24.5	0	0.216	0.0465	0.037	34.5	24.9	7.63	7.95	7.93	7.85
0.00268	1780	28	24.5	0	0.216	0.0465	0.037	34.5	24.9	8.86	8.58	8.56	8.45
0.00293	1780	28	24.5	0	0.216	0.0465	0.037	34.5	24.9	8.24	8.81	8.79	8.67
0.00352	1780	28	24.5	0	0.216	0.0465	0.037	34.5	24.9	8.79	9.31	9.29	9.14
0.00436	1780	28	24.5	0	0.216	0.0465	0.037	34.5	24.9	9.99	10.01	9.96	9.81
0.00488	1780	28	24.5	0	0.216	0.0465	0.037	34.5	24.9	10.90	10.42	10.36	10.21

Table A4.5 : Data for Figure 3.5
Drum : Sandpaper lined PVC. Material : Ballotini

Feed Rate (Kg/s)	Density (Kg/m3)	Dynamic Angle of rep. (Deg)	Static Angle of rep. (Deg)	Slope (Deg)	Length (m)	Drum Rad. (m)	Constriction Radius (m)	Drum Speed (RPM)	% Critical Speed (-)	Filling Exper.(%)	Model with segregated bath assumption (%)
0.00043	1780	28	24.5	0	0.216	0.0465	0.037	34.5	24.9	6.20	6.77
0.00095	1780	28	24.5	0	0.216	0.0465	0.037	34.5	24.9	6.80	7.19
0.00125	1780	28	24.5	0	0.216	0.0465	0.037	34.5	24.9	7.02	7.61
0.00199	1780	28	24.5	0	0.216	0.0465	0.037	34.5	24.9	7.63	8.55
0.00268	1780	28	24.5	0	0.216	0.0465	0.037	34.5	24.9	8.86	9.36
0.00293	1780	28	24.5	0	0.216	0.0465	0.037	34.5	24.9	8.24	9.61
0.00352	1780	28	24.5	0	0.216	0.0465	0.037	34.5	24.9	8.79	10.25
0.00436	1780	28	24.5	0	0.216	0.0465	0.037	34.5	24.9	9.99	11.07
0.00488	1780	28	24.5	0	0.216	0.0465	0.037	34.5	24.9	10.90	11.59

Table A4.6 : Data for Figure 5.1
Taken from Abouzeid & Fuerstenau [1981]. Dynamic angle from Abouzeid et al [1980]

Feed Rate (Kg/s)	Density (Kg/m3)	Dynamic Angle of rep. (Deg)	Static Angle of rep. (Deg)	Slope (Deg)	Length (m)	Drum Rad. (m)	Constriction Radius (m)	Drum Speed (RPM)	% Critical Speed (-)	Filling Exper.(%)	Model (%)
0.000	1400	39	35	0	0.24	0.04	0.0225	42	28.1	17.70	16.20
0.001	1400	39	35	0	0.24	0.04	0.0225	42	28.1	20.02	19.60
0.002	1400	39	35	0	0.24	0.04	0.0225	42	28.1	22.03	21.95
0.003	1400	39	35	0	0.24	0.04	0.0225	42	28.1	23.95	24.04
0.004	1400	39	35	0	0.24	0.04	0.0225	42	28.1	25.90	26.02

Table A4.7 : Data for Figure 5.2
Curve of Abouzeid & Fuerstenau uses data of Table A4.6
Other curves: Drum : PVC. Material : Ballotini.

Feed Rate (Kg/s)	Density (Kg/m3)	Dynamic Angle of rep. (Deg)	Static Angle of rep. (Deg)	Slope (Deg)	Length (m)	Drum Rad. (m)	Constriction Radius (m)	Drum Speed (RPM)	% Critical Speed (-)	Filling Exper.(%)	Model (%)
(1) Lower Curves											
0.00000	1780	24.2	24.5	0	0.216	0.0465	0.037	38.9	28	8.36	5.27
0.00340	1780	24.2	24.5	0	0.216	0.0465	0.037	38.9	28	9.00	8.65
0.00471	1780	24.2	24.5	0	0.216	0.0465	0.037	38.9	28	10.20	9.56
0.00600	1780	24.2	24.5	0	0.216	0.0465	0.037	38.9	28	10.80	10.38
0.00782	1780	24.2	24.5	0	0.216	0.0465	0.037	38.9	28	11.60	11.46
0.00995	1780	24.2	24.5	0	0.216	0.0465	0.037	38.9	28	12.60	12.65
0.01270	1780	24.2	24.5	0	0.216	0.0465	0.037	38.9	28	13.40	14.03
0.01620	1780	24.2	24.5	0	0.216	0.0465	0.037	38.9	28	14.60	15.69
(2) Upper curves											
0.00000	1780	28	24.5	0	0.216	0.0465	0.0262	38.5	27.9	18.39	16.39
0.00337	1780	28	24.5	0	0.216	0.0465	0.0262	38.5	27.9	21.33	20.50
0.00460	1780	28	24.5	0	0.216	0.0465	0.0262	38.5	27.9	22.30	21.55
0.00593	1780	28	24.5	0	0.216	0.0465	0.0262	38.5	27.9	23.20	22.63
0.00769	1780	28	24.5	0	0.216	0.0465	0.0262	38.5	27.9	24.30	23.96
0.00926	1780	28	24.5	0	0.216	0.0465	0.0262	38.5	27.9	25.30	25.10
0.01240	1780	28	24.5	0	0.216	0.0465	0.0262	38.5	27.9	26.60	27.30
0.01590	1780	28	24.5	0	0.216	0.0465	0.0262	38.5	27.9	28.20	29.65

Table A4.8 : Data for Figure 5.3
Unlined drum data as for lower curves Table A4.7.
Sandpaper lined drum data below. Material : Ballotini

Feed Rate (Kg/s)	Density (Kg/m3)	Dynamic Angle of rep. (Deg)	Static Angle of rep. (Deg)	Slope (Deg)	Length (m)	Drum Rad. (m)	Constriction Radius (m)	Drum Speed (RPM)	% Critical Speed (-)	Filling Exper.(%)	Model (%)
0.00346	1780	28	24.5	0	0.216	0.0465	0.037	38.9	28	8.52	9.01
0.00468	1780	28	24.5	0	0.216	0.0465	0.037	38.9	28	9.14	9.95
0.00602	1780	28	24.5	0	0.216	0.0465	0.037	38.9	28	10.00	10.89
0.00785	1780	28	24.5	0	0.216	0.0465	0.037	38.9	28	11.10	12.09
0.00995	1780	28	24.5	0	0.216	0.0465	0.037	38.9	28	11.30	13.34
0.01270	1780	28	24.5	0	0.216	0.0465	0.037	38.9	28	12.30	14.82
0.01620	1780	28	24.5	0	0.216	0.0465	0.037	38.9	28	14.20	16.70

Table A4.9 : Data for Figure 5.4
Upper and Lower Ballotini curves use experimental data from Table A4.7
Data for sand as bulk material given below.

Feed Rate (Kg/s)	Density (Kg/m3)	Dynamic Angle of rep. (Deg)	Static Angle of rep. (Deg)	Slope (Deg)	Length (m)	Drum Rad. (m)	Constriction Radius (m)	Drum Speed (RPM)	% Critical Speed (-)	Filling Exper.(%)
(1) Upper sand curve.										
0.00000	1470	36	35	0	0.216	0.0465	0.0262	38.9	28	20.90
0.00357	1470	36	35	0	0.216	0.0465	0.0262	38.9	28	24.22
0.00635	1470	36	35	0	0.216	0.0465	0.0262	38.9	28	28.70
0.01073	1470	36	35	0	0.216	0.0465	0.0262	38.9	28	31.44
0.01740	1470	36	35	0	0.216	0.0465	0.0262	38.9	28	34.80
(2) Lower sand curve										
0.00000	1470	36	35	0	0.216	0.0465	0.0262	38.9	28	8.70
0.00343	1470	36	35	0	0.216	0.0465	0.0262	38.9	28	12.71
0.00627	1470	36	35	0	0.216	0.0465	0.0262	38.9	28	14.76
0.01075	1470	36	35	0	0.216	0.0465	0.0262	38.9	28	17.42
0.01737	1470	36	35	0	0.216	0.0465	0.0262	38.9	28	20.90

Table A4.10 Data for figure 5.5
Experimental data is that for lower curve Table A4.9

Feed Rate (Kg/s)	Filling Exper.(%)	Model with Dynamic angle 28.6	Model with Dynamic angle 35	Model with Dynamic angle 44.5
0.00000	8.70	5.70	5.70	5.70
0.00343	12.71	9.46	9.54	11.40
0.00627	14.76	11.50	13.25	14.56
0.01075	17.42	14.30	16.82	19.00
0.01737	20.90	18.46	21.20	24.60

Table A4.11 Data for Figure 5.7
Experimental data from [A4]. Dynamic angle from [A10].

Feed Rate (Kg/s)	Density (Kg/m3)	Dynamic Angle of rep. (Deg)	Static Angle of rep. (Deg)	Slope (Deg)	Length (m)	Drum Rad. (m)	Constriction Radius (m)	Drum Speed (RPM)	% Critical Speed (-)	Filling Exper.(%)	Model with $\alpha_d = \alpha_s + m/4_c$ (%)	Model with Dynamic angle 39 (%)
0.0026	1400	39	35	0	0.24	0.04	0.0225	20	13.4	23.30	28.45	27.29
0.0026	1400	39	35	0	0.24	0.04	0.0225	40	26.7	23.10	25.73	23.42
0.0026	1400	39	35	0	0.24	0.04	0.0225	60	40.1	23.30	25.49	22.05
0.0026	1400	39	35	0	0.24	0.04	0.0225	80	53.5	23.94	26.71	21.36
0.0026	1400	39	35	0	0.24	0.04	0.0225	100	66.9	25.55	29.51	20.93

Table A4.12 Data for Figure 5.8
Drum : PVC Material : Ballotini

Feed Rate (Kg/s)	Density (Kg/m3)	Dynamic Angle of rep. (Deg)	Static Angle of rep. (Deg)	Slope (Deg)	Length (m)	Drum Rad. (m)	Constriction Radius (m)	Drum Speed (RPM)	% Critical Speed (-)	Filling Exper.(%)	Model (%)
0.00309	1780	24.7	24.5	1	0.216	0.0465	0.037	3.16	2.3	13.90	17.92
0.00309	1780	26.2	24.5	1	0.216	0.0465	0.037	23.3	16.8	6.94	7.75
0.00309	1780	27.3	24.5	1	0.216	0.0465	0.037	34.5	24.9	6.67	7.12
0.00309	1780	28.0	24.5	1	0.216	0.0465	0.037	41.3	29.8	6.54	6.64
0.00309	1780	29.5	24.5	1	0.216	0.0465	0.037	55.2	39.8	6.37	5.92
0.00309	1780	33.0	24.5	1	0.216	0.0465	0.037	69	49.7	6.50	5.79
0.00309	1780	34.0	24.5	1	0.216	0.0465	0.037	76	54.8	6.30	5.68
0.00309	1780	35.0	24.5	1	0.216	0.0465	0.037	94	67.8	6.17	5.47

Table A4.13 Data for Figure 5.9
Upper curve experimental data from Table A4.4. with Model (2)
Lower curve data below. Drum : PVC+Sandpaper Material : Ballotini

Feed Rate (Kg/s)	Density (Kg/m3)	Dynamic Angle of rep. (Deg)	Static Angle of rep. (Deg)	Slope (Deg)	Length (m)	Drum Rad. (m)	Constriction Radius (m)	Drum Speed (RPM)	% Critical Speed (-)	Filling Exper.(%)	Model (%)
0.00041	1780	28	24.5	2	0.216	0.0465	0.037	34.5	24.9	2.87	3.05
0.00093	1780	28	24.5	2	0.216	0.0465	0.037	34.5	24.9	3.20	3.31
0.00141	1780	28	24.5	2	0.216	0.0465	0.037	34.5	24.9	3.87	3.56
0.00152	1780	28	24.5	2	0.216	0.0465	0.037	34.5	24.9	4.07	3.61
0.00203	1780	28	24.5	2	0.216	0.0465	0.037	34.5	24.9	4.40	4.40
0.00269	1780	28	24.5	2	0.216	0.0465	0.037	34.5	24.9	4.77	4.32
0.00347	1780	28	24.5	2	0.216	0.0465	0.037	34.5	24.9	5.30	4.85
0.00415	1780	28	24.5	2	0.216	0.0465	0.037	34.5	24.9	5.60	5.39
0.00516	1780	28	24.5	2	0.216	0.0465	0.037	34.5	24.9	6.00	6.30

Table A4.14 : Data for Figure 5.10

Feed Rate (Kg/s)	Density (Kg/m3)	Dynamic Angle of rep. (Deg)	Static Angle of rep. (Deg)	Slope (Deg)	Length (m)	Drum Rad. (m)	Constriction Radius (m)	Drum Speed (RPM)	% Critical Speed (-)	Filling Exper.(%)	Model (%)
(1) Literature [K3]											
0.00157	1300	39	35	0	0.24	0.04	0.0175	40	26.7	33.70	29.24
0.00157	1300	39	35	0	0.24	0.04	0.0250	40	26.7	20.90	17.94
0.00157	1300	39	35	0	0.24	0.04	0.0300	40	26.7	14.20	12.07
0.00157	1300	39	35	0	0.24	0.04	0.0350	40	26.7	8.30	7.90
(2) Experiment											
0.0034	1780	24.2	24.5	0	0.216	0.0465	0.037	38.9	28	9.00	8.65
0.0034	1780	28	24.5	0	0.216	0.0465	0.0262	38.5	27.9	21.33	29.50

Table A4.15 : Data for Figure 5.14
This Figure uses the data of Table A4.6 and the upper curves data of Table A4.7
In this instance the feed rates are expressed in dimensionless form as given on Figure 5.14.

(1) Literature data. [A4] Dimensionless Parameter	Filling (%) Experimental	Model	(2) Experimental Dimensionless Parameter	Filling (%) Experimental	Model
0.00000	17.70	16.20	0.00434	21.33	20.50
0.00484	20.02	19.60	0.00592	22.00	21.55
0.00968	22.03	21.95	0.00764	23.20	22.63
0.01452	23.95	24.04	0.00990	24.30	23.96
0.01936	25.90	26.02	0.01200	25.30	25.16
			0.01590	26.60	27.30
			0.02050	28.20	29.65

Table A4.16 : Data for Figures 5.15.5.16.5.17.
Data generated to assess predicted filling trends for drums of various dimensions.

Feed Rate (Kg/s)	Density (Kg/m3)	Dynamic Angle of rep. (Deg)	Static Angle of rep. (Deg)	Slope (Deg)	Length (m)	Drum Rad. (m)	Constriction Radius (m)	Drum Speed (RPM)	% Critical Speed (-)	Predicted Filling (%)	Dimensionless Param Fig 5.1 x 1000	Dimensionless Param Fig 5.1 x 1000	Graphic symbol Assigned.
0.005	1780	28	24.5	0	0.25	0.05	0.025	33.4	25	25.21	6.71	5.04	
0.010	1780	28	24.5	0	0.25	0.05	0.025	33.4	25	29.20	13.40	10.08	
0.020	1780	28	24.5	0	0.25	0.05	0.025	33.4	25	36.66	26.80	21.31	•
0.030	1780	28	24.5	0	0.25	0.05	0.025	33.4	25	44.34	40.20	31.97	
0.040	1780	28	24.5	0	0.25	0.05	0.025	33.4	25	49.85	53.70	42.71	
0.005	1780	28	24.5	0	0.5	0.05	0.025	33.4	25	26.47	13.40	8.96	
0.010	1780	28	24.5	0	0.5	0.05	0.025	33.4	25	31.50	26.80	17.92	
0.020	1780	28	24.5	0	0.5	0.05	0.025	33.4	25	40.77	53.70	35.91	o
0.030	1780	28	24.5	0	0.5	0.05	0.025	33.4	25	47.15	80.50	53.83	
0.040	1780	28	24.5	0	0.5	0.05	0.025	33.4	25	49.88	107.30	71.76	
0.005	1780	28	24.5	0	1	0.05	0.025	33.4	25	28.87	26.80	15.07	
0.010	1780	28	24.5	0	1	0.05	0.025	33.4	25	35.83	53.70	30.20	
0.020	1780	28	24.5	0	1	0.05	0.025	33.4	25	45.34	107.30	60.34	+
0.030	1780	28	24.5	0	1	0.05	0.025	33.4	25	48.56	161.00	90.54	
0.040	1780	28	24.5	0	1	0.05	0.025	33.4	25	49.89	215.00	120.90	
0.010	1780	28	24.5	0	5	0.25	0.125	15	25	20.23	0.96	0.54	
0.050	1780	28	24.5	0	5	0.25	0.125	15	25	21.92	4.78	2.69	
0.100	1780	28	24.5	0	5	0.25	0.125	15	25	23.65	9.56	5.38	
0.200	1780	28	24.5	0	5	0.25	0.125	15	25	26.67	19.12	10.75	x
0.100	1780	36	24.5	0	5	0.25	0.125	15	25	24.61	13.06	7.34	
0.200	1780	36	24.5	0	5	0.25	0.125	15	25	28.38	26.12	14.69	
0.100	1780	36	27.5	0	5	0.25	0.125	15	25	24.49	13.06	7.34	
0.005	1780	28	24.5	0	5	0.05	0.025	33.4	25	42.51	134.20	50.47	
0.010	1780	28	24.5	0	5	0.05	0.025	33.4	25	46.91	268.30	100.90	
0.020	1780	28	24.5	0	5	0.05	0.025	33.4	25	49.07	536.60	201.80	⊘
0.030	1780	28	24.5	0	5	0.05	0.025	33.4	25	49.69	804.90	302.70	
0.040	1780	28	24.5	0	5	0.05	0.025	33.4	25	49.90	1073.20	403.60	
0.005	1780	28	24.5	0	10	0.05	0.025	33.4	25	46.23	268.30	84.84	
0.010	1780	28	24.5	0	10	0.05	0.025	33.4	25	48.43	536.60	169.70	
0.020	1780	28	24.5	0	10	0.05	0.025	33.4	25	49.53	1073.20	339.40	⊘
0.030	1780	28	24.5	0	10	0.05	0.025	33.4	25	49.83	1609.80	509.10	
0.040	1780	28	24.5	0	10	0.05	0.025	33.4	25	49.90	2146.40	678.80	
0.600	1780	28	24.5	0	5	0.25	0.125	15	25	36.73	57.35	32.25	
0.700	1780	28	24.5	0	5	0.25	0.125	15	25	39.06	66.91	37.63	
0.800	1780	28	24.5	0	5	0.25	0.125	15	25	41.14	76.47	43.00	
0.900	1780	28	24.5	0	5	0.25	0.125	15	25	42.78	86.02	48.37	△
1.000	1780	28	24.5	0	5	0.25	0.125	15	25	44.06	95.59	53.75	
1.100	1780	28	24.5	0	5	0.25	0.125	15	25	45.10	105.15	59.12	
1.200	1780	28	24.5	0	5	0.25	0.125	15	25	45.99	114.71	64.51	
0.600	1780	28	24.5	0	10	0.25	0.125	15	25	43.04	114.71	54.24	
0.700	1780	28	24.5	0	10	0.25	0.125	15	25	44.50	133.82	63.28	▲
0.800	1780	28	24.5	0	10	0.25	0.125	15	25	45.53	152.94	72.32	
0.900	1780	28	24.5	0	10	0.25	0.125	15	25	46.39	172.06	81.36	
1.000	1780	28	24.5	0	10	0.25	0.125	15	25	47.00	191.18	90.40	
0.300	1780	28	24.5	0	5	0.25	0.125	15	25	29.39	28.68	16.13	
0.400	1780	28	24.5	0	5	0.25	0.125	15	25	31.95	38.23	21.50	□
0.500	1780	28	24.5	0	5	0.25	0.125	15	25	34.37	47.79	26.87	
1.000	1780	28	24.5	0	10	0.25	0.125	15	25	25.49	19.12	9.04	
2.000	1780	28	24.5	0	10	0.25	0.125	15	25	30.02	38.24	18.08	
3.000	1780	28	24.5	0	10	0.25	0.125	15	25	34.12	57.35	27.12	■
4.000	1780	28	24.5	0	10	0.25	0.125	15	25	37.97	76.47	36.16	
5.000	1780	28	24.5	0	10	0.25	0.125	15	25	41.03	95.59	45.20	
0.100	1300	35	30	0	10	0.25	0.125	15	25	28.66	34.50	16.31	
0.100	1300	29	25	0	10	0.25	0.125	15	25	27.43	27.30	12.91	◇
0.100	600	30	25	0	10	0.25	0.125	15	25	34.82	61.60	29.13	
0.200	600	30	25	0	10	0.25	0.125	15	25	43.62	123.30	58.30	

Appendix 5

Particle Size Distributions of Bulk Materials Used in this Investigation

	Diameter (mm)	Content (%)
Glass Ballotini	1.165 - 1.515	80
	0.895 - 1.165 }	20
	1.515 - 2 }	

	Size (μm)	Content (%)
Sand	<355	19
	355 - 600	80
	>600	1

NOMENCLATURE

A	(1) Initial location of particle in movement cycle. (Figure 2.2) (2) Constant defined by (2.42), (2.43)	(-)
B	(1) Point of particle exit from bed in movement cycle (Figure 2.2) (2) Constant of proportionality in (A2.4)	(-)
b	Perpendicular distance between drum axis and bed surface	(m)
C	(1) Point of particle re-entry to bed in movement cycle(Figure 2.2) (2) Constant defined by (3.7)	(-)
C_b	Parameter related to filling used in (3.39)	(m)
c	Chord length joining particle entrance and exit points from bed (Figure 3.1)	(m)
D	(1) Drum diameter (2) Longitudinal dispersion coefficient (2.47)	(m) (cm^2/sec)
E	Angle of slope with respect to drum axis down which particles cascade at exit (Figure 3.6)	(rad)
F	Mass flow rate through drum	(kg/s)
F*	Constant defined by (2.40)	(-)
Fc	Cumulative fractional filling in drum	(-)
f	Denotes "a function of"	
fc	Fractional filling at any cross section	(-)
g	Acceleration due to gravity	(m/s^2)
H	Hold up in drum	(kg)
H_d	Bed height at discharge from (3.40)	(m)
H_{lim}	Limiting filling bed height.	(m)
h	Bed height at any point (2.12)	(m)
h_i	Bed height at inlet	(m)
h_m	Bed height at minimum fractional filling in drum	(m)
h_o	Bed height at outlet of drum	(m)
m	Empirical constant (2.36)	(-)
N	Rate of drum rotation	(RPM)
N_{CR}	Number of cascades per revolution	(-)
P	Distance covered in parabolic flight (Figure3.1)	(m)
q	Volumetric flowrate through drum	(m^3/s)
R_b	Radial polar coordinate in (3.39)	(m)
R_d	Drum radius	(m)
R_c	Constriction radius	(m)
r	Radial coordinate	(m)

S	Bed / Wall contact arc length	(m)
s	Axial transport distance per cascade	(m)
t	(1) Time	(s)
	(2) Mean residence time in drum	(min)
v	Axial transport velocity	(m/s)
w	Rate of drum rotation. N.B. When used in expressions for dimensionless feed rate Ψ, w is in RPM to be consistent with literature usage .	(rad/s)
w_c	Critical speed of drum $\sqrt{g/R_d}$.	(rad/s)
x	Distance along drum axis from discharge end.	(m)
Y	Constant defined by(3.7).	(rad/s)
Z	Height above a weir.	(m)

α	General symbol for angle of repose.	(rad)
α_d	Dynamic angle of repose (Deg in 3.11).	(rad)
α_s	Static angle of repose.	(rad)
β	Angle between bed surface and drum axis	(rad)
Γ	Angle between horizontal and line of particle descent in bed surface.	(rad)
δ	Angle of return from parabolic flight (Fig 3.1)	(rad)
Δ	Small increment	
ξ	Angle of particle ejection from bed (Fig 3.1)	(rad)
θ_x	Filling angle at a distance x along the drum. (Figure 2.3)	(rad)
θ_r	Filling angle for particle of path radius r.	(rad)
μ	(1) Coefficient of interparticle friction on the bed surface.	(-)
	(2) Apparent viscosity of Bingham fluid.	(Nsm^{-2})
π	22/7	
ρ	Material bulk density.	
ϕ	Angle at which particle cascades down surface (Figure 2.2)	(rad)
Ψ	Dimensionless feed rate.	(-)
ψ	Drum slope.	(rad)
ψ_b	Angular polar coordinate in (3.39)	(rad)
τ	Time particle spends locked in the bed plus cascading on the surface	(s)
τ_y	Yield stress of Bingham fluid	(Nm^{-2})

References

[A1] Abouzeid A Z M A
The transport and mixing behaviour of particulate solids through rotary drums
PhD Dissertation University of California, Berkeley, California (1973)

[A2] Austin L G & Flemmer R L C
A note on the flowrate of dry powder in horizontal rotating cylinders under open ended discharge conditions
Chem Eng Sci, 29, 1286-1289 (1974)

[A3] Austin L G, Shoji K, Hogg R, Carlson J & Flemmer R L C
Flow rates of dry powders in inclined rotating cylinders under open ended discharge conditions
Powd Tech, 20, 219-225 (1978)

[A4] Abouzeid A Z M A & Fuerstenau D W
A study of the hold-up in rotary drums with discharge end constrictions
Powd Tech, 25, 21-29 (1980)

[A5] Abouzeid A Z M A & Fuerstenau D W
Mechanism and rate of passage of materials in rotary kilns
Powd Tech, 25, 65-70 (1980)

[A6] Akerman K, Hoffman P & Zablotny W
Mechanism and rate of passage of materials in rotary kilns
Brit Chem Eng, 11 (1), 26-29 (1966)

[A7] Akerman K
Anwendung radioaktiver indikatoren sur intersuchung der material bewegung in drehofen. (Use of radioactive isotopes for understanding material movement in rotary dryers.) In German
Eurisotop 80, Serie: Monograph 26 (1973)

[A8] × Austin L G, Luckie P T & Atey B G
Residence time distribution in mills
Cem & Conc Res, 1, 241-256 (1971)

[A9] × Abouzeid A Z M, Mika S, Fuerstenau D W & Sastry K V S
The influence of operating variables on RTD for material transport in a continuous rotary drum
Powd Tech, 10, 273-288 (1974)

[A10] Abouzeid A Z M, Fuerstenau D W & Sastry K V S
Transport behaviour of particulate solids in rotary drums: Scale up of residence time distributions using the axial dispersion model
Powd Tech, 27, 241-250 (1980)

[A11] × Augenstein D A & Hogg R
Friction factors for powder flow
Powd Tech, 10, 43-49 (1974)

[B1] × Bayard R A
New formula developed for kiln time
Chem & Metall Eng, 52 (3), 100-102 (1945)

[B2] Boguslavskii N M
Method of computation of the motion of free flowing materials in rotary kilns
Khim Prom, 89-97 (1956). **Original**
Dept of Sci & Ind Res Lending Library Unit. Russian translating program RTS 1504 (1960). **English translation**

[B3] Bachmann D
Unpublished work quoted by Matz W
Spanger-Verlag OHG Berlin (1954)

[B4] Barth W
Tech Mech Thermo Dynam, 1, 321 (1930)

[B5] × Briscoe B J, Pope L & Adams M J
Interfacial friction of powders on concave counterfaces
Powd Tech, 37, 169-181 (1984)

[C1] × Costa H & Petermann K
Investigations on the movement of material and the formation of dust in rotary furnaces of the cement industry, using radioactive isotopes
English translation by ICI _ ICI Numbers 5296, 5297, 5298
Silikattechn, 10, (4) 209-210, (5) 253-259, (6) 345-350, (1959)

[C2] × Cross M
Pellet movement through a rotary kiln
Brit Steel Corp Rep No GS/Tech/553/1/74/C

[D1] Dalmia J H
Simulation of a wet process cement rotary kiln
Univ of Urbana Illinois Co-ord Science Lab
Report No R-392 Cong Cat AD-675.336

[D2] Davis E W
Trans Am Inst Min (Metall) Engrs, 61, 250 (1919)

[F1]× Friedman S J & Marshall W R Jr
Studies in rotary drying. Part 1: Hold-up and dusting
Chem Eng Prog, 45, 482-493 (1949)

[F2]× Fritts S S
A practical evaluation of kiln performance
Cement Technology, 7 (6), 212-213 (1976)

[F3] Fan L T & Ahn Y K
Axial dispersion of solids
Appl Sci Res, A10, 465-470 (1961)

[F4]× Franklin F C & Johanson L N
Flow of granular material through an orifice
Chem Eng Sci, 4, 121-122 (1955)

[G1]× Gilbert W
The rotary kiln in cement manufacture. Part 6
Cem & Cem Manuf, 5 (1), 36-48 (1932)

[G2] Ginstling A M, Z'ilberman D & Gvozdev N V
In Russian
Khim Mashinostroenie, 8 (8), 8-9 (1939)

[G3] Gibbs R
Rock Products p58 (1942)

[G4]× Gibbs R
Chart for estimating performance and production rates in rotary kilns
Chem & Metall Eng, 50, 117-118 (1943)

[G5] Gardner R G, Mitchell J J & Scott R
Radioactive tracer method for estimating the retention time of seaweed in a rotary louvre dryer
Chem & Ind p448 (1952)

[G6] Grasland G
Etude du cheminement de la matiere dans le fours rotatifs a l'aide de traceurs radioactifs. (Examination of the material transport in rotary kilns using radioactive tracers.) **In French**
Silicates Industriels, 39, 554-556 (1965)

[G7]× Gorczyca et al
Mathematical modelling of a rotary kiln using a hybrid computer
Pomidry Autom Kontrola, 20 (6), 265-268 (1974)

[H1]× Hogg R, Shoji K & Austin L G
The axial transport of dry powders in horizontal rotating cylinders
Powd Tech, 9, 99-106 (1974)

[H2] Hogrebe K & Lehmann W S
"Tracer"-Versuche an drehofen mit La^{140}. (Tracer tests in rotary kilns with La^{140}). **In German**
Zem Gips, 9, 210-215 (1956)

[H3]× Hehl H, Kroeger H, Helmrich H, Schugerl K
Longitudinal mixing in horizontal rotary drum reactors
Powder Tech, 20, 29-37 (1978)

[H4]× Hogg R & Fuerstenau D W
Transverse mixing in rotating cylinders
Powd Tech, 6, 139-148 (1972)

[H5]× Henein H, Brimacombe J K & Watkinson A P
Experimental study of transverse bed motion in rotary kilns
Metallurgical Transactions B, 14B, 191-205 (1983)

[H6]× Henein H, Brimacombe J K & Watkinson A P
The modelling of transverse solids motion in rotary kilns
Metallurgical transactions B, 14B, 207-220 (1983)

[I1]× Ivanets V N, Moiseenko V I & Lukyanov P I
Method of determining the intensity of longitudinal mixing of free flowing materials in flow through apparatus
Int Chem Eng, 9, 198-201 (1968)

[J1]× Jinescu V V & Jinescu I
Design data for rotary drum plants. **English translation by ICI** - ICI Number 5291
Aufbrereitungstechnik, 9, 573-578 (1972)

[J2] Jaeger J C
An introduction to applied mathematics
University Press Oxford (1963)

[J3]× Johnstone R E & Thring M W
Pilot plants and scaled up methods in chemical engineering [K1]
McGraw Hill (1957)

[K1] × Kramers H & Croockewit P
The passage of granular solids through inclined rotary kilns
Chem Eng Sci, 1, 253-258 (1952)

[K2] × Karra V K & Fuerstenau D W
Scale up of axial profile of material hold up in horizontal rotating cylinders
Powd Tech, 19, 265-269 (1978)

[K3] Karra V K & Fuerstenau D W
Material transport in a continuous rotating drum: The effect of discharge plate geometry
Powder Tech, 16, 23-28 (1977)

[K4] Kröger H, Hehl M, Helnirich H & Schugerl K
Decomposition of powders in horizontal rotary drum reactors
Powder Tech, 22, 1-10 (1979)

[K5] Knight P C
The role of particle collisions in determining high strain rate flow behaviour
Powd Tech, 37, 183-193 (1984)

[K6] Kaye B H & Sparrow D B
The role of surface diffusion as a mixing mechanism in a barrel mixer (Parts 1 & 2)
Ind Chem, April, 200-205, 245-250 (1964)

[L1] Luoto V A & Rotkirch E G
Tracer techniques in the Finnish Industry
UN International Conference on Peaceful uses of Atomic Energy
19, 28-33 (1958)

[L2] Lyons J W, Mins H S, Parisot P S & Paul J Y
Computer simulation of a wet process cement kiln operation
ISA Proc Inst Automation Conference, Preprint 202-LA-61
Los Angeles California (1961)

[L3] Lyons J W, Mins H S, Parisot P S & Paul J Y
Experimentation with a wet process rotary cement kiln via the analogue computer
I & E C Proc Des Dev, 1 (1), 29-33 (1962)

[L4] Lehmberg J, Hehl M & Schügerl
Transverse mixing and heat tranfer in horizontal rotating drum reactors
Powd Tech, 18, 149-163 (1977)

[M1] Mu J & Perlmutter DD
The mixing of granular solids in a rotary cylinder. (Part 1: Model derivation)
AIChEJ, 26 (6), 928-934 (1980)

[M2] Mu J & Perlmutter D D
The mixing of granular solids in a rotary cylinder. (Part 2: Experimental results and parameter estimation
J Chem E Symp Ser No 59, 5:7/1-5:7/20 (1980)

[M3] Mukherjee S G & Ghosh B B
Effect of dam hold-up in a rotary kiln
Indian J Tech, 15, 232-234 (1977)

[M4] Miskell F & Marshall W R Jr
A study of retention time in rotary drier
Chem Eng Prog, 52, 35-38 (1956)

[M5] Merz A & Molerus O
Ermittlung der transportkeoffizienten von Schuttgütern in einen drehrohr unde ihre abhangigkeit von korngrisse und markiersfunktion
Dechema Mono, Bd 69, Nr 1292-1326 Tiel 2, 675-697 (1972)

[M6] Miller C O, Smith B A & Schuette W M
Factors influencing the performance of rotary driers: II The rotary drier as a heat exchanger
Trans Am Inst Chem Eng, 38, 841-864 (1942)

[O1] Osiowski A
Isotope absorption & radioactive tracer methods in the cement industry
Cem Wapno Gips, 18/28 (11), 237-240 (1963)

[O2] Oyama Y
Particle motion in horizontal rotating cylinders (original 1933)
Int Chem Eng, 20 (1), 36-55 (1980)

[P1] Pickering R W, Feakes F & Fitzgerald M L
Time for passage of material through rotary kilns
J Appl Chem, 1, 13-19 (1951)

[R1] Rykvin V D, Telyatnikov G V & Broginskii L N
Calculation of the residence time and effective coefficient of longitudinal mixing of material in rotating furnaces
Theor Found Chem Eng, 6 (3), 362-366 (1972)

[R2] Rutle J
Investigation of material transport in wet process rotary kilns by radio isotopes
Pit & Quarry, 48 (1), 120-139 (1955)

[R3] Rutgers R
Longitudinal mixing of granular material flowing through a rotating cylinder. Part 1: Descriptive and theoretical. Part 2: Experimental
Chem Eng Sci, 20, 1079-1087, 1089-1100 (1965)

[R4] Rogers R S C, Gardner R P
Monte Carlo method for simulating dispersion & transport through horizontal rotating cylinders
Powder Tech, 23,

[R5] Riffaud J B, Koehret B & Coupal B
Modelling and simulation of an Alumina kiln
Brit Chem Eng & Proc Tech, 17, 413-418 (1972)

[R6] Rose H E & Sullivan R M E
A treatise on the internal mechanics of tall, tube and rod mills
Chem Pub Co NY (1958)

[S1] Sullivan J D, Maier G C & Ralston O C
US Bureau of Mines Technical Paper 384 (1927)

[S2] Saeman W C
Passage of solids through rotary kilns: Factors affecting time of passage
Chem Eng Prog, 47, 508-514 (1951)

[S3] Saeman W C
Title as above
Pit and Quarry p97 Oct (1952)

[S4] Shoji K
Some results on the breakage and mass transfer of particles in tumbling mills
PhD Dissertation. Pennsylvania State University (1974)

[S5] Sribner N G
Analysis of the movement of free flowing solid materials in rotating drums
Khim Prom, 11, 258-262 (1979)

[S6] Shevstov B I, Kubyshev N N, Cherepivskii A A & Bogdanov Yu.
Determination of the rate of movement of the charge in rotary kilns by means of radioactive isotopes
Int Chem Eng, 11 (2), 252-254 (1971)

[S7] Suzuki A & Tanaka T
Measurement of flow properties of powders along an inclined plane
I & E C Fund, 10 (1), 84-91 (1971)

[T1] Train D
Some aspects of the property of angle of repose of powders
J Pharm & Pharmacol, 10, 127T (1958)

[V1] Van Krevelen D W & Hoftijzer P J
Drying of granulated materials. Part 1: Drying of a single granule
J Soc Chem Ind, 68, 59-66 (1949)

[V2] Vahl L
Het transport in continu werkende droogtrommels
Conveyance in continuously operating drying drums. **English translation by ICI** - ICI Number 5303
Chemisch Weekblad, 45, 325-329 (1949)

[V3] Vahl L & Kingma W G
Transport of solids through horizontal rotary cylinders
Chem Eng Sci, 1, 253-258 (1952)

[V4] Varentzov P V & Yufa M S
The movement of a bed of solid particles in rotary kilns
Int Chem Eng, 1, 88-92 (1961)

[V5] Vogel R
The movement of bulk material in a model rotary tube as a basis for the design and appraisal of cylindrical rotary furnaces.
Parts 1 and 2
English translation by ICI - ICI Numbers 5311, 5317
Wiss Z Hochsch Archit u Bauwesen, Weimar, 12 (1), 57-67, 288-293 (1965)

[V6] Vogel R
Beweging und verweilzeit von shüttgut in einen drehrohr
Maschinebautechnik, 14, 461-4 (1965)

[Z1] Zablotny W W
The movement of the charge in rotary kilns
Int Chem Eng, 5, 360-366 (1965)

[Z2] Zablotny W W et al
Radioactive isotopes in investigating the movement of materials in kilns, **In Polish**
Cem Wapno Gips, 26, 45-51 (1971)